



GEO SOFT



**G E O F E A**®

redefining simplicity for geotechnical engineers

**USER GUIDE**





**G E O F E A**<sup>®</sup>  
redefining simplicity for geotechnical engineers

## USER GUIDE

*Copyright:* GeoSoft Pte Ltd, 31 Changi South Avenue 2, Singapore 486478. Without limiting the rights under copyright, no part of this document may be reproduced, stored in or introduced into a retrieval system, or transmitted in any form or by any means (electronic, mechanical, photocopying, recording, or otherwise), or for any purpose, without written permission from GeoSoft Pte Ltd. GeoSoft Pte Ltd may have trademarks, copyrights or other intellectual property rights covering subject matter in this document. Except as expressly provided in any written license agreement from GeoSoft Pte Ltd, the furnishing of this document does not give you any license to these trademarks, copyrights, or other intellectual property.

*Disclaimer:* The authors of this program have used their best efforts in preparing this program. These efforts include the development, research, and testing of the theories to determine their effectiveness. The author makes no warranty of any kind, expressed or implied, with regard to the theories contained herein. The author shall not be liable in any event for incident or consequential damages in connection with, or arising out of, the furnishing, performance, or use of these theories. The authors are not attempting to render engineering or other professional services through the use of this program. If such services are required, the assistance of an appropriate professional should be sought.

This page is intentionally left blank.

# Contents

Contents	i
Chapter 1	Project setup..... 1
1.1	Conventions..... 1
1.2	Plane Strain ..... 2
1.3	Axisymmetry..... 2
1.4	3-dimensions ..... 2
1.5	Drained and undrained analyses ..... 3
1.6	Consolidation analyses ..... 4
1.7	Limitations..... 4
1.8	Units of measurement..... 4
Chapter 2	Workspace operations group..... 5
2.1	Zoom ..... 7
2.2	Pan ..... 7
2.3	Orbit ..... 7
2.4	Selecting objects ..... 8
2.5	Hiding objects..... 9
2.6	Workgrid ..... 9
Chapter 3	Workflow explorer ..... 11
Chapter 4	View panel ..... 15
4.1	View workgroup..... 15
4.1.1	Perspective ..... 16
4.1.2	Axonometric..... 16
4.1.3	Wireframe..... 16
4.1.4	Transparency..... 16

	4.1.5	Shaded .....	16
	4.2	Grid workgroup .....	17
	4.3	Camera workgroup.....	17
Chapter 5		Geometry panel .....	19
	5.1	Objects in geometry .....	19
	5.1.1	Point.....	19
	5.1.2	Line.....	20
	5.1.3	Surface.....	20
	5.1.4	Volume .....	20
	5.2	Entities in finite element mesh .....	20
	5.2.1	Node .....	20
	5.2.2	Edge.....	21
	5.2.3	Face.....	21
	5.2.4	Solid.....	21
	5.3	Draw workgroup.....	21
	5.3.1	Point  .....	22
	5.3.2	Line  .....	22
	5.3.3	Circle  .....	23
	5.3.4	Ellipse  .....	23
	5.3.5	Arc  .....	24
	5.3.6	Freestyle Curve  .....	24
	5.3.7	Import Files  (     ).....	25
	5.4	Create workgroup.....	25
	5.4.1	Surface  .....	25
	5.4.2	Revolve  .....	26
	5.4.3	Extrude  .....	26
	5.4.4	Sweep  .....	27
	5.4.5	Loft  .....	27
	5.5	Modify workgroup.....	28
	5.5.1	Trim  .....	28
	5.5.2	Extend  .....	28
	5.5.3	Split  .....	29

5.6	Transform workgroup .....	29
5.6.1	Move  .....	30
5.6.2	Copy  .....	30
5.6.3	Array  .....	31
5.6.4	Mirror  .....	31
5.6.5	Rotate  .....	32
5.6.6	Normal Align  .....	32
5.7	Combine workgroup .....	33
5.7.1	Stitch  .....	33
5.7.2	Degenerate  .....	33
5.7.3	Join  .....	33
5.8	Mesh workgroup .....	33
5.8.1	Mesh solid settings  .....	34
5.8.2	Mesh line setting  .....	35
Chapter 6	Material panel .....	37
6.1	Elastic workgroup .....	37
6.2	Elastic perfectly plastic workgroup .....	38
6.3	Critical state workgroup .....	38
6.4	Special workgroup .....	38
6.5	Structure workgroup .....	39
6.6	Defining materials .....	39
6.7	Material models and element types .....	42
6.8	Constitutive soil models .....	43
6.8.1	Coefficient of lateral earth pressure at rest, <b>K<sub>0</sub></b> .....	43
6.8.2	Over-consolidation ratio, <b>OCR</b> .....	47
6.9	Elastic .....	49
6.9.1	Linear variation elastic  .....	56
6.9.2	Anisotropic elastic  .....	56
6.10	Elastic perfectly plastic .....	57
6.10.1	Tresca  .....	58
6.10.2	von Mises  .....	60
6.10.3	Mohr Coulomb  .....	61

	6.10.4	Drucker Prager 	.....69
6.11		Critical states .....	70
	6.11.1	Original Cam clay 	.....74
	6.11.2	Modified Cam clay 	.....76
	6.11.3	Hyperbolic Cam clay 	.....77
	6.11.4	Schofield 	.....82
6.12		User definable.....	83
6.13		Structure interaction .....	83
	6.13.1	Bar elements 	.....85
	6.13.2	Beam elements 	.....85
Chapter 7		In-Situ panel.....	89
	7.1	In-situ stress workgroup.....	89
		7.1.1 Ignore.....	90
		7.1.2 Auto .....	90
		7.1.3 Manual.....	91
	7.2	Translation (in-situ) workgroup.....	91
		7.2.1 Node translational restraint .....	92
		7.2.2 Edge translational restraint.....	92
		7.2.3 Face translational restraint.....	92
	7.3	Rotation (in-situ) workgroup.....	93
		7.3.1 Node rotational restraint.....	93
	7.4	Pore pressure (in-situ) workgroup.....	93
		7.4.1 Node assignment.....	94
		7.4.2 Edge assignment.....	94
		7.4.3 Face assignment .....	94
		7.4.4 Constraints removal.....	94
		7.4.5 Constraints release.....	95
	7.5	Load (in-situ) workgroup .....	95
		7.5.1 Loads removal.....	96
		7.5.2 Loads release .....	96
	7.6	Common (in-situ) workgroup.....	96
	7.7	State (in-situ) workgroup .....	97
Chapter 8		Stages panel .....	99
	8.1	Staged construction.....	99

8.2	Translation (stage) workgroup .....	100
8.2.1	Node translational restraint .....	101
8.2.2	Edge translational restraint.....	101
8.2.3	Face translational restraint.....	102
8.3	Rotation (stage) workgroup .....	103
8.3.1	Node rotational restraint .....	103
8.4	Pore pressure (stage) workgroup .....	104
8.4.1	Node assignment.....	105
8.4.2	Edge assignment.....	105
8.4.3	Face assignment .....	105
8.5	Load (stage) workgroup.....	106
8.5.1	Node assignment.....	107
8.5.2	Edge assignment.....	107
8.5.3	Face assignment .....	108
8.6	Common (stage) workgroup .....	108
8.7	State (stage) workgroup .....	108
Chapter 9	Solution panel.....	109
9.1	Solver .....	109
9.2	Coordinates update .....	109
9.2.1	Coordinates not updated.....	109
9.2.2	Coordinates updated .....	110
9.2.3	Updated Lagrangian scheme .....	110
9.3	Error correction.....	110
9.4	Running the analysis.....	111
Chapter 10	Result panel.....	115
10.1	Point.....	115
10.2	Line .....	118
10.3	Bar.....	118
10.4	Beam .....	121
10.5	Deform shape.....	123
10.6	Contour .....	124
10.7	Vector.....	125
10.8	Stress point.....	126
Chapter 11	Model explorer .....	129
References	137	

*Notes conventions:*

***Good practice:*** *That's the right way to do it.*

***Tips:*** *Just something to highlight.*

***Bad practice:*** *Best check yourself, it is not looking good.*

***Warning:*** *Don't ever do this!*

# Chapter 1 Project setup

## 1.1 Conventions

In rock and soil mechanics, compressive stresses are positive by convention because we shall almost exclusively be dealing with them and tensile stresses are negative. Shear stresses are positive if the implied rotation is anticlockwise. GeoFEA adopted this familiar soil mechanics derivation in our code. A Cartesian frame of reference is adopted:  $x$  = horizontal,  $y$  = vertical and  $z$  = out-of-plane. Positive  $x$  is to the right and positive  $y$  is upward. Positive  $z$  follows the middle finger's pointing direction in the right-hand rule where the pointing directions of thumb and index finger correspond to the positive  $x$ - and positive  $y$ -directions respectively.

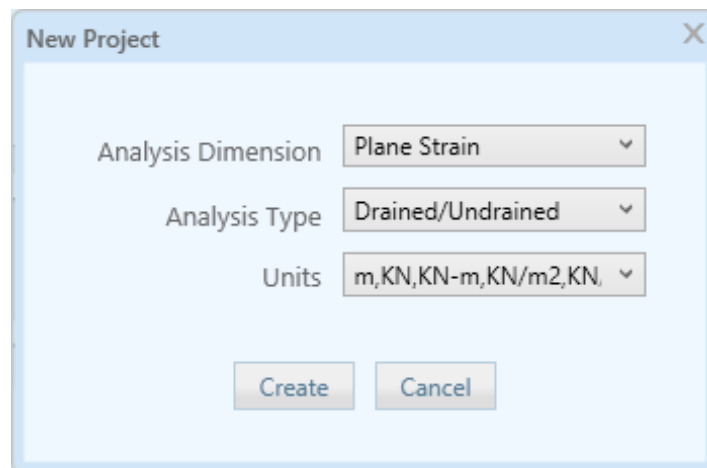


Figure 1: New project interface

## 1.2 Plane Strain

In a plane strain analysis, the strain associated along the out-of-plane direction (i.e. z-direction) is zero. Plane strain deals with the situation where the dimension of the model in one direction is very large in comparison with its dimensions in the other two directions.

Some practical applications of this representation occur in the analysis of dams, embankments, strip footings and to a lesser extent, tunnels.

## 1.3 Axisymmetry

An axisymmetry analysis is one in which the geometry, loading, boundary condition, material zones and properties are symmetrical about a vertical axis. In such a case, a radial section is sufficient to represent the entire domain of the problem. The axis of symmetry is always the vertical y-axis passing through the origin (0, 0). One edge of the mesh must be coincident with this vertical axis. The analysis is performed on a unit radian. One radian of the solid element and loading condition is modeled when using axisymmetric analysis. The field stress must be axisymmetric with the existence of a circumferential field stress. Thus, the loading, boundary and the underlying soil conditions must be axisymmetrical.

**Warning:** Do not set the axisymmetrical axis to any other values other than  $x = 0$ .

**Warning:** Do not use bar or beam structural elements in axisymmetric models!

Single pile, circular footings or small-scale cofferdams constructions are amenable to an axisymmetrical representation.

## 1.4 3-dimensions

A mesh with full 3-dimensional stress state will be able to define a construction model arbitrarily. Such analyses clearly embrace all the practical cases giving more realistic behaviour for both the soil and the structures.

The number of finite elements will be considerably greater than the plane strain or axisymmetric assumptions in practical problems.

Practical application of 3-dimensional analyses include irregularly shaped excavation, tunnel construction, irregular pile group arrangement and undulating soil profiles with pockets of weak soil.

## 1.5 Drained and undrained analyses

Total stress and effective stress analyses can be carried out using total stress and effective stress parameters respectively. Total stress parameters include the response of pore water in the material as the name suggests. On the other hand, effective stress parameters do not consider pore water together with the soil behaviour.

Material response	Effective stress	Total stress	Consolidation
<b>Drained</b>	$E', \nu'$	$E', \nu'$	$E', \nu', t \rightarrow t_\infty$
<b>Undrained</b>	$E', \nu', K_w$	$E_u, \nu_u = 0.5$	$E', \nu', t \rightarrow t_0$
<b>Time-dependent</b>	—	—	$E', \nu', t$

This is different from the common understanding of drained and undrained analyses where "drained" and "effective stress" are used interchangeably. Drained (or effective stress) analyses are rather straightforward as pore water does not take part in the solution. Thus, effective stress (or drained) parameters are used.

In some cases, consolidation analysis is not really necessary because the duration of the consolidation process is short compared to the time scale of the problem considered. This can be investigated by evaluating the dimensionless time expression,  $c_v t / h^2$ , where  $h$  is the average drainage length, and  $t$  is a characteristic time. When the value of this parameter is large compared to 1, the condition is nearly drained, consolidation may be disregarded. In such cases, the behaviour of the soil is said to be fully drained. No excess pore pressures need to be considered for the analysis of the behaviour of the soil.

Sometimes, an "undrained" may be confused with a "total stress" analysis. An undrained analysis can be performed using either total stress or effective stress parameters. The effect of pore water is deemed inclusive in the total stress parameters while a separate treatment must be considered for the effect of pore water when effective stress parameters are used. A bulk modulus of water is used together with effective stress parameters to this effect. When the effect of water is considered separately in the solution equation, pore water pressure can be evaluated as an output field variable.

In an undrained analysis, the material has a shear modulus equal to the drained shear modulus, but a bulk modulus that is practically infinite; this is representative of a material that is volumetrically incompressible. This condition is satisfied by a Poisson's ratio,  $\nu$  of 0.5 when the soil is undrained.

$$G = \frac{E'}{2(1 + \nu')} = \frac{E_u}{2(1 + 0.5)} \quad (1)$$

However, during the setting of in-situ stresses, the groundwater table is required in drained/undrained analyses so that the total stress level in the beginning of the analyses can be determined. The lateral stress coefficient from the groundwater table is

unity and is considered separately from the lateral earth pressure coefficient during the computation of in-situ stresses.

## 1.6 Consolidation analyses

Consolidation analyses should be conducted using effective stress parameters. The dissipation or accumulation of pore water pressure will manifest itself in the analyses. Consolidation is the transition between an undrained and a drained condition govern by the permeability of soils and the duration considered for the loading sustained.

Consolidation analyses are usually implemented either by Terzaghi-Rendulic uncoupled theory (Terzaghi, 1943; Rendulic, 1936) or Biot's consolidation coupled theory (Biot, 1941). The uncoupled solution solves the stress-deformation and the pore pressure dissipation equations independently. The coupled solution solves the stress-deformation and the pore pressure dissipation equations simultaneously.

For uncoupled formulation, the pore pressure dissipation equation is first solved to evaluate the pore pressure, which is then used to solve the stress deformation equation. The stress-deformation problem is solved using the equations of equilibrium, in which the gradient of the pore pressure acts as a known body force. It is difficult to say under what conditions such approximation is acceptable.

Biot's consolidation coupled theory, which is considered to be more rigorous, is used in this finite element formulation. In general, the system of equations of three-dimensional consolidation involves solving the storage equation together with the three equations of equilibrium simultaneously, because these equations are coupled. This coupling is accomplished through conditions of soil skeleton compressibility and flow continuity. The compressibility becomes part of the overall formulation and the calculation of the generated excess pore pressure becomes part of the solution. This three-dimensional theory of consolidation, as developed by Biot may lead to solutions that are significantly different from the theory proposed by Terzaghi.

Cryer compared the three-dimensional consolidation theories of Biot and Terzaghi (Cryer, 1963).

## 1.7 Limitations

This software is not suitable for dynamic events, nor is it capable of handling partially saturated conditions.

## 1.8 Units of measurement

The user can select from 4 sets of units. The input of parameters shall follow the set of units selected. It cannot be changed thereafter. The parameters derived from any in-built libraries will be in accordance with the selected unit measure.

## Chapter 2 Workspace operations group

Workspace occupies the most area on the computer screen. It is an area where the finite element model will be constructed. The orientation of the model's global coordinates system is reflected on the lower left of the Workspace together with the cursor's location. The color convention for the axes are red for  $x$ -axis, green for  $y$ -axis and blue for  $z$ -axis. The vertical  $y$ -axis in the coordinates system is gravity-related. This is also the usual right-handed coordinate system seen in Computer Graphics.

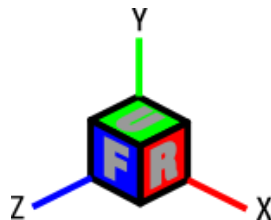


*Figure 2: Coordinates system*

The tools required for common operations of the Workspace is located in the Workspace Operations group. The operations include:

- setting of preset views,
- fitting the extent of view and
- rubber band zooming.



*Figure 3: Preset views: front, back, up, down, left and right*



Figure 4: View area controls: fit to window and zoom area

Clicking on "Show" will reveal 4 options for visual entities:

- Show Grid
- Show Load
- Show Fixity
- Show Pore Pressure

Selecting the options will reveal the stated visual entities. All options are selected by default. Uncheck the item will hid the stated visual entity.

Clicking the "Element" will bring up an element checking window with "Mesh" and "Element" tabs. The "Mesh" tab reflects the average mesh quality for the various entities comprising of continuum elements. Six different quality measures are used. The "Element" tab allows a specific element to be located and the six quality measures for that element is presented.

A set of common tools that are required over the whole analysis workflow. These can be found to the right of the Workflow explorer panel. The operations include:

- orientating the Workgrid and
- selecting different types of geometry objects.



Figure 5: Workgrid position and orientation: move, x-y grid, y-z grid and x-z grid

Pressing "F1", "F2" and "F3" shortcut keys will set x-y grid, y-z grid and x-z grid respectively.



Figure 6: Objects selection tools: auto-select, point, line, surface and volume

Wheel mouse is the recommended pointing device.

## 2.1 Zoom

Scrolling the wheel button of the mouse changes the view magnification. The zoom interaction also keeps the cursor over a fixed point.



*Figure 7: Scroll to zoom*

## 2.2 Pan

Pan moves the view parallel to the screen plane. Pan the Workspace by dragging with the right mouse button held down while any tool is active.



*Figure 8: Hold right mouse button to pan*

## 2.3 Orbit

This function is only available in 3-dimensional analyses. Orbit rotates your view around a view centre. Orbit the camera view by dragging with the wheel button held down.



*Figure 9: Hold mouse wheel button to orbit*

## 2.4 Selecting objects

A single click will select the object on which the mouse cursor is resting. Multiple objects selection is enable my holding down the “SHIFT” key on the keyboard. Clicking with the mouse cursor on an empty portion of the Workspace will deselect everything.



*Figure 10: Click left mouse button to select*

Rectangular selection box can be defined with a start and an end points representing the diagonal of the selection box traversed by the mouse pointer while holding down the left mouse button. Depending on the box definition, the box selects objects:

- that are fully in the defined rectangular area when the start point is at the top left and the end corner of the box is at the bottom right,
- that are fully or partly (intersected) in the defined area when the start point is at any corner of the selection box other than the top left.

## 2.5 Hiding objects

It is sometime necessary to hide some objects in a model, especially for complicated ones. It is more convenient to remove the unwanted objects from view and work only with the relevant objects of the model. Right click on the any objects to bring up the "Hide" menu options: (1) Hide Selected, (2) Hide Unselected and (3) Hide None.

## 2.6 Workgrid

The Workgrid is the grid plane on which geometrical objects are drawn. The local axes convention on the Workgrid is presented as red and green lines. The intersection of these two lines represents the origin of the Workgrid. The Workgrid's orientation determines the breadth, height and depth onto which the cursor will snap to. The cursor will only snap to the grid other than the drawn objects on the screen. The Workgrid only appears as  $x$ - $y$  plane in 2-dimensional analyses. A new Workgrid will be a 200 units by 100 units.

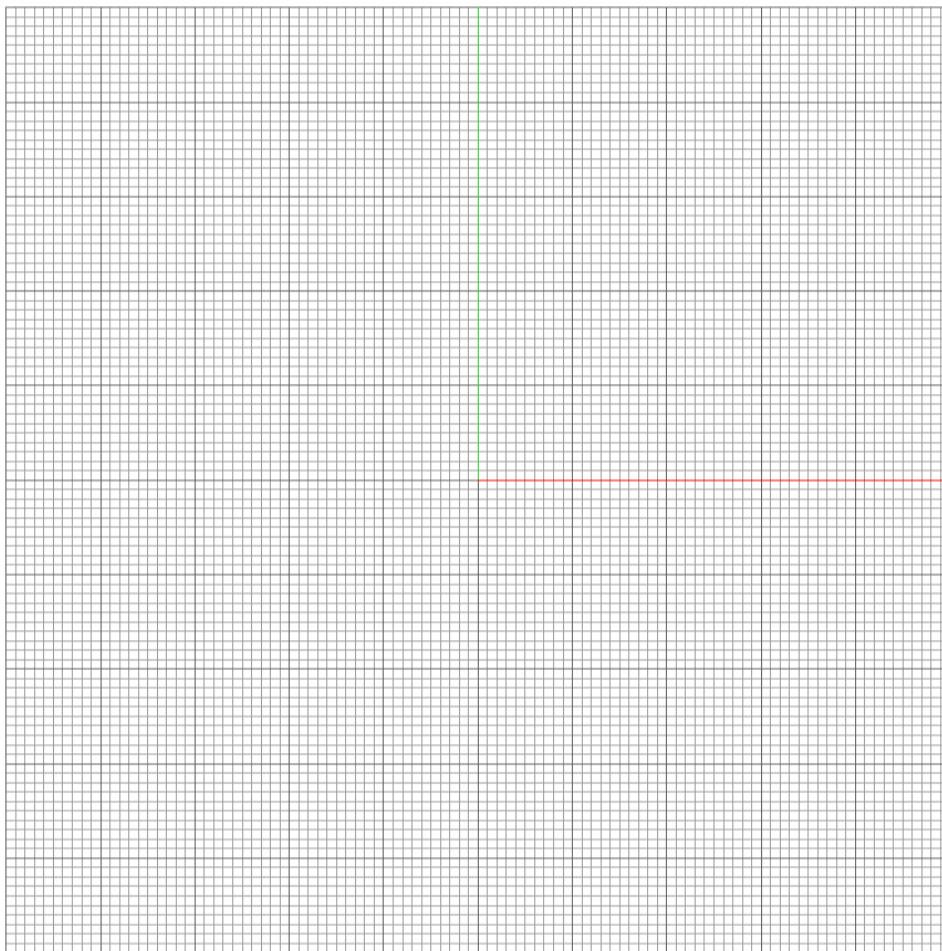


*Figure 11: Workgrid*

There are two explorer-type windows aligned vertically to the left of the Workspace.  
They are:

- Workflow explorer and
- Model explorer

## Chapter 3 Workflow explorer

The Workflow explorer located on the left side of the screen provides a guide on the actions required by user in completing the finite element analyses.

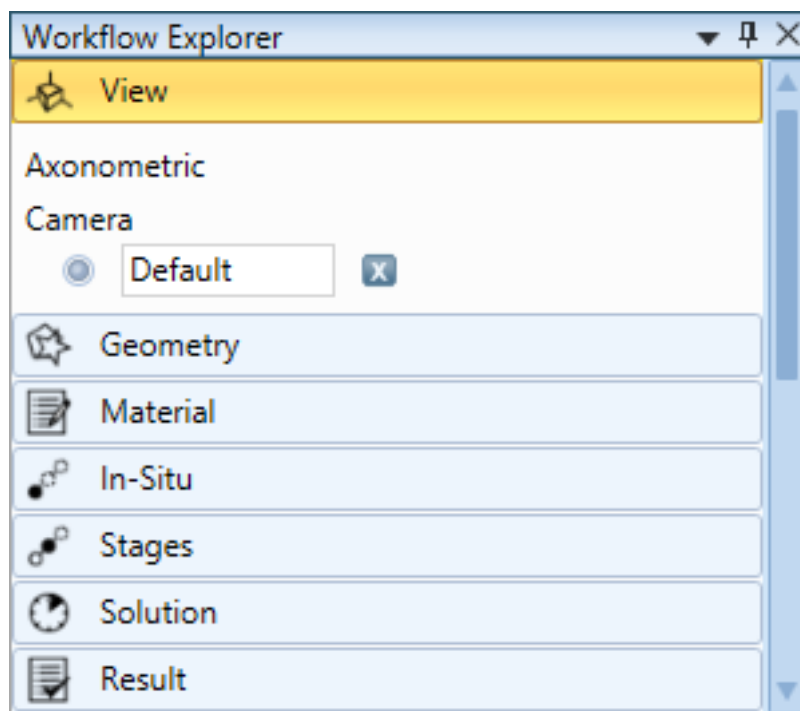


*Figure 12: Workflow explorer*

It comprises clickable bars labeled as **View**, **Geometry**, **Material**, **In-Situ**, **Stages**, **Solution** and **Result**. The user will only be able to view the contents of the clickable bars one at a time.

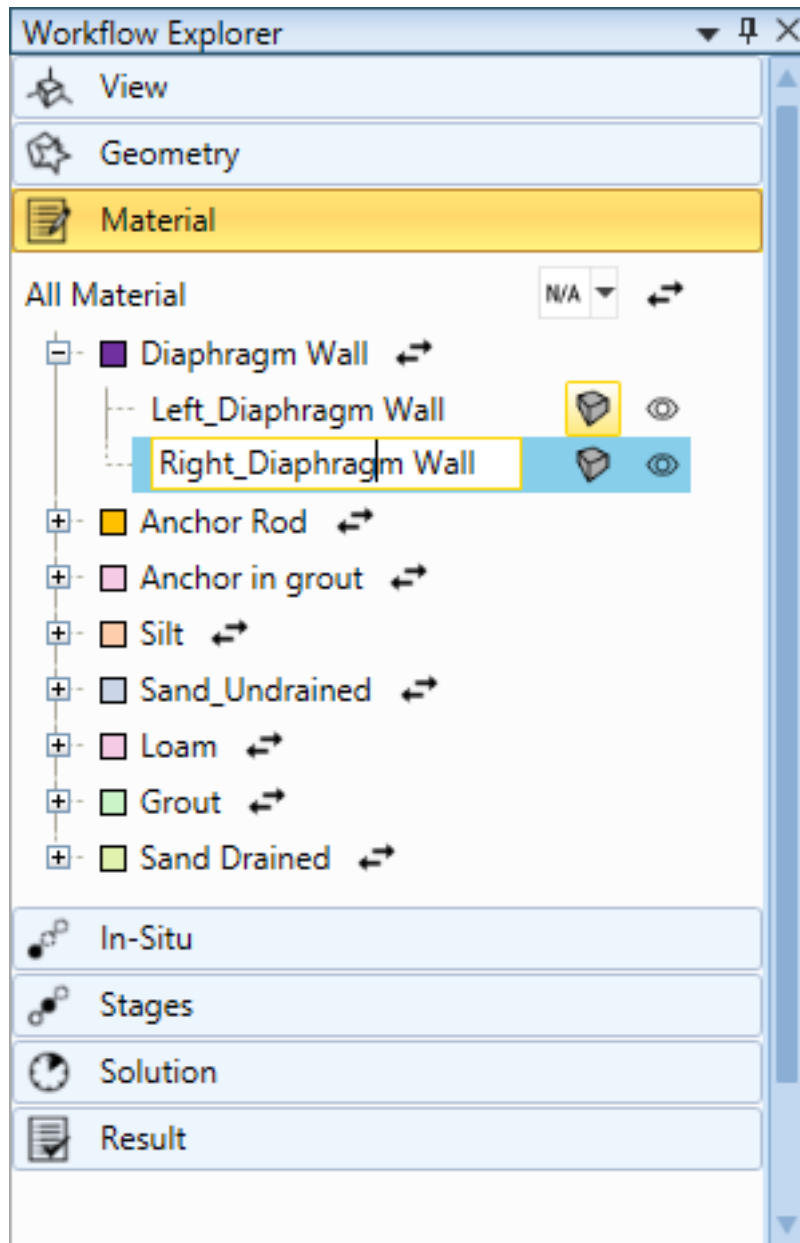


*Figure 13: Editing information in Workflow Explorer*

The contents under these clickable bars present information about each work process in a tree view. Some items presented in an edit box under the tree view is editable. Double-click on the information to edit. Others are actionable with right click options.

Each click on the bars will reveal a different set of tools organized as workgroups in the work panel. The typical finite element workflow is as follow.

---

<b>Step</b>	<b>Description</b>
<b>1</b>	Create geometry.
<b>2</b>	Generate mesh.
<b>3</b>	Assign material properties.
<b>4</b>	Apply loads and constraints.
<b>5</b>	Analyse problem.
<b>6</b>	Review results.

---

This page is intentionally left blank.

# Chapter 4 View panel

Selecting **View** on the Workflow panel reveals a set of tools on the View panel.

## 4.1 View workgroup

The View Workgroup contains the tools for the manipulating the projections and styles of the model.

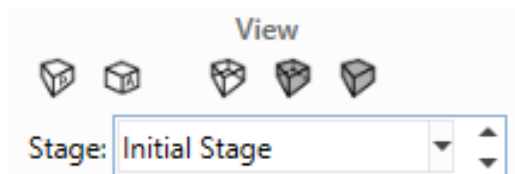


*Figure 14: View settings*

The "Stage" dropdown list allows selection of construction stages. Above this dropdown list are buttons that control the view of the model objects.

Viewports can have one of the two projections: axonometric or perspective. Axonometric view helps you to evaluate the object's shape and size proportions without any distortion, while a perspective view gives you a better sense of space and depth, especially with large objects.



*Figure 15: View projections: perspective and axonometric*

Most overrides for visibility and graphic display are made in the View workgroup. The exception is for individual element overrides; these are made in the view-specific object control under Material workflow.



*Figure 16: View styles: wireframe, transparency and shaded*

#### **4.1.1 Perspective**

In a perspective view, grid lines converge to a vanishing point. This provides the illusion of depth in the viewport. Perspective projection makes objects farther away look smaller.

#### **4.1.2 Axonometric**

Axonometric views are also called orthogonal views in some systems. In an axonometric view, all the grid lines are parallel to each other, and identical objects look the same size, regardless of where they are in space.

#### **4.1.3 Wireframe**

A wireframe model is an edge representation of an object. Wireframe models consist of points, lines, arcs, circle, and other curves that define the edges of objects. The term wireframe comes from the use of metal wire to represent a three-dimensional shape of solid objects. Any edges hidden from view will still be visible as solid lines.

#### **4.1.4 Transparency**

In a transparency model, only edges and fill are drawn on element faces. The edge behind the face in any degree of transparency element is visible to a lesser degree and thus allows the differentiation between hidden and visible lines.

#### **4.1.5 Shaded**

In a shaded model, parts of edges are hidden. An edge can be hidden by the face of any non-transparent element, and by a face of its own.

## 4.2 Grid workgroup

The z-axis of the view coordinates always points directly to the viewer in orthographic projection. The x-axis points to the right, the y-axis points upwards.

The "X Extend" and "Y Extend" define the size of the drawing grid. The spacing between the major and minor gridlines can be changed by editing the relevant editable fields. The default value of 100 units and 50 units for the X and Y Extend will give a 200 units by 100 units Workgrid. The colours of the background, major and minor gridlines can be customised. Clicking on the button after the background colour designation will restore the default colours for background, major and minor grid lines. The "Snap Tolerance" will define the smallest allowable snap interval.

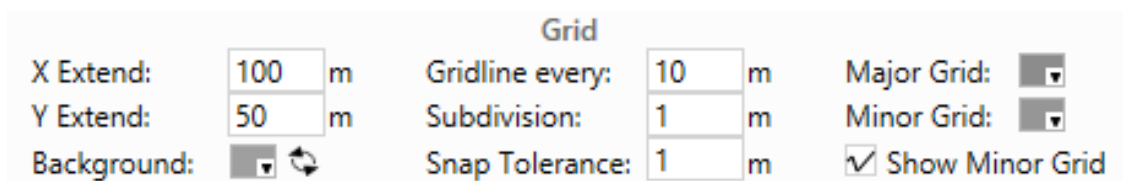


Figure 17: Grid settings

## 4.3 Camera workgroup

An orbit camera in a right-handed coordinate system is used to allow the camera to orbit around an object that is placed in the Workspace. The object doesn't necessarily need to be placed at the origin of the world. An orbit camera doesn't limit the rotation around the object.

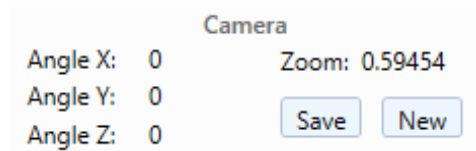
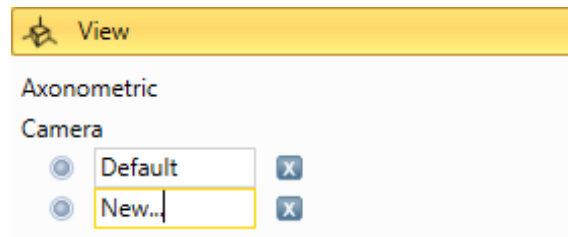


Figure 18: Camera settings

The basic theory of this camera model is that the camera matrix first rotates "pitch" angle about the x-axis (Camera X), then rotates "yaw" angle about the y-axis (Camera X), then translates to some position in the world. The camera is always in an upright position and does not need to "roll" about the z-axis thus the Camera Z is always set to zero.

The zoom function only scales the object up or down. It does not change the field-of-view angle of the object whether in perspective or axonometric mode.

The "New" button will create a new camera view under the Default view in the "View" camera property. This allows different view orientations to be saved when the "Save" button is clicked. To remove the view orientations, click on the button marked with an "X" to the side of the view orientation that is to be deleted.



*Figure 19: View properties tree*

**Tips:** Multiple model views can be created and saved for consistent presentation of the finite element mesh.

# Chapter 5 Geometry panel

Selecting **Geometry** on the Workflow panel reveals a set of tools on the Geometry panel. It consists the following workgroups:

- Draw
- Create
- Modify
- Transform
- Combine
- Mesh

A command panel is appended at the end of these tools as prompt for actions for the tools that is active.

## 5.1 Objects in geometry

The geometry is simplified to create a computationally feasible and efficient model using a combination of points, lines, surfaces and volumes. Geometric objects will not be evaluated in the solution of finite elements.

### 5.1.1 Point

This is a zero-dimension (zeroth-order) geometric object known as 0-simplex. This is the basis upon which a geometric line is drawn. Vertex is an angular point of a polygon.

Points are created graphically by using a pointing device to locate the coordinates and left clicking on the Workgrid. Points can be imported from a list in comma separated value format.

### 5.1.2 Line

This is a one (1)-dimension (first-order) geometric object known as 1-simplex. This is the basis upon which a geometric surface is created. It will be more appropriate to describe a line as a first-order object because a curved line will be described by 2 dimensions even in a local coordinate system.

### 5.1.3 Surface

This is a two (2)-dimension (second-order) geometric object. It is a non-self-intersecting polygon defined by an arbitrary number of connected lines. This is the highest ordered object in a 2-dimension modelling. In a 3-dimension model, this is the basis upon which a geometric volume is created. It cannot be guaranteed that a face is always planar. It will be more appropriate to describe a surface as second-order object because a curved surface will be described by in 3 dimensions even in a local coordinate system.

### 5.1.4 Volume

This is a three (3)-dimension (third-order) geometric object. This is the highest ordered object in a 3-dimension modelling. It will be more appropriate to describe a volume as a third-order object to ensure consistency with the nomenclature of lower ordered objects.

## 5.2 Entities in finite element mesh

A mesh is seen as a partition of an arbitrary domain into simpler geometrical objects (or elements). Those elements are compound of entities such as nodes, edges, faces, solids and the relations between them. Only finite element entities are interpreted during pre-processing. Only nodes and elements are evaluated during solution.

### 5.2.1 Node

A node is also a point. However, a node is a point which is obtained when the domain is discretized and a mesh is generated. It is the simplest entity in a mesh. Nodes are a part of the finite element model. Generation of nodes are automated during mesh procedures, however, the user is allowed to refine the number of nodes along elements' edges.

Loads are applied at the nodes. Any edge or face loads described geometrically as a line or surface distribution patches will eventually be converted to equivalent nodal loads. Nodes are the points where the required values related to degree-of-freedom like displacements and reaction forces are calculated.

### 5.2.2 Edge

An edge links two nodes together. In many cases, edges are treated as vectors, knowing their starting and ending nodes. The edges shared by two elements are counted only once to ensure continuity of field variations between the elements. The edges will also define the shape of the finite elements visually. Each element has 2, 3 or 4 vertices depending on the type of elements user wishes to create.

A fairly simple polynomial expressions known as shape functions reside along these edges. The shape function is the function which interpolates the solution between the discrete values obtained at the mesh nodes. It defines the underlying assumption of how quantities like stiffness, mass, element loads, displacements, strains, stress, internal forces, etc are distributed in an element.

An isoparametric formulation is considered in the program where the shape function defines the element's geometry, and also acts as an interpolation function for the primary variable, the displacement field.

### 5.2.3 Face

Surface meshes form faces. In 2-dimension analyses, it defines the highest element order. It serves as a faithful representation of the finite element model to the real world. To be able to handle arbitrary polygon surfaces (planar or curved), their decomposition to simplexes is required, commonly known as triangulation. The triangles thus generated are 2-simplexes.

### 5.2.4 Solid

Volume meshes form solids. In 3-dimension analyses, it defines the highest element order. It serves as a faithful representation of the finite element model to the real world. Extending the approach followed for the geometric computations of polygons, polyhedrons are treated by applying a decomposition as well. This type of decomposition is known as tetrahedralisation, where the solid is considered as the sum of non-overlapping tetrahedrons, 3-simplexes.

## 5.3 Draw workgroup

Icon	Description
	Draws a point.
	Draws a line segment from 2 points.
	Draws a circle from center and radius.
	Draws a circle from diameter.
	Draws a circle from three points on the circumference.
	Draws an ellipse from center, major radius and minor radius.
	Draws an ellipse by major diameter and minor radius.
	Draws an arc segment from center, start point and end point.
	Draws an arc segment from start point and end point follows by a point on the circumference.
	Draws a smooth freestyle curve from multiple points.
	Import from DXF or CSV file.

### 5.3.1 Point

Insert "Point" allows the insertion of points through mouse input or entering the coordinates of the point in the command box.

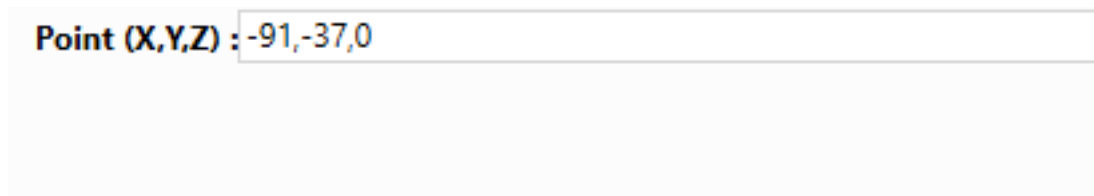


Figure 20: Point input

### 5.3.2 Line

Draw "Line" allows line construction through mouse input or entering the coordinates of the point in the command box.

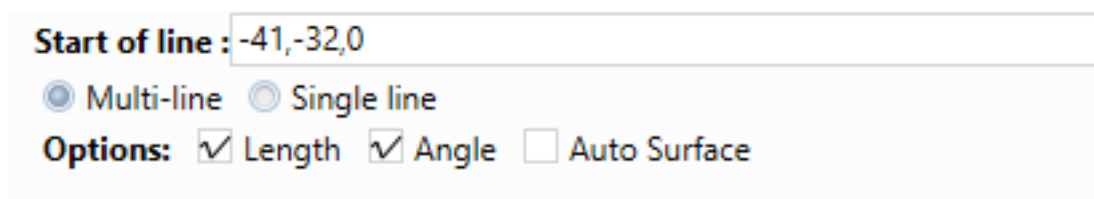
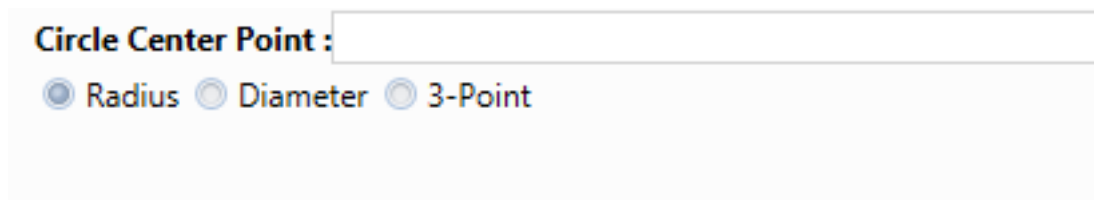


Figure 21: Line input

When using the command box tool, consecutive point coordinates are required to define the line. The "Multi-line" option allows connected sequence of line segments created in a single operation. Press the "ESC" key to terminate the operation. The lines thus created are separate entities. The "Single line" option allows the creation of one line entity each time. The checkboxes for "Length" and "Angle" turn on the measurement displays when checked.

### 5.3.3 Circle

Draw "Circle" allows three ways of circle creation.



*Figure 22: Circle input*

The method of circle creation can be selected from the drop-down list or the radio options. The command box will prompt for the required steps for each method.

### 5.3.4 Ellipse

Draw "Ellipse" provides two ways of ellipse creation.

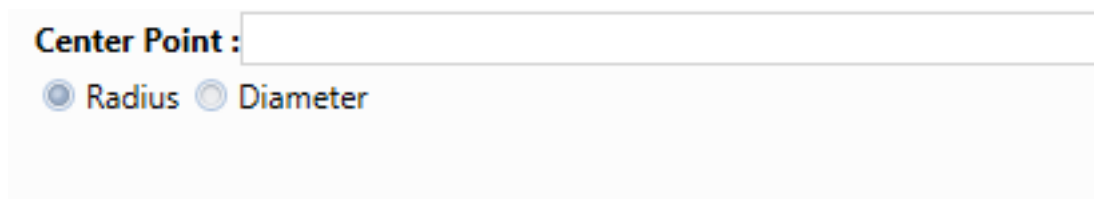
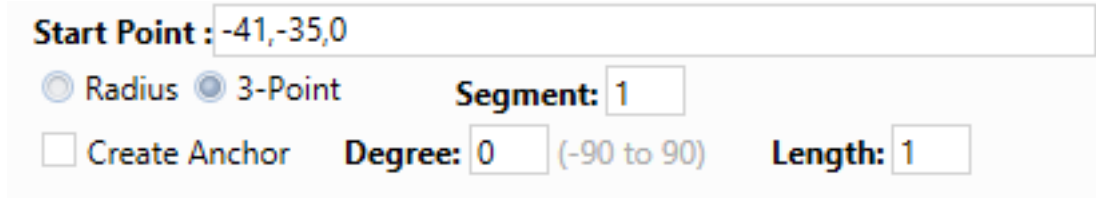


*Figure 23: Ellipse input*

The method of ellipse creation can be selected from the drop-down list or the radio options. The command box will prompt for the required steps for each method.

### 5.3.5 Arc

Draw "Arc" provides two ways of ellipse creation.



Start Point : -41,-35,0

Radius  3-Point Segment: 1

Create Anchor Degree: 0 (-90 to 90) Length: 1

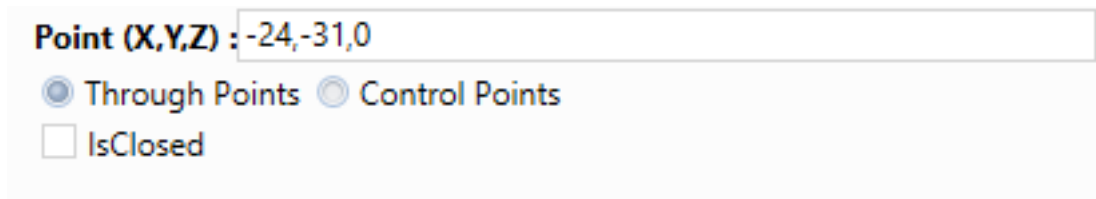
Figure 24: Arc input

The method of ellipse creation can be selected from the drop-down list or the radio options. The creation of arc can be a sequence of segments created in a single operation by specifying the number of segments desired.

Where the arc creation function is used to generate the tunnel outline, user can opt to create the reinforcing anchors in the same operation by checking the "Create Anchor" option. Set the angles of inclination from the horizon and the length of the anchors. A "Reverse Anchor" button will be shown to allow user to toggle between the forward or backward directions of inclination upon defining the arc. Click "OK" to generate the arc with anchors.

### 5.3.6 Freestyle Curve

Draw "Freestyle Curve" creates a B-spline curve based on a linear combination of control points.



Point (X,Y,Z) : -24,-31,0

Through Points  Control Points

IsClosed

Figure 25: Freestyle curve input

The curve can be created by specifying the "Through Points" or the "Control Points". A curve that actually passes through each through point is called an interpolating curve; a curve that passes near to the control points but not necessarily through them is called an approximating curve. The "IsClosed" option makes it possible for the curve to join back on itself to make a closed figure.

### 5.3.7 Import Files

Points can be created from either DXF (AutoCAD Drawing Exchange Format) or CSV (Comma separated values) file formats.

Lines and curves can only be imported from DXF file.

## 5.4 Create workgroup

Icon	Description
	Creates a surface from closed boundary lines and points.
	Creates a line/surface/solid from point/line/surface by an angle around a point or axis.
	Extrudes a point/line/surface to a line/surface/solid.
	Creates a surface/solid from a line/surface along a path.
	Creates a surface between two closed boundary lines.

### 5.4.1 Surface

Create "Surface" generates surface from closed boundary curves and points.

Select objects to find faces. <Press Enter> :

Delete finding shapes:  Yes  No

Surface Only  Split

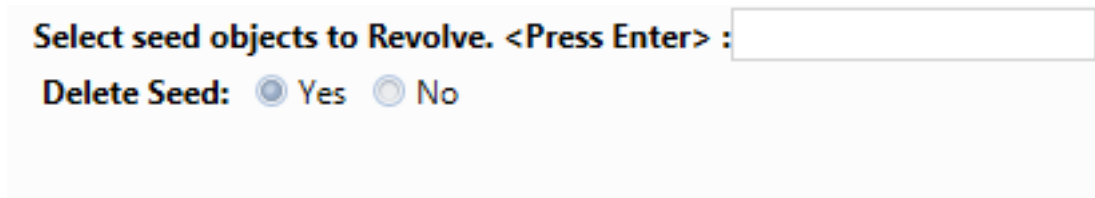
Figure 26: Surface input

Surface can be created from 3 or more boundary curves. Points selected with the boundary curves will create surfaces passing through both the boundary curves and the interior points. When interior curves are included within the boundary curves, the surface will include the interior curves. The selected interior control points or curves can be used to define the surface topology within the closed boundary lines. A set of control points can thus be used to represent an interface between two soil strata. When no boundary lines are selected with the control points, a four-edge boundary will be formed based on the spread of the control points.

Select "Yes" for "Delete finding shapes" if the lines and points are not required after the surface is created.

## 5.4.2 Revolve

"Revolve" generates a higher order entity from an entity an order lower. A point generates a line, a line generates a surface and a surface generates a volume.

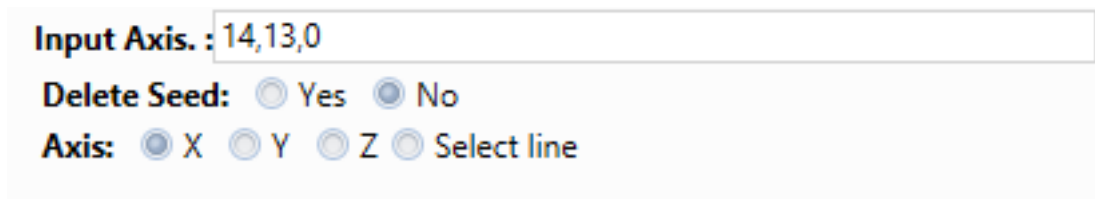


Select seed objects to Revolve. <Press Enter> :

Delete Seed:  Yes  No

*Figure 27: Revolve input*

Select "Yes" for "Delete Seed" if the creation entity is not required after creating the desired object.



Input Axis. :

Delete Seed:  Yes  No

Axis:  X  Y  Z  Select line

*Figure 28: Define revolving axis*

Axis selection will appear in the command space after seed object selection. The axis can be defined in the input box, select the revolving axis follow by specifying the center of revolution or select an existing geometry line.

## 5.4.3 Extrude

"Extrude" lets user pull surfaces or curves in a specified direction to form volumes or surfaces.



Select objects to Extrude. <Press Enter> :

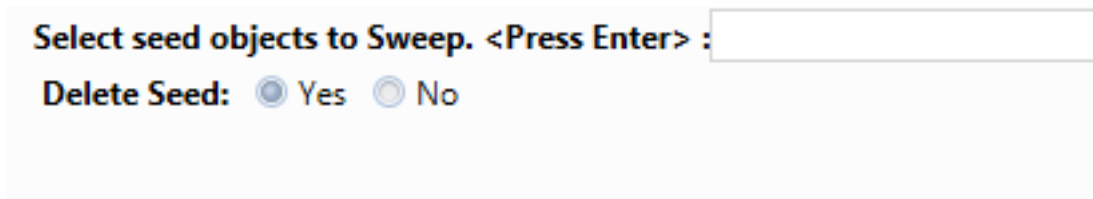
Delete Seed:  Yes  No

*Figure 29: Extrude input*

Select "Yes" for "Delete Seed" if the creation entity is not required after creating the desired object.

#### 5.4.4 Sweep

"Sweep" creates an entity one order higher by sweeping it along a backbone curve. Point generates into line; line into surface and surface into volume. Multiple entities can be swept along a backbone curve.



Select seed objects to Sweep. <Press Enter> :

Delete Seed:  Yes  No

Figure 30: Sweep input

Select "Yes" for "Delete Seed" if the creation entity is not required after creating the desired object.

#### 5.4.5 Loft

"Loft" builds a skin surface or a solid between any number of shape curves or wires. The sequence of curves or wires selection will determine the direction of loft operation.



Select Closed curves/wires to Loft. <Press Enter> :

Delete Seed:  Yes  No

IsSolid  Ruled

Figure 31: Loft input

When a set of closed wires is used in the operation, selecting "IsSolid" will create a solid object. Otherwise, a skin surface will be generated. Selecting "Ruled" will generate a straight edges along the loft direction. Otherwise, curved edges will be formed.

Select "Yes" for "Delete Seed" if the creation entity is not required after creating the desired object.

## 5.5 Modify workgroup

Icon	Description
	Trims a line with respect to another line.
	Extends a line to another line.
	Splits an object with points, lines, surfaces or solids.

### 5.5.1 Trim

"Trim" removes portions of a line that extend past a line intersection. If there is no intersecting boundary in the direction of extension, the line segment will not be trimmed.



*Figure 32: Trim input*

### 5.5.2 Extend

This feature extends line segments to the selected line. If there is no intersecting boundary in the direction of extension, the line segment will not be extended.



*Figure 33: Extend input*

### 5.5.3 Split

"Split" involves operation between entities of the same order or entities of one-order difference. Mesh compatibility can only be ensured under this condition. Points can be positioned on lines, split lines can be placed on surfaces and surfaces can be inserted in volumes.



Figure 34: Split input

The operation is analogous to a heated wire/rod (cutting object) melting through a foam (object-to-split). The cutting object will not disappear after the object-to-split is modified. The operation splits all the geometry along the edges where the selected entities intersect.

Any surface regions, which are in contact with other parts, should be precisely cut into separate surfaces using the split operation in order for interactions to occur between the parts and the surface region. An example is a footing placed directly on a ground surface.

**Good practice:** The cutting object should extend beyond the object to be cut if complete separation is required.

**Tips:** Lines, surfaces or volumes may be split where these entities meet to ensure alignment of nodes and, consequently, compatibility of mesh.

## 5.6 Transform workgroup

Icon	Description
	Moves objects from one point to another by selecting or inputting a direction vector.
	Copies objects from one point to another by selecting or inputting a direction vector.
	Creates an array of objects along a path by selecting or inputting a direction vector.
	Mirrors objects on a mirror plane.

Icon	Description
	Rotates objects by a certain angle around a point or axis.
	Aligns a surface normally to a line passing through it.

### 5.6.1 Move

This function moves objects from one point to another by selecting or inputting a direction vector. The "Move" function requires a from and to location. Pick these locations on the screen or type coordinates at the command box.



Select objects to Move. <Press Enter> :

Option:  Line  Point

*Figure 35: Move input*

Selecting the "Line" option will show the measurement of vector length and angle on screen other than the coordinates. Select the "Point" option to show only the coordinates.

### 5.6.2 Copy

"Copy" creates new copies of the object by specifying the direction vector. Multiple copies of the object can be created by holding the "SHIFT" key while specifying the incremental direction vectors from the previous creation.



Select objects to Copy. <Press Enter> :

Option:  Line  Point

*Figure 36: Copy input*

Selecting the "Line" option will show the measurement of vector length and angle on screen other than the coordinates. Select the "Point" option to show only the coordinates.

### 5.6.3 Array

"Array" make multiple copies of an object equidistant or specific distance from each other.

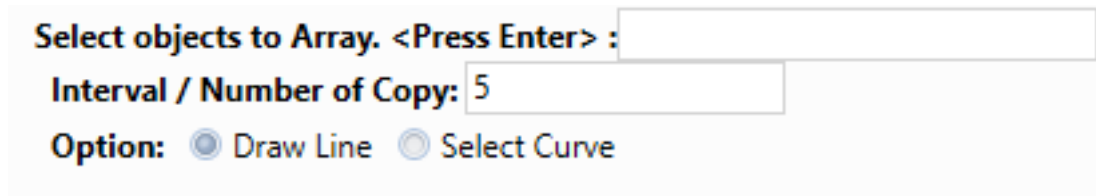


Figure 37: Array input

Inputting a single number in the "Interval/Number of Copies" box represent the number of copies to create during the array operation. Defining a series of numbers separated by commas (,) represent the intervals between successive new objects. These intervals are designated separation distance along a curve.

This feature offers two ways of specifying the direction vector. "Draw Line" requires user to draw a new curve or line. "Select Curve" allows user to pick a geometry curve on the screen.

### 5.6.4 Mirror

"Mirror" flipped the selected object across a symmetry plane.

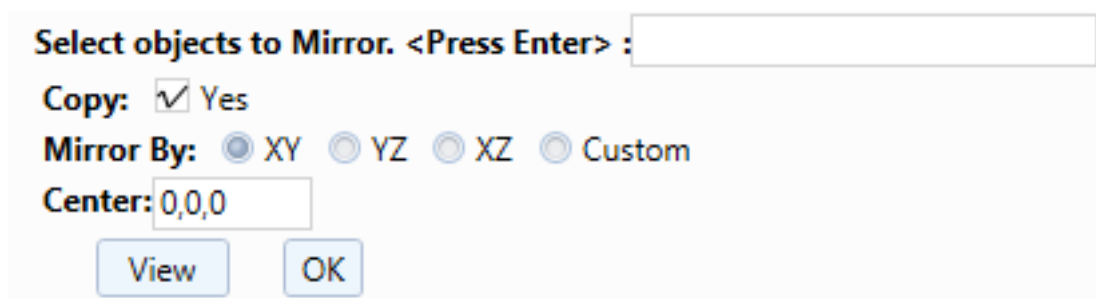


Figure 38: Mirror input

Select the object to be mirrored after activating the function. Press "ENTER" to confirm selection. The selected object will be outlined in red. Check "Copy" will keep the original object.

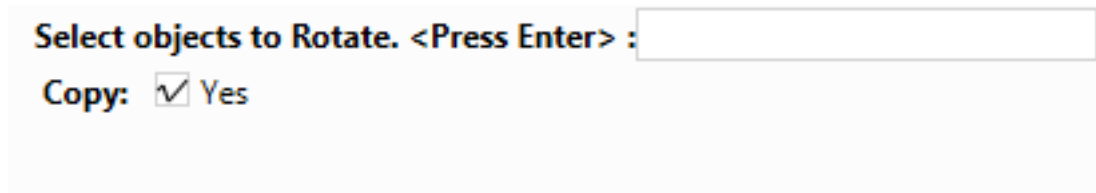
Define the mirror plane. Selecting the respective plane will define the symmetry plane parallel to it. Define the center of mirror by entering the coordinates. The "View" button refresh the preview on screen.

Select "Custom" mirror plane allows user to set the location and orientation of the mirror plane. Check "Show Mirror" to visualise the symmetry plane. The mirror plane will be outlined in green.

Click "Ok" to complete the operation.

### 5.6.5 Rotate

"Rotate" turns it around a fixed point that user designates.



Select objects to Rotate. <Press Enter> :

Copy:  Yes

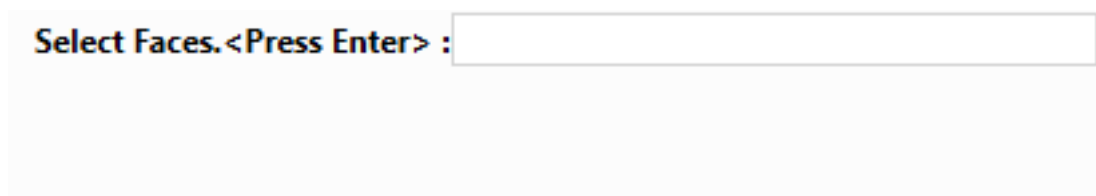
*Figure 39: Rotate input*

Select the object to rotate after activating the function and press "ENTER". Define the point of rotation by selection with mouse or input a coordinate. Define the arm of rotation by specifying a second point. Define angle of rotation and the plane in which this angle lies by specifying a third point. Check "Copy" will keep the original object.

Click "Ok" to complete the operation.

### 5.6.6 Normal Align

This function orientates surfaces normal to a selected curve.



Select Faces. <Press Enter> :

*Figure 40: Normal align input*

Select the surface to align after activating the function and press "ENTER". Next, select the line to which the surface will align and press "ENTER".

If the face contains anchor elements and these elements will need to be aligned together with the face, select the anchor elements together with the face and press "ENTER".

## 5.7 Combine workgroup

Icon	Description
	Groups different objects together. Typically used for ease of selection.
	Turns object into lower level objects by one tier. A solid will degenerate to surfaces and surfaces to closed boundary lines and closed boundary lines to line segments.
	Turns line segments to closed boundary lines. Typically used during loft operation.

### 5.7.1 Stitch

"Stitch" places different surfaces into one object for ease of manipulation.

### 5.7.2 Degenerate

This feature breaks an entity into its components by one order. Thus, a volume degenerates to shell (a collection of surfaces); shell to surfaces; surface to wire (a collection of lines) and wire to lines. "Degenerate" allows recovery of seed objects when an object is erroneously created.

### 5.7.3 Join

This feature connects line segments into a single wire. This operation is typically used before "Loft" operation to join line segments into closed wire.

## 5.8 Mesh workgroup

Icon	Description
	Creates a mesh from surfaces or solids generating faces and volumes in the process.

Icon	Description
	Deletes the mesh from the faces and volumes.
	Creates edge mesh from lines or set divisions to edge boundary of surface and volume mesh.
	Ensures the geometrical objects meet the meshing requirement. This operation is carried out automatically when mesh operation is being carried out. It is provided as a fail-safe measure.

### 5.8.1 Mesh solid settings

The element distribution can be adjusted using 5 global settings: Very coarse, Coarse, Medium, Fine and Very fine. The default setting is medium.

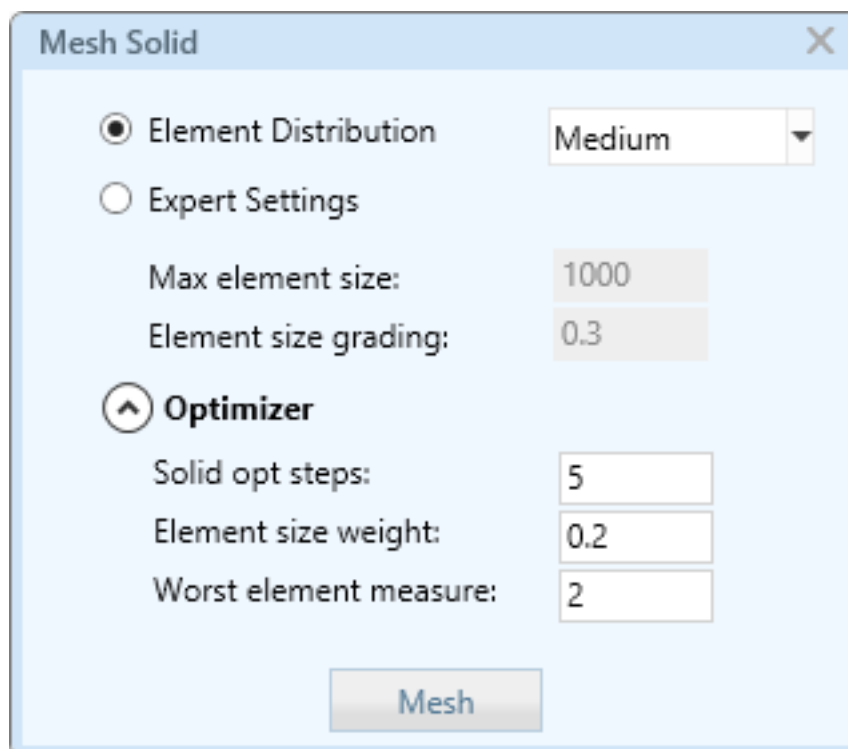


Figure 41: Mesh Solid setting

The maximum element size default value is 1000. This global value refers to the number of minor grid division with respect to the mesh area. All faces will be meshed with this nominal dimension unless local adjustment is done to the edges using the "Mesh Line" function. Select the "Mesh Boundary" option in the "Mesh Line" function to change the mesh edge divisions.

The global element size grading default value is 0.3. This can also be viewed as the element size growth ratio. Reducing this value extends the region in which smaller

elements transition to larger elements. This can help to smooth the mesh in areas of high stress gradients.

Solid mesh is erased using the "Erase Mesh" button (  ).

**Warning:** Do not use the "DELETE" key on the keyboard to erase the mesh!

### 5.8.2 Mesh line setting

The line to be mesh can be a structure or a mesh boundary. While meshing a structure, the nodal compatibility option will be available. If full compatibility is selected, the corresponding nodes on the structural element and the adjacent soil elements will be the same. The number of divisions will follow that of the soil and cannot be specified.

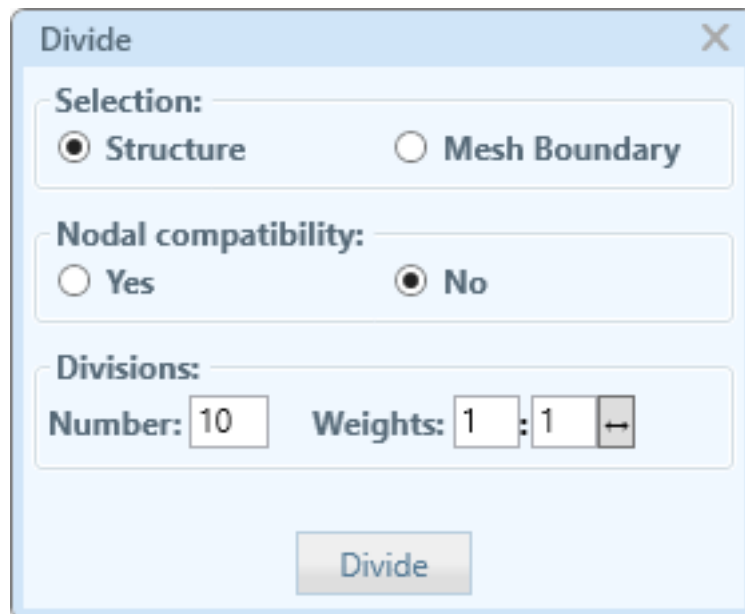


Figure 42: Mesh Line setting

Boundary meshing is carried out if finer or coarser mesh than that generated by global setting is required. Unequal division can be obtained by adjusting the linearly distributed weights of the divisions. The weight ratio reflects the relative division sizes at the distal ends of a line.

This page is intentionally left blank.

# Chapter 6 Material panel

Selecting **Material** on the Workflow panel reveals a set of tools on the Material panel. It consists the following workgroups:

- Elastic
- Elastic Perfectly Plastic
- Critical State
- Special
- Structure

## 6.1 Elastic workgroup

Icon	Description
	Linear variation elastic - not often used in geotechnical analyses as they are only valid where the possibility of yielding and non-linear behaviour can be ruled out.
	Anisotropic elastic - similar to linear variation elastic model. It can also be used for structural members that exhibit stiffness anisotropy where yielding can be ruled out.

## 6.2 Elastic perfectly plastic workgroup

Icon	Description
	Tresca - historically developed for structural rather than geologic material.
	von Mises - similar to Tresca model but with a smooth yield surface.
	Mohr Coulomb - usually restricted to sands and stiff soils which are unlikely to exhibit virgin compression behaviour under the normal range of loading. Available in associated and non-associated flow mode. No tension cut-off.
	Drucker Prager - similar to Mohr Coulomb model but with a smooth yield surface. Only associated flow mode is available. No tension cut-off.

## 6.3 Critical state workgroup

Icon	Description
	Original Cam clay - suitable for soil with $K_0 = 1$ and will often give an overly-stiff behaviour in soft soil after yielding.
	Modified Cam clay - suitable for soft normally consolidated and light over-consolidated clays, to a certain extent, residual soils where non-linearity before yielding is not a real concern since yielding will occur more readily for soft clays.
	Hyperbolic Cam clay - similar to Modified Cam clay but accounts for non-linearity in stress-strain curves before yielding that will make significant difference to ground movement prediction in stiff soil.
	Schofield - formulated to model the Hvorslev surface and tensile cracking behaviour of heavily over-consolidated soils.

## 6.4 Special workgroup

Icon	Description
	User definable constitutive model through a compiled dynamic library (UMOD.DLL).

## 6.5 Structure workgroup

Icon	Description
	3-noded bar element. In 2D, 2 degree-of-freedoms (u, v-displacements) are required in each node. In 3D, 3 degree-of-freedoms (u, v, w-displacements) are required in each node.
	3-noded beam element based on Euler-Bernoulli hypothesis. In 2D, 3 degree-of-freedoms (u, v-displacements and z-rotation) are required in each node. In 3D, 6 degree-of-freedoms (u, v, w-displacements and x, y, z-rotations) are required in each node.

## 6.6 Defining materials

Defining the material involves two steps; create a list material zones and assign the properties to the relevant element entities.

**Modified Cam-Clay** [X]

Name:

Color:

Use As Structural Material

**Model Parameters**

$y_{ref}$	<input type="text" value="0"/>	m
$c_s$	<input type="text" value="0.09"/>	-
$\kappa$	<input type="text" value="0.0451666261179382"/>	-
$c_c$	<input type="text" value="0.8"/>	-
$\lambda$	<input type="text" value="0.347435585522601"/>	-
$p'$	<input type="text" value="50"/>	kN/m <sup>2</sup>
$e_o$	<input type="text" value="1.800"/>	-
$e_{cs}$	<input type="text" value="3.06092054895488"/>	-
$\phi'_{cs}$	<input type="text" value="22.000"/>	°
$M$	<input type="text" value="0.856115336794377"/>	-
$\nu'$	<input type="text" value="0.35"/>	-
$\gamma_w$	<input type="text" value="10"/>	kN/m <sup>3</sup>
$\gamma_{bulk}$	<input type="text" value="15"/>	kN/m <sup>3</sup>
$k_x$	<input type="text" value="1E-08"/>	m/sec
$k_y$	<input type="text" value="5E-09"/>	m/sec

**Insitu-Stress Options**

$OCR_{ref}$	<input type="text" value="1.1"/>	-
$m_{OCR}$	<input type="text" value="0.000"/>	-
$K_D$	<input type="text" value="0.70"/>	-

**Soil Library**

Type:  [v]

Figure 43: Material definition for Mohr Coulomb model

Creating a new material involves selecting a constitutive model for the soil, naming it and specifying values for the various soil parameters associated with that model. A greyed out text box indicates a computed values from related parameters or the value has been specified in a previous stage. Clicking the "OK" button on the material properties dialog window store the input values for subsequent assignment to the soil

or structural element entities. The actual material property values can be defined at any time before solving the analysis.

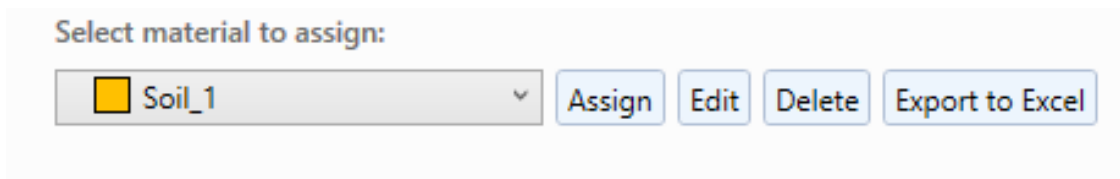


*Figure 44: Material assignment*

Assigning the stored material to the element entities involves selecting the material from the material drop down list defined in the aforementioned step. Select the element entity. Multiple entities can be selected by holding down the "SHIFT" key while clicking successively on the entities. Click on the "Assign" button to apply the properties.

The material properties can be changed by clicking on the "Edit" button. The same material properties dialog window will be called up for editing of the values.

If the material is no longer required, it can be removed by selecting it from the drop down list and clicking the "Delete" button.

The material data can be exported to a Microsoft Excel format database using the "Export to Excel" button. The material database is presented in two Excel Worksheets, one for "Soil", the other for "Structure".

Parameter	Symbol	UOM	Sand Fill	Dredged Clay	Residual Soil	SVI-50	SVI-100	SVI-200
Type		-	Mohr Coulomb	Modified Cam-Clay	Mohr Coulomb	Mohr Coulomb	Mohr Coulomb	Mohr Coulomb
Extra Info		-	NAF	-	NAF	NAF	NAF	NAF
Bulk unit weight	$\gamma_{bulk}$	kN/m <sup>3</sup>	17	15	18	20.5	20.5	21
Unit weight of water	$\gamma_w$	kN/m <sup>3</sup>	10	10	10	10	10	10
Reference depth	$v_{ref}$	m	0	0	0	0	0	0
Young's modulus at $v_{ref}$	$E'_{ref}$	kN/m <sup>2</sup>	8000	-	4050.088	2544.048	4618.651	17739.614
Rate of change of Young's modulus with $d_e$		kN/m <sup>2</sup> /m	0	-	0	0	0	0
Young's modulus in the horizontal plane	$E'_h$	kN/m <sup>2</sup>	-	-	-	-	-	-
Young's modulus in the vertical plane	$E'_v$	kN/m <sup>2</sup>	-	-	-	-	-	-
Poisson ratio	$\nu'$	-	0.3	0.35	0.3	0.3	0.3	0.3
Poisson ratio in the horizontal plane	$\nu'_{hh}$	-	-	-	-	-	-	-
Poisson ratio in the vertical plane	$\nu'_{vh}$	-	-	-	-	-	-	-
Shear modulus in the vertical plane	$G_{sv}$	kN/m <sup>2</sup>	-	-	-	-	-	-
Bulk modulus of water	$K_w$	kN/m <sup>2</sup>	10	10	10	10	10	10
Cohesion at $v_{ref}$	$c'_{ref}$	kN/m <sup>2</sup>	0.01	-	2	0.1	0.1	40
Rate of change of cohesion with depth	$m_c$	kN/m <sup>2</sup> /m	0	-	0	0	0	0
Internal angle of friction	$\phi'$	°	31	-	27	35	32	36
Angle of dilation	$\psi$	°	4	-	4	4	4	4
Slope of swelling line	$\kappa_c$	-	-	0.09	-	-	-	-
Critical state slope of swelling line	$\kappa$	-	-	0.045166626	-	-	-	-
Slope of normal compression line	$\lambda_c$	-	-	0.8	-	-	-	-
Critical state slope of normal compression	$\lambda$	-	-	0.347435586	-	-	-	-
Mean effective stress	$p'$	kN/m <sup>2</sup>	-	50	-	-	-	-
Initial void ratio	$e_0$	-	-	1.8	-	-	-	-
Critical state void ratio	$e_{cs}$	-	-	3.060920549	-	-	-	-
Critical state friction angle	$\phi_{cs}$	°	-	22	-	-	-	-

Figure 45: Material parameters export

## 6.7 Material models and element types

Soil behaviour can be defined using available constitutive soil models. A soil model library is provided for Singapore soil type. The finite element type for the soil will be automatically selected according to the required dimensions, type and intent of analysis.

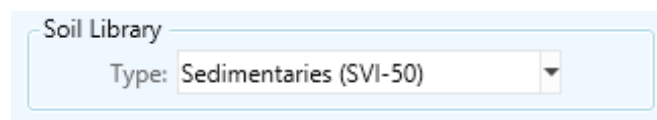


Figure 46: Soil library

Structures are defined using bar, beam and plate element types. Plate element is not available in current version. Structural designation library is provided for common hot-rolled steel sections and steel sheet pile sections. If continuum elements are used for structures, effective stress material properties are required. Elastic, Tresca or von Mises material models are recommended.

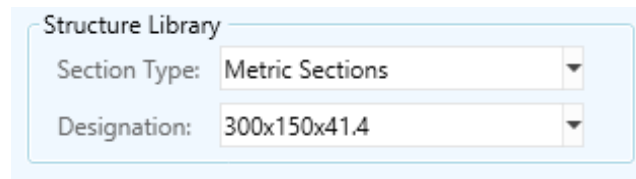


Figure 47: Structure library

Interface elements are not available in the current version.

## 6.8 Constitutive soil models

The constitutive soil models are divided into three major categories and a user definable model. They are:

1. Elastic
  - Linear variation elastic
  - Anisotropic elastic
2. Elastic perfectly plastic
  - Tresca
  - von Mises
  - Mohr Coulomb
  - Drucker Prager
3. Critical states
  - Original Cam clay
  - Modified Cam clay
  - Hyperbolic Cam clay
  - Schofield
4. User definable

### 6.8.1 Coefficient of lateral earth pressure at rest, $K_0$

The horizontal in-situ effective stresses ( $\sigma'_h$ ) were calculated from the vertical effective stresses ( $\sigma'_v$ ) using the relation:

$$\sigma'_h = K_0 \sigma'_v \quad (2)$$

where  $K_0$  is the coefficient of lateral earth pressure at rest.

From elastic theory,

$$K_0 = \frac{\nu}{1 - \nu} \quad (3)$$

where  $\nu$  is the Poisson's ratio.

Experimental evidence does indicate that the coefficient of earth pressure,  $K_0$ , is dependent on the stress history or over-consolidation ratio,  $OCR$ , of the soil. Jaky (1944) empirical relationship is a sufficiently accurate estimate of lateral earth coefficient at rest for most engineering in normally consolidated soil:

$$K_{0,NC} = (1 - \sin\phi_{crit}') \left( \frac{1 + \frac{2}{3} \sin\phi_{crit}'}{1 + \sin\phi_{crit}'} \right) \quad (4)$$

which was simplified to:

$$K_{0,NC} = 1 - \sin\phi'_{tc} \quad (5)$$

where  $\phi_{crit}'$  is the critical state friction angle and  $\phi'_{tc}$  is the effective friction angle from triaxial compression test.

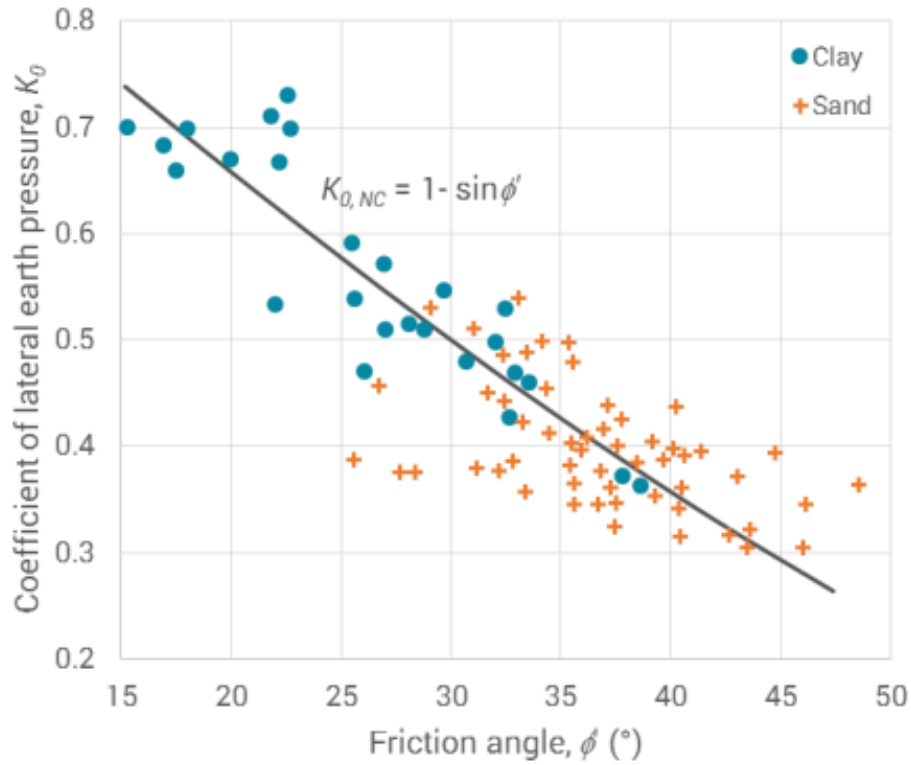


Figure 48: Relationship between  $K_{0,NC}$  and internal angle of friction,  $\phi'$

The relation is valid for cohesive soils but only moderately valid for cohesionless soils. It is often observed that  $K_{0,NC}$  varies with the density condition showing increases with decreasing relative density.

Holtz and Kovacs (1981) suggested a relationship with  $PI$ :

$$K_{0,NC} = 0.44 + 0.42 \frac{PI}{100} \quad (6)$$

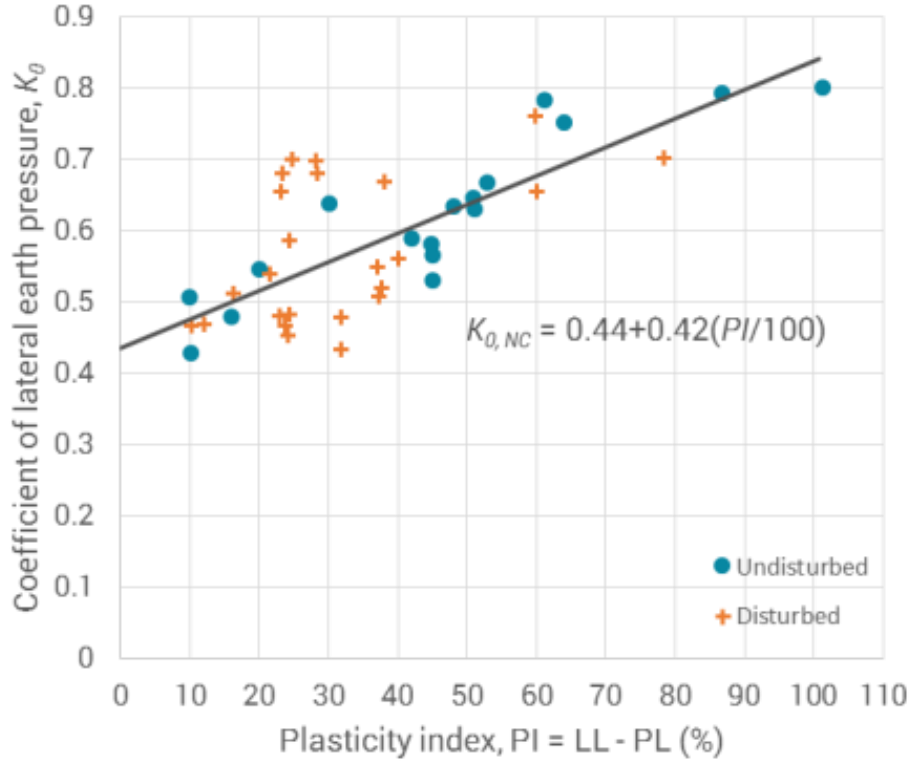


Figure 49: Relationship between  $K_{0,NC}$  and plasticity index,  $PI$

Considering the stress-state for cohesionless soil, Lee et al. (2016) proposed:

$$K_{0,NC} = \left( \frac{1 - \sin \beta \phi_{crit}'}{1 + \sin \beta \phi_{crit}'} \right) \quad (7)$$

where  $\beta = a[D_r(\%)]^b$ ,  $a=0.1$ ,  $b=0.44$  and  $D_r$  is the relative density of cohesionless soil.

From the critical states framework using modified Cam clay, the lateral earth coefficient at rest in normally consolidated soil can be derived as:

$$K_{0,NC} = \frac{1}{2} \left( \frac{3(3 - \sin \phi_{crit}')}{\sqrt{17 \sin^2 \phi_{crit}' - 6 \sin \phi_{crit}' + 9}} - 1 \right) \quad (8)$$

The above relation consistently predicts higher value than Jaky's prediction by approximately 0.15 to 0.18. The original Cam Clay predicts even higher  $K_0$ , in fact, it can be readily shown that the  $K_{0,NC}$  predicted by the original Cam Clay is always equal to 1.0 for a wide range of friction angles. This is clearly unrealistic. The modified Cam Clay is more realistic, but nonetheless still differs from Jaky's rule.

Typical values of the coefficient of lateral earth pressure at rest for various soil types are shown below:

Soil Type	$K_0$
Dense sand	0.35
Loose sand	0.6
Normally consolidated clays	0.5 – 0.6
Lightly over-consolidated clays	1.0
Heavily over-consolidated clays	3.0

### 6.8.2 Over-consolidation ratio, $OCR$

Since both isotropic compression data from triaxial tests and one-dimensional data from oedometer tests are required for parameter determination, the definition of over-consolidation ratio ( $OCR$ ) for each type of tests should be clearly defined. The definition of  $OCR$  is important for Cam clay models which are formulated using the isotropic stress state as a reference point. On the other hand, most of the laboratory tests relating to consolidation are one-dimensional compression tests.

The preconsolidation pressure ( $p'_0$ ) is the maximum effective vertical overburden stress that a particular soil sample has sustained in the past. The ratio of the preconsolidation pressure to current mean effective stress ( $p'$ ) is known as the over-consolidation ratio ( $OCR$ ):

$$OCR = \frac{p'_0}{p'} \quad (9)$$

However under one-dimensional oedometer tests, the over-consolidation ratio is defined as:

$$OCR_{oedo} = \frac{\sigma_{v0}'}{\sigma_v'} \quad (10)$$

In firm to stiff clays which are not highly sensitive nor structured, the approximation to apparent preconsolidation stress ( $\sigma'_p$ ) proposed by Kulhawy & Mayne (1990) is:

$$\sigma'_p \approx 0.47N_{60} \cdot p_{atm} \quad (11)$$

where  $p_{atm} = 1 \text{ atmosphere} = 1 \text{ bar} = 100 \text{ kPa}$

In clean sands,  $\sigma'_p$  can be estimated from the relationship modified in generalized form (Mayne, 1992):

$$\sigma'_p \approx 0.47(N_{60})^m \cdot p_{atm} \quad (12)$$

where  $m = 0.6$  for clean quartzitic sands,  $0.8$  for silty sands to sandy silts, and  $m = 1.0$  for intact "vanilla" clays to clayey silts. Assuming  $\sigma'_p = \sigma'_{v0}$ , the generalized form derived by Mayne (1992) can be re-cast in terms of  $OCR$  as follows:

$$OCR \approx \frac{0.47(N_{60})^m \cdot p_{atm}}{\sigma'_v} \quad (13)$$

Based on statistical analysis of laboratory consolidation test data by Stas and Kulhawy (1984) on clays with sensitivity 1 to 10,  $OCR$  can be estimated from liquidity index,  $LI(\%)$ :

$$OCR = \left(\frac{p_{atm}}{\sigma'_v}\right) \times 10^{(1.11 - \frac{1.62LI}{100})} \quad (14)$$

Schmidt (1966) determined a simple expression from plotting, against over-consolidation ratio in primary unloading condition. He also proposed that an exponent related to the effective angle of friction, be assigned to:

$$K_0 = K_{0,NC} \cdot OCR^{1.2 \sin \phi'_{crit}} \quad (15)$$

Mayne and Kulhawy (1982) suggested that, for granular materials:

$$K_0 = K_{0,NC} \cdot OCR^{\sin \phi'_{tc}} \quad (16)$$

where  $\phi'_{crit}$  is the critical state friction angle and  $\phi'_{tc}$  is the effective friction angle from triaxial compression test.

Material properties e.g. Young's modulus ( $E$ ), cohesion ( $c$ ) and over-consolidation ratio ( $OCR$ ) can vary with depth ( $y$ ) in some models. The reference elevation ( $y_{ref}$ ) is the same for all varying properties in the model. Specifying zero for the rate of change ( $m_{E/c/OCR}$ ) for a property will enforce constant value for that property.

The convention used for specifying these properties are as follows:

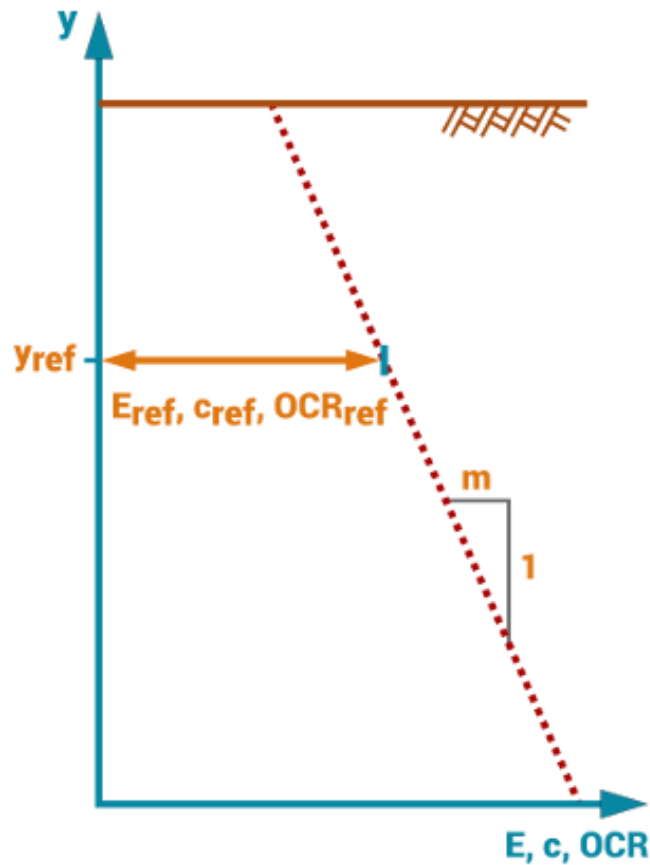


Figure 50: Variation of material properties with depth

$$E = E_{ref} + m_E(y_{ref} - y) \quad (17)$$

$$c = c_{ref} + m_c(y_{ref} - y) \quad (18)$$

$$OCR = OCR_{ref} + m_{OCR}(y_{ref} - y) \quad (19)$$

## 6.9 Elastic

The models obey Hooke's law that describes a linear relationship between stress and strain. This law is commonly stated as a relationship between force,  $F$  and corresponding extension displacement,  $x$ . It can also be stated as a relationship between stress and strain:

$$\sigma = \varepsilon E \quad (20)$$

where  $E$  is known as Young's modulus.

For homogeneous isotropic materials, simple relations exist between elastic constants (Young's modulus  $E$ , shear modulus  $G$ , bulk modulus  $K$ , and Poisson's ratio  $\nu$  that allow calculating them all as long as two are known:

$$E = 2G(1 + \nu) = 3K(1 - 2\nu) \quad (21)$$

Most elastic materials exhibit linear elasticity for a small amount of deformations.

### Poisson's ratio, $\nu$

Poisson's ratio ( $\nu$ ) gives the ratio of elastic horizontal strain to vertical strain. It is required to describe the elastic response of the soil. Values of Poisson's ratio are typically arbitrarily selected and often assume. Wroth (1975) indicates some dependence of Poisson's ratio on the plasticity index ( $PI$ ). In addition to classification,  $PI$  is an important property that affects geo-material behaviour, such as swelling/shrinkage potential, permeability and strength.

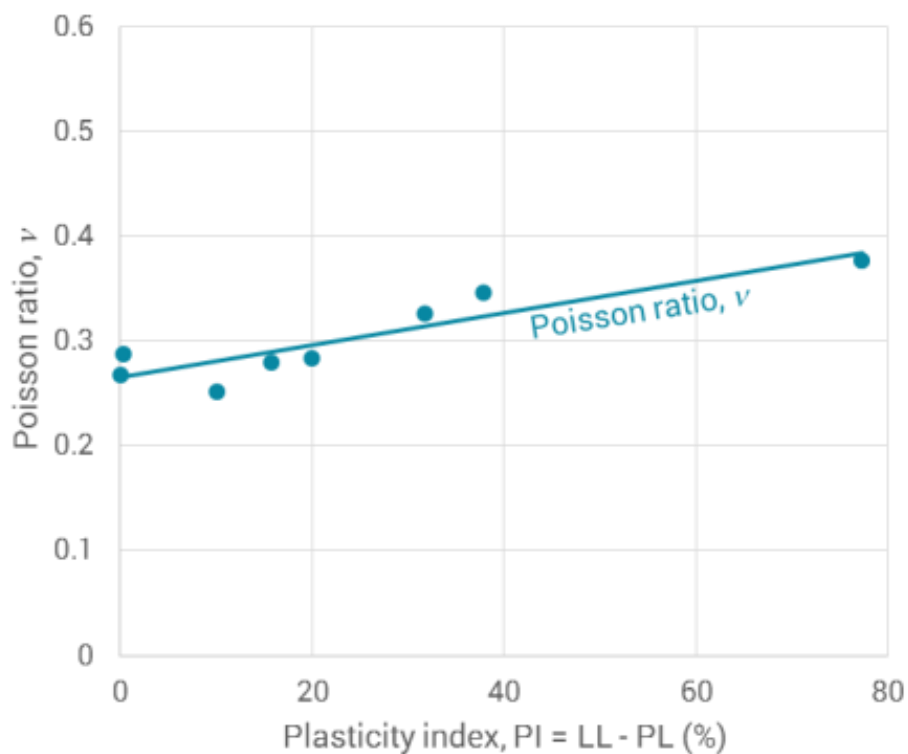


Figure 51: Relationship between Poisson's ratio and plasticity index

The relationship between effective Poisson's ratio ( $\nu'$ ) and plasticity index  $PI(\%)$  can be approximated with the following best-fit equation:

$$\nu' = 0.0015PI + 0.2654 \quad (22)$$

Kulhawy and Mayne (1990) suggested that the drained Poisson's ratio of cohesionless soil can be estimated from:

$$\nu' = 0.1 + 0.3 \left( \frac{\phi' - 25^\circ}{45^\circ - 25^\circ} \right) \quad \phi' < 45^\circ \quad (23)$$

### Young's modulus, $E$

Young's modulus ( $E$ ) is a parameter used as a measure of soil stiffness. It is required in determining deformations. In cohesionless soil,  $E$  can be derived through standard penetration test (SPT) data. Kulhawy and Mayne (1990) suggested that for normally consolidated clean sands:

$$\frac{E'}{p_{atm}} \approx 10N_{60} \quad (24)$$

and for sands with fines:

$$\frac{E'}{p_{atm}} \approx 5N_{60} \quad (25)$$

where  $p_{atm} = 1 \text{ atmosphere} = 1 \text{ bar} = 100 \text{ kPa}$

The  $N$ -values obtained from the field shall be corrected before they are used in design so that they are consistent with the correlation being used. If energy efficiency ( $E_f$ ) is measured, then the energy-corrected SPT  $N$ -value adjusted to 60% efficiency ( $N_{60}$ ) is given by:

$$N_{60} = \frac{E_f}{60} N_{measured} \quad (26)$$

where  $N_{measured}$  is the  $N$ -value measured in the field during the test.

The possible ranges of correction for  $N_{60}$  (Skempton, 1986) are:

<b>Equipment Variable</b>	<b>Correction (<math>\frac{E_f}{60}</math>)</b>
<b>Donut Hammer</b>	0.5 to 1.0
<b>Safety Hammer</b>	0.7 to 1.2
<b>Automatic Hammer</b>	0.8 to 1.5

Theoretically, it is mandatory to measure  $E_f$  to get the proper correction to  $N_{60}$ . Typically,  $E_f=60$  for rope and cathead systems, i.e., donut and safety hammers and  $E_f=80$  for automatic hammer systems.

An empirical correlation relating plasticity index,  $PI(\%)$ , and overconsolidation ratio,  $OCR$ , to an elastic stiffness provided by Duncan and Buchignani (1976) allows the range of  $E_u/c_u$  or  $G/c_u$  to be estimated. The  $E_u$  in this ratio represents the undrained secant modulus.

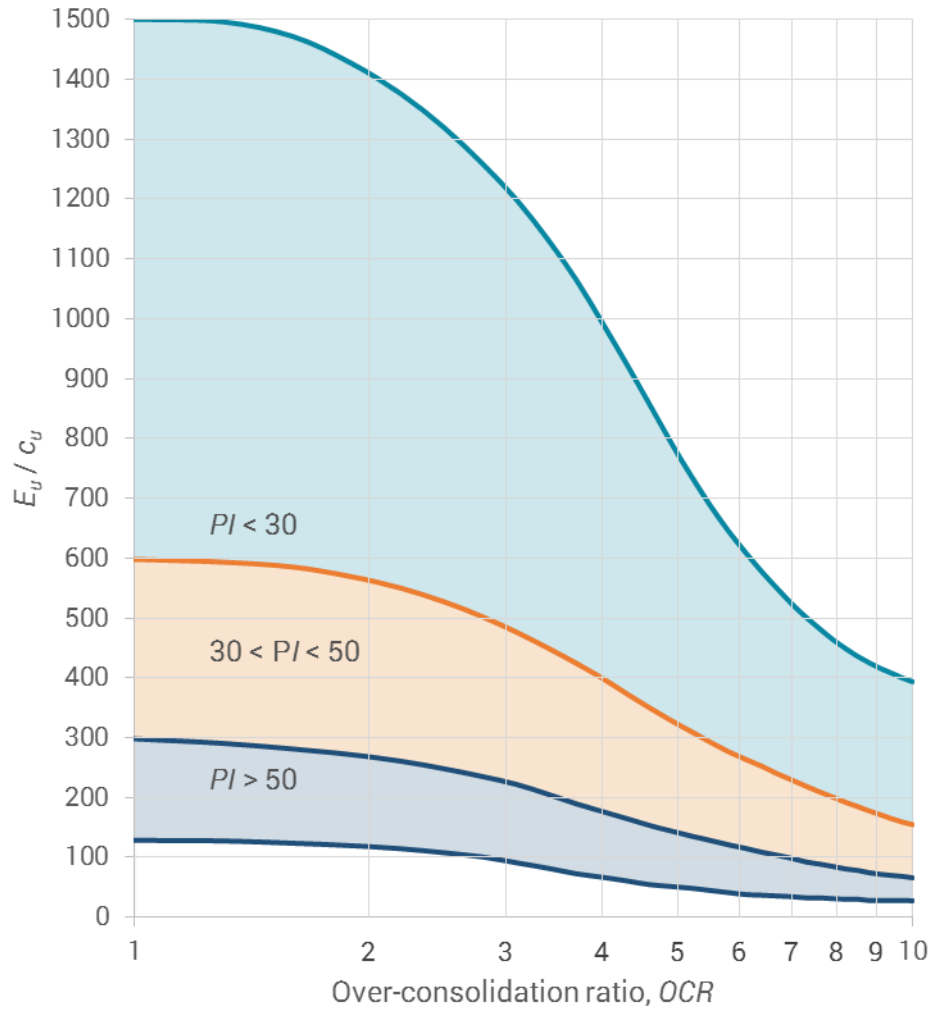


Figure 52: Relationship between plasticity index and over-consolidation ratio with soil stiffness

Kulhawy and Mayne (1990) suggested a relationship for the undrained initial tangent modulus ratio based on more fundamental soil properties:

$$\frac{E_u}{c_u} = \frac{64M(1 + e_0)[1 + \ln OCR]}{c_c OCR^\Lambda} \quad (27)$$

where  $M$  is the critical state frictional constant,  $e_0$  is the initial void ratio,  $c_c$  is the slopes of compression line and  $\Lambda (= \frac{\lambda - \kappa}{\lambda}) \approx 0.8$ . The symbol  $\Lambda$  represents the plastic volumetric strain ratio, being the ratio of the plastic to the total component of the volumetric strain increment in normal consolidation.

## Permeability, $k$

Estimates of the in-situ permeability should be made using in-situ permeability tests. The correlations proposed below should only be used when in-situ permeability test data are unavailable.

In-situ vertical permeability,  $k_v$  (m/s), for clays can be estimated using plasticity index,  $PI(\%)$ , clay fraction,  $CF(\%)$ , and void ratio,  $e$ , as suggested by Tavenas et al. (1983):

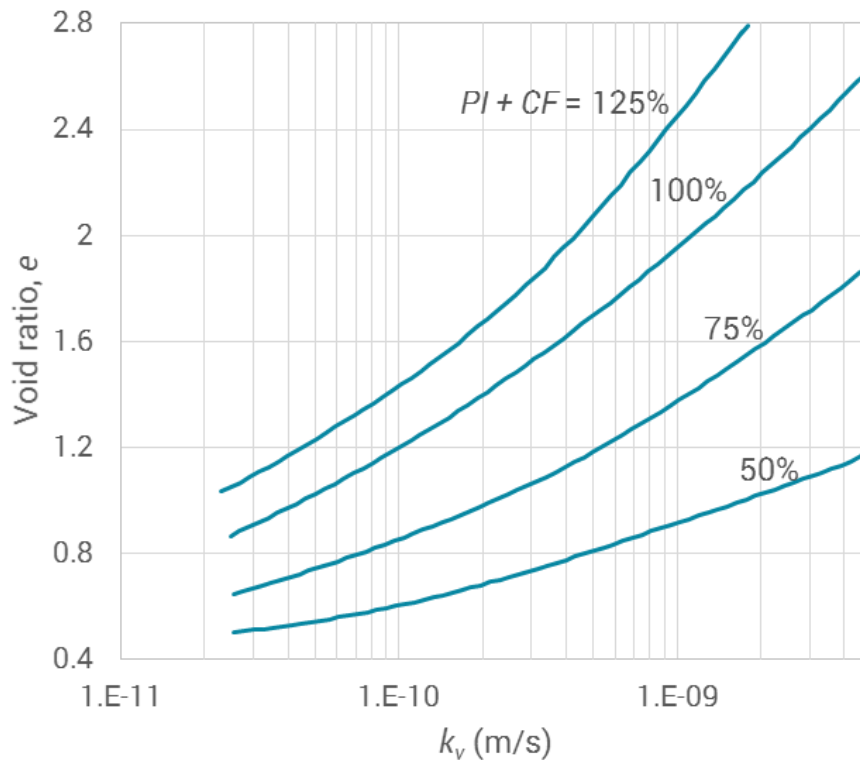


Figure 53: Relationship between plasticity index, clay fraction, void ratio and vertical permeability

An approximate relationship between plasticity index, clay fraction, void ratio and vertical permeability derived from power function fitting is as follow:

$$k_v \text{ (m/s)} = \sqrt[0.17203]{\frac{1.5612 \times e^{0.91011}}{(PI + CF)}} \quad (28)$$

Permeability,  $k$  (m/s), for non-swelling or limited swelling clays can be estimated using plasticity index,  $PI(\%)$  suggested by Dolinar and Škrabl (2013):

$$k \text{ (m/s)} = \frac{6.31 \times 10^{-7}}{(PI - 8.74)^{3.03}} e^{2.66} (PI - 8.74)^{0.234} \quad (29)$$

where  $e$  is the void ratio.

The external specific surface area and the clay minerals content for non-swelling or limited swelling clays can be expressed in terms of  $PI$ .

The permeability of soil can also be estimated from one-dimensional consolidation parameters:

$$k_v = m_v c_v \gamma_w \quad (30)$$

where  $k_v$  is the vertical coefficient of permeability;  $m_v$  is the vertical coefficient of compressibility;  $c_v$  is the vertical coefficient of consolidation and  $\gamma_w$  is the unit weight of water.

**Tips:** It should be noted that the field permeability may be up to fifty times higher than the measured laboratory values (Poulos et al., 1989; Balasubramanian et al., 1989).

In cohesionless soil, the Kozeny-Carman relationship (Carman, 1956) can be used. The coefficient of permeability or Darcy's permeability,  $k$ , is given by:

$$k \text{ (m/s)} = 8.3 \times 10^{-3} \times \left( \frac{\rho_w g}{\mu} \right) \left[ \frac{e^3}{1 + e} \right] D_{10}^2 \quad (31)$$

where  $\rho_w$  = density of water ( $kg/m^3$ ),  $g$  = acceleration due to gravity ( $m/s^2$ ),  $\mu$  = dynamic viscosity coefficient of water ( $Ns/m^2$ ),  $e$  = void ratio and  $D_{10}$  = particle size for which 10% of the material is finer ( $m$ ),  $0.0005m \leq D_{10} \leq 0.004m$ . The dynamic viscosity of water in relation to temperature is:

$$\mu \text{ (Ns/m}^2\text{)} = 2.414 \times 10^{-5} \times 10^{\left( \frac{247.8}{133.15 + T} \right)} \quad (32)$$

where  $T$  is temperature in  $^{\circ}C$ .

Density of water,  $\rho_w$ , at  $10^{\circ}C$  and  $20^{\circ}C$  are  $999.75 \text{ kg/m}^3$  and  $998.21 \text{ kg/m}^3$  respectively. Dynamic viscosities,  $\mu$ , at  $10^{\circ}C$  and  $20^{\circ}C$  are  $1.307 \times 10^{-3} \text{ Ns/m}^2$  and  $1.002 \times 10^{-3} \text{ Ns/m}^2$  respectively.

### 6.9.1 Linear variation elastic

This model is sometimes referred to as ‘Gibson soil’ where increasing confining pressure (with depth) often leads to a linearly increasing stiffness with depth.

The material parameters required are:

Parameter	Definition
$y_{ref}$	reference elevation
$E_{ref}$	reference Young's modulus
$m_E$	Young's modulus rate of change with depth
$\nu$	Poisson's ratio
$K_w$	bulk modulus of water (0 for drained material)
$\gamma_w$	unit weight of water
$\gamma_{bulk}$	bulk unit weight of soil
$k_x$	permeability in $x$ direction
$k_y$	permeability in $y$ direction
$K_0$	lateral earth pressure coefficient

The unit weight of water ( $\gamma_w$ ) is typically assumed to be  $10 \text{ kN/m}^3$ . The bulk unit weight ( $\gamma_{bulk}$ ) is simply defined as the weight per unit volume of soil.

### 6.9.2 Anisotropic elastic

This is an elastic model which allows for cross anisotropic behaviour. For simple cross anisotropy in a 3-dimensional space, Young's modulus in the horizontal directions is the same. Since the  $x$  and  $z$  directions are horizontal directions, the subscript  $h$  can be used in place of  $x$  and  $z$ . Similarly, the subscript  $v$  (for vertical) can be used in place of  $y$ . The relationships between Young's moduli, shear moduli and Poisson's ratios are as follows:

$$E_x = E_z \quad (33)$$

$$\nu_{xz} = \nu_{zx} \quad (34)$$

$$\nu_{yz} = \nu_{yx} \quad (35)$$

$$\nu_{zy} = \nu_{xy} \quad (36)$$

$$G_{zy} = G_{xy} = G_{hv} \quad (37)$$

$$\frac{\nu_{zy}}{E_z} = \frac{\nu_{yz}}{E_y} = \frac{\nu_{xy}}{E_x} = \frac{\nu_{yx}}{E_y} \quad (38)$$

$$\therefore \frac{\nu_{hv}}{E_h} = \frac{\nu_{vh}}{E_v} \quad (39)$$

$$G_{zx} = \frac{E_z}{2(1 + \nu_{zx})} \quad (40)$$

$$\therefore G_{hh} = \frac{E_h}{2(1 + \nu_{hh})} \quad (41)$$

The material parameters required are:

Parameter	Definition
$E_h$	Young's modulus in the horizontal plane
$E_v$	Young's modulus in the vertical plane
$\nu_h$	Poisson's ratio in the horizontal plane
$\nu_v$	Poisson's ratio in the vertical plane
$G_h$	shear modulus in the vertical plane
$K_w$	bulk modulus of water (0 for drained material)
$\gamma_w$	unit weight of water
$\gamma_{bulk}$	bulk unit weight of soil
$k_x$	permeability in $x$ direction
$k_y$	permeability in $y$ direction
$K_0$	lateral earth pressure coefficient

## 6.10 Elastic perfectly plastic

The elastic perfectly plastic models provide a means of imposing limiting shear stress on what would otherwise be an elastic response. There is no hardening or softening of the yield surface during plastic yielding. Non-homogeneity of elastic stiffness and

strength is allowed, with both quantities being permitted to vary linearly with depth. Full isotropy of stiffness and strength are enforced.

### 6.10.1 Tresca

The Tresca model is a maximum shear stress (single shear) criterion that assumes that the material is frictionless. The yield criterion is:

$$\max\left(\frac{|\sigma_1 - \sigma_2|}{2}, \frac{|\sigma_2 - \sigma_3|}{2}, \frac{|\sigma_3 - \sigma_1|}{2}\right) = c_u \quad (42)$$

where  $c$  is the yield stress of the material determined from the pure shear test and  $\sigma_1$ ,  $\sigma_2$  and  $\sigma_3$ , are the major, minor or intermediate principal stresses.

The yield surface represents a prismatic surface, the cross section of which is a regular hexagon. The prism is centred on the hydrostatic axis, the line on which all three principal stresses are equal. The yield strength of which is insensitive to the hydrostatic pressure thus limiting its use to situations of loading of fully saturated soil (clays) using a total stress approach.

Cohesion (total stress),  $c_u$

Skempton's correlation (Skempton, 1954 and 1957) for the vane shear strength of normally consolidated soils as a function of plasticity index is often used:

$$\frac{c_u}{\sigma_v'} = 0.11 + 0.37\left(\frac{PI}{100}\right) \quad (43)$$

where  $\sigma_v'$  is the in situ vertical effective stress and  $PI$  is the plasticity index.

From the definition of :

$$K_0 = \frac{\sigma'_h}{\sigma'_v} \quad (44)$$

and  $p'$ :

$$p' = \frac{\sigma_v'(1 + 2K_0)}{3} \quad (45)$$

$$\frac{c_u}{p'} = \frac{0.33 + 1.11\left(\frac{PI}{100}\right)}{1 + 2K_0} \quad (46)$$

Taking a  $PI(\%) = 39$ , results in a commonly used relationship,

$$\frac{c_u}{\sigma_v'} = 0.11 + 0.37\left(\frac{39}{100}\right) = 0.254 \quad (47)$$

Variation of  $c_u$  with depth can also be estimated from SPT blow counts. Stroud (1974) gives a chart for the plasticity index influences on  $c_u/N_{60}$  for stiff clays which can be fitted with the following relationship by Vardanega and Bolton (2011):

$$\frac{c_u}{N_{60}} = 10PI^{-0.22} \quad (kN/m^2) \quad (48)$$

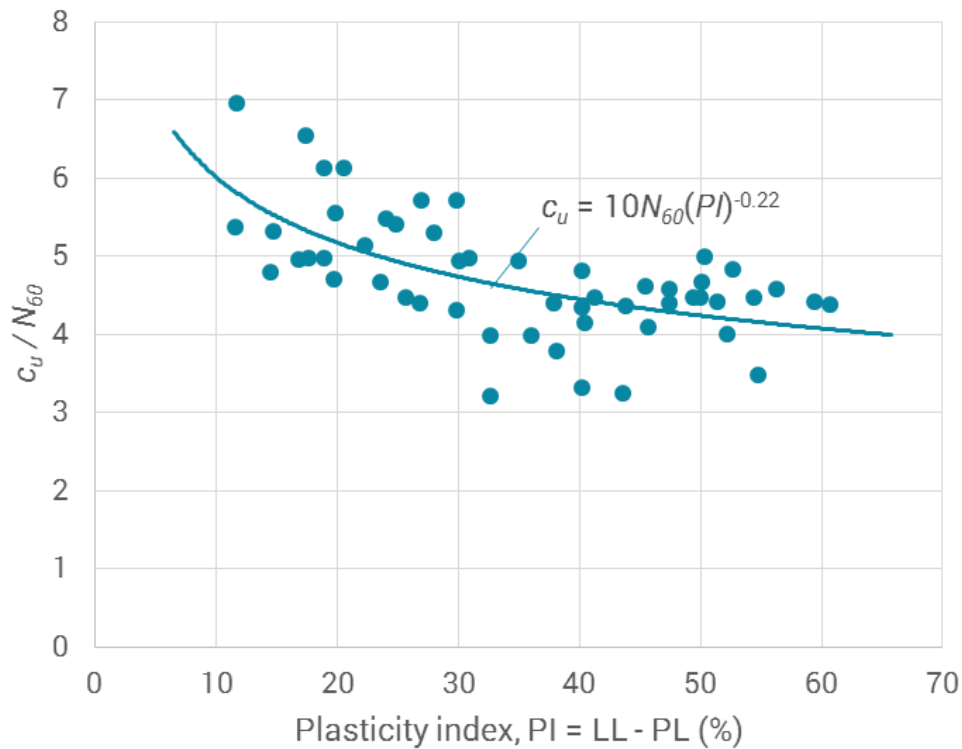


Figure 54: Relationship between plasticity index with soil stiffness

Taking a  $PI(\%) = 23$ , results in a commonly used relationship,

$$c_u = 10N_{60}(23)^{-0.22} = 5.0N_{60} \quad (kN/m^2) \quad (49)$$

Over-consolidation ratio has a significant effect on undrained shear strength. Ladd et al. (1977) on empirical grounds and Muir Wood (1990) additionally from theoretical relations based on critical state soil mechanics both show:

$$\frac{c_u}{\sigma_v'} = \left(\frac{c_u}{\sigma_v'}\right)_{NC} OCR^\Lambda \quad (50)$$

where  $\sigma_v'$  is the in situ vertical effective stress, subscript *NC* indicates normal consolidation, *OCR* is the over-consolidation ratio, and  $\Lambda (= \frac{\lambda - \kappa}{\lambda})$  varies from 0.85 to 0.75 as *OCR* increases.

The material parameters required are:

Parameter	Definition
$y_{ref}$	reference elevation
$E_{ref}$	reference Young's modulus
$m_E$	Young's modulus rate of change with depth
$c_{ref}$	reference cohesion
$m_c$	cohesion rate of change with depth
$\nu$	Poisson's ratio
$K_w$	bulk modulus of water (0 for drained material)
$\gamma_w$	unit weight of water
$\gamma_{bulk}$	bulk unit weight of soil
$k_x$	permeability in <i>x</i> direction
$k_y$	permeability in <i>y</i> direction
$OCR_{ref}$	over-consolidation ratio
$m_{ocr}$	increment rate of <i>OCR</i> with depth
$K_0$	lateral earth pressure coefficient

### 6.10.2 von Mises

The von Mises model is an octahedral shear stress yield criterion that is based on a critical value of the distortional energy stored in an isotropic material. This yield criterion is suitable for total stress analyses similar to the Tresca model.

$$\frac{1}{2} [(\sigma_1 - \sigma_2)^2 + (\sigma_2 - \sigma_3)^2 + (\sigma_3 - \sigma_1)^2] = (2c_u)^2 \quad (51)$$

where  $2c_u$  is the yield stress in uniaxial tension.

The material parameters required are:

Parameter	Definition
$y_{ref}$	reference elevation
$E_{ref}$	reference Young's modulus
$m_E$	Young's modulus rate of change with depth
$c_{ref}$	reference cohesion
$m_c$	cohesion rate of change with depth
$\nu$	Poisson's ratio
$K_w$	bulk modulus of water (0 for drained material)
$\gamma_w$	unit weight of water
$\gamma_{bulk}$	bulk unit weight of soil
$k_x$	permeability in $x$ direction
$k_y$	permeability in $y$ direction
$OCR_{ref}$	over-consolidation ratio
$m_{ocr}$	increment rate of $OCR$ with depth
$K_0$	lateral earth pressure coefficient

### 6.10.3 Mohr Coulomb

This yield criterion is commonly used for modelling soil. The Mohr-Coulomb yield criterion can be written as the equation for the line that represents the yield envelope. The general equation is:

$$\tau = c + \sigma' \tan \phi' \quad (52)$$

where  $\tau$  is the shear stress on the yield envelope,  $c$  is the apparent cohesion,  $\sigma'$  is the normal effective stress on the yield envelope and  $\phi'$  is the internal angle of friction.

In 3-dimensional stress space, the yield criterion describes an irregular hexagonal pyramid.

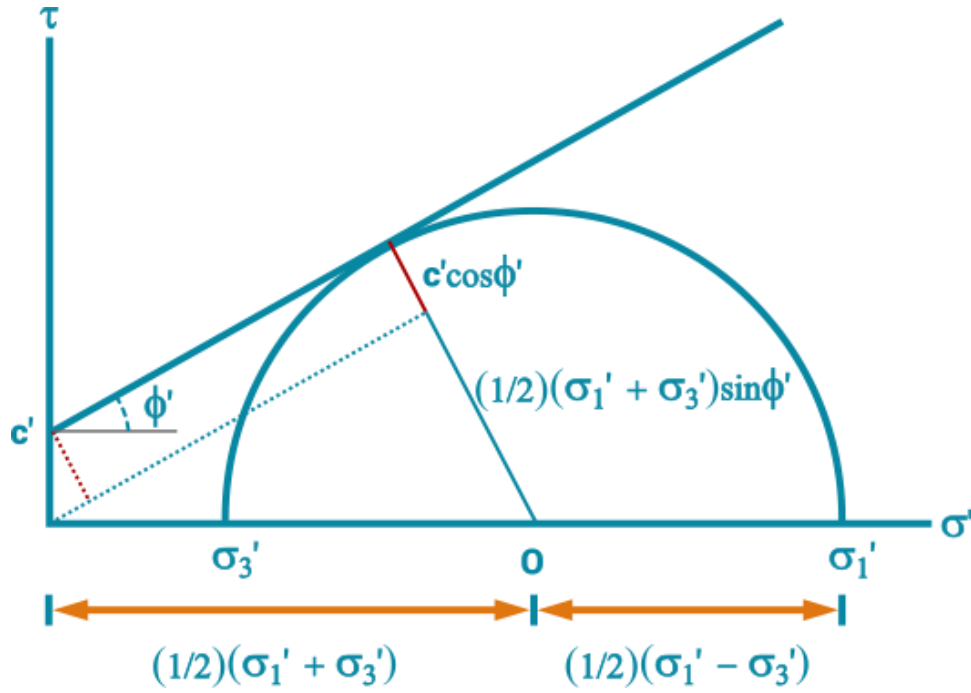


Figure 55: Relationship between principal stresses and friction angle in Mohr Coulomb

The failure criterion can be expressed in terms of the relationship between the principal stresses. From the geometry of the Mohr circle:

$$\left(\frac{\sigma_1' - \sigma_3'}{2}\right) = \left(\frac{\sigma_1' + \sigma_3'}{2}\right)\sin\phi' + c'\cos\phi' \quad (53)$$

Alternatively, the relationship can be written in term of stress invariants  $p'$  (mean effective stress) and  $q$  (deviator stress) as:

$$\left[\frac{1}{\sqrt{3}\cos\phi'}\sin\left(\theta + \frac{\pi}{3}\right) - \frac{1}{3}\tan\phi'\cos\left(\theta + \frac{\pi}{3}\right)\right]q - p'\tan\phi' = c' \quad (54)$$

where  $\theta$  is the lode angle (positive cosine convention) where triaxial compression and extension correspond to  $\pi/3$  and 0 respectively.

### Cohesion (effective stress), $c'$

The effective cohesion can be derived from its undrained counterpart and the Mohr Coulomb criterion by assuming  $\sigma_1' = \sigma_v'$  and  $\sigma_3' = \sigma_h'$ .

$$\left(\frac{\sigma_1' - \sigma_3'}{2}\right) = c_u = \sin\phi' \left[\left(\frac{\sigma_v' + \sigma_h'}{2}\right) + c'\cot\phi'\right] \quad (55)$$

$$c' = \left[ \frac{c_u}{\cos\phi'} - \left( \frac{\sigma_v' + \sigma_h'}{2} \right) \tan\phi' \right] \quad (56)$$

Expressing the effective cohesion in terms of  $c_u$ ,  $p'$  and  $K_0$ :

$$c' = \left[ \frac{c_u}{\cos\phi'} - \frac{3(1 + K_0)p'}{2(1 + 2K_0)} \tan\phi' \right] \quad (57)$$

The value of undrained shear strength is greatly affected by the amount of water in the soil. In the case where the tested soil is not fully saturated, the value will not be representative and will greatly decrease upon saturation of the soil. Using the lower  $c_u$  may result in a negative  $c'$ .

### Internal friction angle, $\phi'$

The following chart will demonstrate the relationship between plasticity index,  $PI(\%)$ , and internal friction angle for cohesive soil.

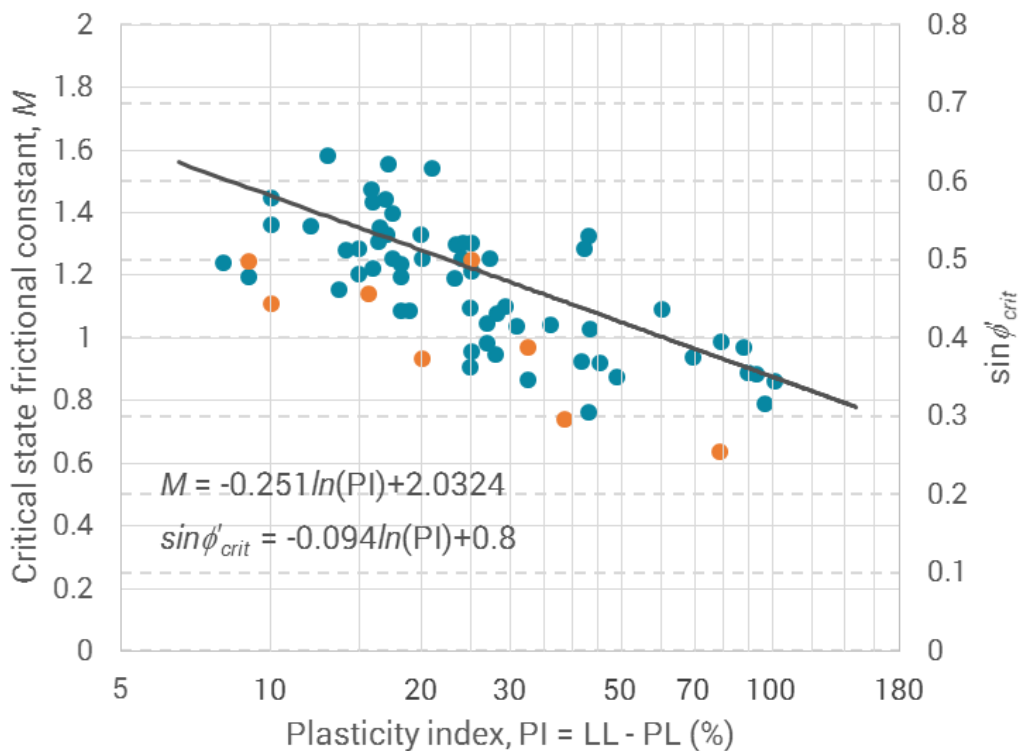


Figure 56: Relationship between plasticity index and internal friction angle

The effective internal friction angle of cohesionless soil can be derived from the relationship proposed by Hatanaka and Uchida (1996):

$$\phi' = 20^\circ + \sqrt{15.4(N_1)_{60}} \quad 3.5 \leq (N_1)_{60} \leq 30 \quad (58)$$

where  $(N_1)_{60} = N_{60} \sqrt{\frac{p_{atm}}{\sigma_{v'}}$  and  $p_{atm} = 1 \text{ atmosphere} = 1 \text{ bar} = 100 \text{ kPa}$

The dependence of the internal friction angle on the effective overburden pressure is indirectly accounted for by the correction factor,  $N_1$  proposed by Liao and Whitman (1986).

In the absence of reliable laboratory test data, the conservative values of  $\phi'_{crit}$  for clay soils given in BS 8002 (BSI, 2015) may be used, with  $c' = 0 \text{ kPa}$ .

Plasticity index (%)	$\phi'_{CRIT}$ (°)
15	30
30	25
50	20
80	15

The peak and critical state angles of shearing resistance for siliceous sands and gravels may be estimated from the following equations from BS 8002 (BSI, 2015):

The estimated peak effective angle of shearing resistance is given by:

$$\phi'_{max} = 30^\circ + A + B + C \quad (59)$$

The estimated critical state angle of shearing resistance is given by:

$$\phi'_{crit} = 30^\circ + A + B \quad (60)$$

The values of:

$A$  = angularity of the particles

$B$  = grading of the sand/gravel

$C$  = results of standard penetration test

<b>A-Angularity</b>	<b>(°)</b>
<b>Rounded</b>	0
<b>Sub-angular</b>	2
<b>Angular</b>	4

Angularity is estimated from visual description of soil.

<b>B-Grading of soil</b>	<b>(°)</b>
<b>Uniform</b>	0
<b>Moderate grading</b>	2
<b>Well graded</b>	4

Grading can be determined from grading curve by use of uniformity coefficient,  $\frac{D_{60}}{D_{10}}$  where  $D_{10}$  and  $D_{60}$  are particle sizes such that in the sample, 10% of the material is finer than  $D_{10}$  and 60% is finer than  $D_{60}$ .

<b>Grading</b>	<b>Uniformity coefficient</b>
<b>Uniform</b>	<2
<b>Moderate grading</b>	2 to 6
<b>Well graded</b>	6

A step-graded soil should be treated as uniform or moderately graded soil according to the grading of the finer fraction.

<b>C-N' (blows/305mm)</b>	<b>(°)</b>
<b>&lt; 10</b>	0
<b>20</b>	2
<b>40</b>	6
<b>60</b>	9

$N'$  from results of standard penetration test shall be modified where necessary using the following equation that approximates the figure in BS 8002 (BSI, 2015) for the derivation of  $N'$  from  $N$ .

$$\frac{N'}{N} = 1.26 - 0.94 \ln\left(\frac{\sigma_v'}{p_{atm}}\right) \quad 1.0 \leq \frac{N'}{N} \leq 3.0 \quad (61)$$

where  $p_{atm} = 1 \text{ atmosphere} = 1 \text{ bar} = 100 \text{ kPa}$

The following indicative values of the effective angle of friction in BS 8002 (BSI, 2015) relate to rocks which can be treated conservatively as composed of granular fragments, i.e. they are closely and randomly jointed or otherwise fractured, having an RQD (rock quality designation) value close to zero.

Stratum	$\phi'_{CRIT}$ (°)
Chalk	35
Clayey marl	28
Sandy marl	33
Weak sandstone	42
Weak siltstone	35
Weak mudstone	28

The presence of a preferred orientation of joints, bedding or cleavage in a direction near that of a possible failure plane may require a reduction in the above values, especially if the discontinuities are filled with weaker materials.

### External friction angle, $\delta$

Where the external friction angle,  $\delta$ , is required for the modeling of interface material, the following relation can be used:

$$\delta = [0.67\phi', 0.93\phi'] \quad (62)$$

Values of the external friction angle,  $\delta$ , for different interfaces according to the NAVFAC (1986):

Interface material	External Friction Angle $\delta$ (°)
<b><i>Mass concrete on the following foundation materials:</i></b>	
Clean sound rock	35
Clean gravel, gravel-sand mixtures, coarse sand	29 - 31

<b>Interface material</b>	<b>External Friction Angle <math>\delta</math> (°)</b>
Clean fine to medium sand, silty medium to coarse sand, silty or clayey gravel	24 - 29
Clean fine sand, silty or clayey fine to medium sand	19 - 24
Fine sandy silt, non-plastic silt	17 - 19
Very stiff and hard residual or preconsolidated clay	22 - 27
Medium stiff and stiff clay and silty clay	17 - 19
<b><i>Steel sheet piles against the following soils:</i></b>	
Clean gravel, gravel-sand mixtures, well-graded rock fill with spalls	22
Clean sand, silty sand-gravel mixture, single size hard rock fill	17
Silty sand, gravel or sand mixed with silt or clay	14
Fine sandy silt, non-plastic silt	11
<b><i>Formed concrete or concrete sheet piling against the following soils:</i></b>	
Clean gravel, gravel-sand mixture, well-graded rock fill with spalls	22 - 27
Clean sand, silty sand-gravel mixture, single size hard rock fill	17 - 22
Silty sand, gravel or sand mixed with silt or clay	17
Fine sandy silt, non-plastic silt	14

In the absence of large shear box test results the representative strength, in terms of effective stress, BS 8002 (BSI, 2015) recommends that the external friction angle should not exceed values calculated using:

- $\delta = \phi'_{crit}$  for the soil, for rough surfaces with a texture coarser than that of the median particle size;
- $\delta = 20^\circ$  for smooth surfaces with a texture finer than that of the median particle size.

No effective adhesion,  $c'$ , should be taken for walls or bases in contact with soil. In case of uncertainty, it is always safer to assume smaller value of  $\delta$ .

### Dilation angle, $\psi$

Non-associated flow is allowed for better prediction of dilation. The angle of dilation,  $\psi$ , needs to be specified. The angle of dilation controls the amount of plastic volumetric strain developed during plastic shearing. Clays are characterised by a low dilation angle ( $\psi \approx 0$ ). Non-cohesive soil's dilation angle depends on its relative density,  $D_r$  (%), and

the grain type. The formulated stiffness matrix is non-symmetric. The angle of dilation can be expressed in terms of a relative index,  $I_r$ , as defined by Bolton (1986):

$$I_r = I_D [Q - \ln(100 \frac{p'}{p_{atm}})] - R \quad (63)$$

where  $I_D = D_r/100$ ,  $p'$  is the mean effective stress ( $kN/m^2$ ),  $Q$  is the coefficient for grain type,  $R = 1$  and  $p_{atm} = 100 kN/m^2$ .

Sand Classification	SPT- $N_{60}$ (blows/305mm)	$D_r$ (%)
Very loose	0-4	0-15
Loose	4-10	15-35
Medium dense	10-30	35-65
Dense	30-50	65-85
Very dense	50-100	85-100

Grain type	$Q$
Quartz and feldspar	10
Limestone	8
Anthracite	7
Chalk	5.5

Schanz and Vermeer (1996) developed the following empirical relationship:

$$\psi = \sin^{-1}(\frac{I_r}{6.7 + I_r}) \quad (64)$$

The material parameters required are:

Parameter	Definition
$y_{ref}$	reference elevation
$E_{ref}$	reference Young's modulus
$m_E$	Young's modulus rate of change with depth
$c_{ref}$	reference cohesion
$m_c$	cohesion rate of change with depth
$\nu$	Poisson's ratio

Parameter	Definition
$\phi$	internal angle of friction
$\psi$	angle of dilation (only for non-associated flow)
$K_w$	bulk modulus of water (0 for drained material)
$\gamma_w$	unit weight of water
$\gamma_{bulk}$	bulk unit weight of soil
$k_x$	permeability in $x$ direction
$k_y$	permeability in $y$ direction
$OCR_{ref}$	over-consolidation ratio
$m_{ocr}$	increment rate of $OCR$ with depth
$K_0$	lateral earth pressure coefficient

Both the internal angle of friction ( $\phi$ ) and angle of dilation ( $\psi$ ) are specified in degrees ( $^\circ$ ).

The table below summarises the various methods for modelling undrained conditions with Mohr Coulomb model where the Young's modulus and Poisson's ratio represent the stiffness parameters; cohesion and angle of friction represent the strength parameters.

Method	Young's modulus	Poisson's ratio	Cohesion	Angle of friction
<b>A</b>	$E'$ (with $K_w$ )	$\nu'$	$c'$	$\phi'$
<b>B</b>	$E'$ (with $K_w$ )	$\nu'$	$c_u$	0
<b>C</b>	$E_u$ (set $K_w = 0$ )	0.499	$c_u$	0

#### 6.10.4 Drucker Prager

The simplification of Mohr-Coulomb model where the hexagonal shape of the failure cone was replaced by a simple cone was known as the Drucker-Prager model (Drucker and Prager, 1952). This yield criterion is suitable for effective stress analyses. Both inscribing (inner cone) and circumscribing (outer bound cone) criteria are implemented. A compressive meridian match gives:

$$\sqrt{J_2} = aI_1 + k \quad a = \frac{2\sin\phi'}{\sqrt{3}(3 - \sin\phi')} \quad k = \frac{6c\cos\phi'}{\sqrt{3}(3 - \sin\phi')} \quad (65)$$

where  $I_1 = 3p$  and  $J_2 = q^2/3$  are the first invariant principle stress and the second invariant of deviator stress tensor respectively.

Under plane strain condition,

$$a = \frac{\tan\phi'}{\sqrt{9 + 12\tan^2\phi'}} \quad k = \frac{3c}{\sqrt{9 + 12\tan^2\phi'}} \quad (66)$$

The flow rule is fully associated.

The material parameters required are:

Parameter	Definition
$y_{ref}$	reference elevation
$E_{ref}$	reference Young's modulus
$m_E$	Young's modulus rate of change with depth
$c_{ref}$	reference cohesion
$m_c$	cohesion rate of change with depth
$\nu$	Poisson's ratio
$\phi$	internal angle of friction
$K_w$	bulk modulus of water (0 for drained material)
$\gamma_w$	unit weight of water
$\gamma_{bulk}$	bulk unit weight of soil
$k_x$	permeability in $x$ direction
$k_y$	permeability in $y$ direction
$OCR_{ref}$	over-consolidation ratio
$m_{ocr}$	increment rate of $OCR$ with depth
$K_0$	lateral earth pressure coefficient

The internal angle of friction ( $\phi$ ) is specified in degrees ( $^\circ$ ).

## 6.11 Critical states

The Original Cam clay (Roscoe and Burland, 1968), Modified Cam clay (Roscoe and Schofield, 1963), Schofield and Hyperbolic Cam clay (Nasim, 1999) models are available. All of these models are specific formulations within the framework of critical state soil mechanics that describe 3 important aspects of soil behaviour:

- Strength
- Compression or dilatancy
- Critical state at which soil can experience unlimited distortion without any changes in stress or volume

In critical state mechanics, the state of a soil sample is characterized by three parameters, mean effective stress ( $p'$ ), deviator stress ( $q$ ) and specific volume ( $v$ ). Under general stress conditions, the mean effective stress ( $p'$ ) and the deviator stress ( $q$ ) can be calculated in terms of principal stresses  $\sigma'_1$ ,  $\sigma'_2$  and  $\sigma'_3$  as:

$$p' = \frac{1}{3}(\sigma'_1 + \sigma'_2 + \sigma'_3) \quad (67)$$

$$q = \frac{1}{\sqrt{2}}\sqrt{(\sigma'_1 - \sigma'_2)^2 + (\sigma'_2 - \sigma'_3)^2 + (\sigma'_3 - \sigma'_1)^2} \quad (68)$$

$$v = 1 + e \quad (69)$$

where  $e$  is the void ratio.

One of the major contributions which Cam clays made to soil mechanics is to highlight the difference between yielding and ultimate failure. Prior to Cam clay, yielding is often taken to be synonymous to failure (eg. the Mohr-Coulomb model). In Cam clay, yielding, including yielding under isotropic or constrained compression, is explained by the initiation of large-scale particle slippage. However, this does not necessarily lead to failure. The soil can undergo plastic volumetric hardening (arising to contractancy of the soil skeleton, with particles re-packing into denser arrays), if it is on the wet side of critical. On the dry side of critical, yielding is associated with the tendency to dilate. If dilatancy is allowed to occur, say in a drained test or by the drainage of pore fluid into a thin shear band, volumetric softening, arising from the re-packing of soil particles into a looser array, occurs. On the other hand, if true undrained conditions can be maintained, Cam clay predicts that the tendency to dilate will result in the generation of negative excess pore pressure, thereby leading to an increase in mean effective stress,  $p'$ , and thus deviator stress,  $q$ .

### Frictional constant, $M$

The critical state frictional constant ( $M$ ) is related to triaxial compression  $\phi'_{cs}$  by:

$$M = \frac{6\sin\phi'_{cs}}{(3 - \sin\phi'_{cs})} \quad (70)$$

### Slope of isotropic compression line and swelling line

Bolton (1991) suggested  $\lambda_{oedo}$  and  $\kappa_{oedo}$  in one-dimensional (1D) test and  $\lambda$  and  $\kappa$  isotropic values may be approximately related through the relations:

$$\lambda = \lambda_{oedo} = \frac{c_c}{\ln 10} \quad (71)$$

$$\kappa \approx 1.5\kappa_{oedo} = 1.5 \frac{c_s}{\ln 10} \quad (72)$$

where  $c_c$  and  $c_s$  are slopes of compression line and swelling line respectively.

Estimates of  $\kappa$  are typically obtained from one-dimensional unloading, oedometer test data. Unloading in an oedometer test is not a constant stress ratio unloading process as required by the critical states model.

Without going through the derivation of the  $\kappa/\kappa_{oedo}$  ratio ( $R$ ), the following relationship can be used:

$$\frac{\kappa}{\kappa_{oedo}} = \frac{(1 + 2K_0)(1 - \nu')}{(1 + \nu')} = R \quad (73)$$

Using the empirical relationship:

$$K_0 = (1 - \sin\phi')OCR_{oedo}^{\sin\phi'} \quad (74)$$

where  $OCR_{oedo}$  is the one-dimensional over-consolidation ratio.

The first well-known correlation was presented by Skempton (1944), who gave the following correlation for the compressibility of remoulded soils with liquid limit,  $LL(\%)$ :

$$c_c = 0.007(LL - 10) \quad (75)$$

Terzaghi and Peck (1967) presented a linear correlation more suited for inorganic soil with sensitivity less than 4 as:

$$c_c = 0.009(LL - 10) \quad (76)$$

Wroth and Wood (1978), using critical-state concepts, derived an empirical relation between  $C_c$  and index properties  $PI(\%)$  as:

$$c_c = 0.5 \times \frac{PI}{100} \cdot G_s \quad (77)$$

where  $G_s$  is the specific gravity of the soil.

For soil with low plasticity, Sower (1970) suggested:

$$c_c = 0.75(e_0 - 0.50) \quad (78)$$

For inorganic soil, Hough (1957) suggested:

$$c_c = 0.29(e_0 - 0.27) \quad (79)$$

where  $e_0$  is the initial void ratio of the soil.

Typically, the swelling index,  $c_s$ , is 0.1-0.2 of the compression index,  $c_c$ .

The parameter  $\lambda$  can also be used to guide or check the choice of  $\kappa$  values using the relation:

$$\Lambda = \frac{\lambda - \kappa}{\lambda} \quad (80)$$

$$\kappa = \lambda(1 - \Lambda) \quad (81)$$

Available laboratory strength data indicate that for natural clays the parameter  $\Lambda$  is approximately equal to 0.75, 0.8 and 0.85 for triaxial compression, simple shear and triaxial extension (Kulhawy and Mayne, 1990). Therefore,  $\kappa$  is typically 0.2-0.3 of  $\lambda$ .

The equivalent bulk modulus ( $K$ ), shear modulus ( $G$ ) and Young's modulus ( $E$ ) are related to  $e$ ,  $p'$  and  $\kappa$  by:

$$K = \frac{(1 + e)p'}{\kappa} \quad (82)$$

$$G = \frac{3(1 - 2\nu)(1 + e)p'}{2(1 + \nu)\kappa} \quad (83)$$

$$E = \frac{3(1 + e)p'}{\kappa}(1 - 2\nu) \quad (84)$$

### Critical void ratio, $e_{cs}$

There are several possible ways of estimating  $e_{cs}$ . A direct and intuitive procedure is described below.

The procedure is to extrapolate the one-dimensional (1D) virgin compression line backwards until it intersects the vertical line  $\sigma'_v = 1kPa$ , the void ratio at this point is  $e_{oedo}$ . Substituting  $e_{oedo}$  into the equation gives  $e_{cs}$ .

$$e_{cs} = e_{oedo} + \lambda \ln \frac{1 + 2K_{0,NC}}{3} + (\lambda - \kappa) \ln \left( \frac{\alpha}{2} \right) \quad (85)$$

where:

$$\alpha = 1 + \frac{\eta_0^2}{M^2} \quad (86)$$

in which  $\eta_0 = 0$  for original Cam clay and  $\eta_0 = \sqrt{M^2 + \frac{9}{4} - \frac{3}{2}}$  for modified Cam clay.

#### 6.11.1 Original Cam clay

In the original Cam clay model, the yield surface has a logarithmic spiral shape. This shape is an inconvenient shape that predicts an unrealistic plastic shear strain increments against isotropic compression. The yield surface is given by:

$$q = M \cdot p' \cdot \ln \frac{p'_0}{p'} \quad (87)$$

The incremental constitutive stress-strain relations are given by:

$$\begin{bmatrix} \delta \varepsilon_v \\ \delta \varepsilon_s \end{bmatrix} = \frac{1}{(1+e)p'} \begin{bmatrix} \kappa + \frac{\lambda - \kappa}{M}(M - \eta') & \frac{\lambda - \kappa}{M} \\ \frac{\lambda - \kappa}{M} & \frac{2\kappa(1 + \nu')}{9(1 - \nu')} + \frac{\lambda - \kappa}{M(M - \eta')} \end{bmatrix} \begin{bmatrix} \delta p' \\ \delta q \end{bmatrix} \quad (88)$$

where  $\varepsilon_v$  and  $\varepsilon_s$  are the volumetric and deviatoric strains respectively. The terms for the elastic regime are underlined.

The material parameters required are:

Parameter	Definition
$y_{ref}$	reference elevation
$c_s$	slope of swelling line
$\kappa$	$R \cdot c_s / \ln 10$
$c_c$	slope of normal compression line
$\lambda$	$c_c / \ln 10$
$p'$	mean effective stress
$e_0$	initial void ratio
$e_{cs}$	critical state void ratio
$\phi_{cs}$	critical state friction angle
$M$	critical state frictional constant
$\nu$	Poisson's ratio
$K_w$	bulk modulus of water (0 for drained material)
$\gamma_w$	unit weight of water
$\gamma_{bulk}$	bulk unit weight of soil
$k_x$	permeability in $x$ direction
$k_y$	permeability in $y$ direction
$OCR_{ref}$	one-dimensional over-consolidation ratio
$m_{OCR}$	increment rate of $OCR$ with depth
$K_0$	lateral earth pressure coefficient

Critical state void ratio ( $e_{cs}$ ) is required to define the position of the critical state line in the compression plane but also to calculate the initial voids ratio,  $e_0$ , from the known stress history of the soil. The critical state void ratio can be derived from the following relationship:

$$e_{cs} = e_0 + (\lambda - \kappa) \ln\left(\frac{p'OCR}{2.718}\right) + \kappa \ln(p') \quad (89)$$

where  $p'$  is the mean effective stress experienced by the soil with void ratio  $e_0$ .

The OCR in relation to the  $OCR_{oedo}$  is given by:

$$OCR = \frac{OCR_{oedo}(1 + 2K_{0,NC})}{1 + 2K_0} \exp\left[\frac{3}{M} \cdot \frac{1 - K_{0,NC}}{1 + 2K_{0,NC}}\right] \quad (90)$$

Given Jaky's relationship, the above equation can be rewritten as:

$$OCR = \frac{OCR_{oedo}(3 - 2\sin\phi_{cs})}{1 + 2(1 - \sin\phi_{cs})OCR_{oedo}^{\sin\phi_{cs}}} \exp\left[\frac{3}{M} \cdot \frac{\sin\phi_{cs}}{3 - 2\sin\phi_{cs}}\right] \quad (91)$$

### 6.11.2 Modified Cam clay

The modified Cam clay model is an isotropic, non-linear elastic, strain-hardening plastic model developed at Cambridge University. The term "modified" was added to distinguish it from the Original Cam clay model. The yield surface is an ellipse centred around the mean effective stress axis:

$$q^2 = M^2 \cdot p'(p'_0 - p') \quad (92)$$

The modified Cam Clay has several advantages over the original Cam Clay, as follows:

- It matches real remoulded soil data better under conditions of low stress ratio.
- Isotropic compression will not give rise to any shear strain increment, which seems more intuitively correct.
- Under 1-D compression, the  $K_0$  value is less than 1.0, which is also in better agreement with real soil behaviour.

The incremental constitutive stress-strain relations are given by:

$$\begin{bmatrix} \delta\varepsilon_v \\ \delta\varepsilon_s \end{bmatrix} = \frac{1}{(1+e)p'} \begin{bmatrix} \kappa + \frac{(\lambda - \kappa)(M^2 - \eta'^2)}{(M^2 + \eta'^2)} & \frac{2\eta'(\lambda - \kappa)}{(M^2 + \eta'^2)} \\ \frac{2\eta'(\lambda - \kappa)}{(M^2 + \eta'^2)} & \frac{2\kappa(1 + \nu')}{9(1 - \nu')} + \frac{4\eta'^2(\lambda - \kappa)}{(M^4 - \eta'^4)} \end{bmatrix} \begin{bmatrix} \delta p' \\ \delta q \end{bmatrix} \quad (93)$$

where  $\varepsilon_v$  and  $\varepsilon_s$  are the volumetric and deviatoric strains respectively. The terms for the elastic regime are underlined.

The material parameters required are:

Parameter	Definition
$y_{ref}$	reference elevation
$c_s$	slope of swelling line
$\kappa$	$R \cdot c_s / \ln 10$
$c_c$	slope of normal compression line
$\lambda$	$c_c / \ln 10$
$p'$	mean effective stress

$e_0$	initial void ratio
$e_{cs}$	critical state void ratio
$\phi_{cs}$	critical state friction angle
$M$	critical state frictional constant
$\nu$	Poisson's ratio
$K_w$	bulk modulus of water (0 for drained material)
$\gamma_w$	unit weight of water
$\gamma_{bulk}$	bulk unit weight of soil
$k_x$	permeability in $x$ direction
$k_y$	permeability in $y$ direction
$OCR_{ref}$	one-dimensional over-consolidation ratio
$m_{OCR}$	increment rate of $OCR$ with depth
$K_0$	lateral earth pressure coefficient

The critical state void ratio ( $e_{cs}$ ) can be derived from the following relationship:

$$e_{cs} = e_0 + (\lambda - \kappa) \ln\left(\frac{p' \cdot OCR}{2}\right) + \kappa \ln(p') \quad (94)$$

The OCR in relation to the  $OCR_{oedo}$  is given by:

$$OCR = \frac{OCR_{oedo}(1 + 2K_{0,NC})}{1 + 2K_0} \left[1 + \frac{9(1 - K_{0,NC})^2}{M^2(1 + 2K_{0,NC})^2}\right] \quad (95)$$

Given Jaky's relationship, the above equation can be rewritten as:

$$OCR = \frac{OCR_{oedo}(3 - 2\sin\phi_{cs})}{1 + 2(1 - \sin\phi_{cs})OCR_{oedo}^{\sin\phi_{cs}}} \left[1 + \frac{9(\sin\phi_{cs})^2}{M^2(3 - 2\sin\phi_{cs})^2}\right] \quad (96)$$

### 6.11.3 Hyperbolic Cam clay

The hyperbolic Cam clay model comprises of the modified Cam clay yield criterion and approximates the stress-strain relationship with a hyperbola in the elastic loading regime. The initial tangent of the hyperbolic curve is expressed by the initial shear modulus. The unloading regime is defined by the Masing's (1926) rule. The ultimate deviator stress within the yield criterion is defined by the critical state of the model.

The hyperbolic function based on Hardin-Drnevich (1972) model used by Nasim (1999) is given by:

$$q = \frac{(S_0 - S_\infty)\varepsilon_s}{1 + \frac{(S_0 - S_\infty)|\varepsilon_s|}{q_f}} + S_\infty \cdot \varepsilon_s \quad (0 < \varepsilon_s < \varepsilon_y) \quad (97)$$

where  $S_0$  is the initial tangential stiffness,  $S_\infty$  is the tangential stiffness at very large strain,  $\varepsilon_s$  is the shear strain,  $\varepsilon_y$  is the shear strain at yielding  $q_f$  is the deviator stress at failure.

Assuming:

$$S = \frac{\delta q}{\delta \varepsilon_s} = 3G \quad (98)$$

Differentiating  $q$  with respect to  $\varepsilon_s$  leads to a variation of shear modulus  $G$  with shear strain  $\varepsilon_s$  that is given by:

$$G = \frac{(G_0 - G_\infty)}{\left[1 + \frac{(G_0 - G_\infty)|\varepsilon_s|}{q_f}\right]^2} + G_\infty \quad (99)$$

where  $G_0$  is the initial shear modulus and  $G_\infty$  is the shear modulus at very large strain which can be assumed to be zero.

In the unloading regime, Masing's rule is incorporated using similar expression proposed by Hashiguchi (1993):

$$\varepsilon_s - \varepsilon_{ur} = f\left(\frac{\sigma_s - \sigma_{ur}}{L}\right) \quad (100)$$

with shape factor  $L=1$  in primary loading and  $L=2$  in unloading and reloading. The strain and stress levels  $\varepsilon_s$  and  $\sigma_s$  denote the last load reversal point in stress-strain space, where  $\varepsilon_{ur}$ , and  $\sigma_{ur}$  specify the actual strain and stress respectively. The unloading variation of  $G$  incorporating Masing's rule can be derived as follow:

$$G = \frac{G_0}{\left[1 + \frac{3G_0}{q_f} \frac{|\varepsilon_s - \varepsilon_{ur}|}{2}\right]^2} \quad (101)$$

Hardin & Black (1969) proposed an empirical relationship between the initial shear modulus,  $G_0$ , and the over-consolidation ratio,  $OCR$ , of the form:

$$G_0 \propto OCR^m \quad (102)$$

Hardin & Richart (1963) proposed the following relationship between the initial shear modulus,  $G_0$ , and the effective confining stress,  $p'$ :

$$G_0 \propto p'^n \quad (103)$$

For cohesive soils, the exponent  $n=0.5$  used by Hardin & Richart themselves is controversial. Combining the above two equations, the initial shear modulus,  $G_0$ , is in turn related to the current state of soil by the relation:

$$G_0 = C \cdot OCR^m \cdot p'^n \quad (104)$$

where  $C$  is a constant,  $m$  is the  $OCR$  exponent and  $n$  is the effective stress ( $p'$ ) exponent.

The values of  $m$  reported typically range from 0.2 to 0.3 whereas  $n$  typically ranged from 0.5 to 0.9. For coarse-grained soils,  $n$  could reasonably be approximated by 0.58. For normally consolidated clay,  $n$  is approximately 0.85. The value of  $m$  depended on the history of over-consolidation or compaction. Since the hyperbolic shear modulus variation is based purely on an empirical relationship, matching with laboratory tests is essential in determining the soil parameters  $C$ ,  $m$  and  $n$ . These values can be determined by simulating a consolidated undrained triaxial test using finite elements. It is likely that some errors will be incurred in the fitting process since conventional triaxial tests with external strain measurements often tend to return lower soil stiffness than the true values. The relationship between the plasticity index and the two exponents are shown in the following chart (Viggiani & Atkinson, 1995). For clays with  $10 < PI(\%) < 40$ , Viggiani & Atkinson found  $0.20 < m < 0.25$ .

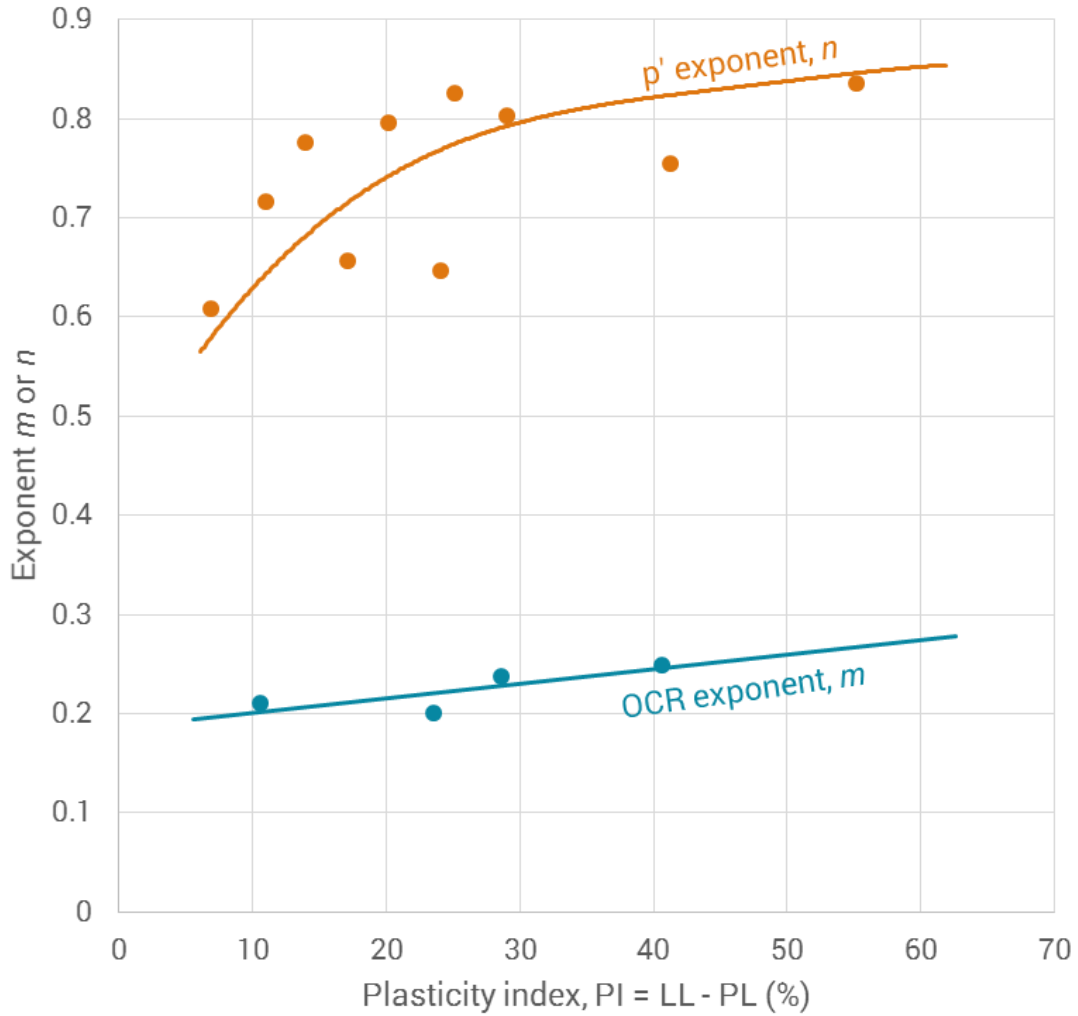


Figure 57: Relationship between plasticity index versus OCR and  $p'$  exponents

Alternatively, the OCR exponent can be approximated using a hyperbolic relationship as follow for  $PI(\%) > 5$ :

$$n = \frac{0.060PI}{0.894 + 0.095PI} + 0.308 \quad (105)$$

A linear relationship approximates the  $p'$  exponent as follow for  $PI(\%) > 5$ :

$$m = 0.0015PI + 0.1863 \quad (106)$$

The shear variation constant,  $C$ , should be derived from the stress-strain relationship of consolidated undrained (CU) triaxial tests. In the absence of CU triaxial test data, the following approximation by Viggiani and Atkinson (1995) can be used for  $PI(\%) > 5$ :

$$C = 3790 \exp[-0.045PI] \quad (107)$$

The material parameters required are:

Parameter	Definition
$\gamma_{ref}$	reference elevation
$c_s$	slope of swelling line
$\kappa$	$R \cdot c_s / \ln 10$
$c_c$	slope of normal compression line
$\lambda$	$c_c / \ln 10$
$p'$	mean effective stress
$e_0$	initial void ratio
$e_{cs}$	critical state void ratio
$\phi_{cs}$	critical state friction angle
$M$	critical state frictional constant
$\nu$	Poisson's ratio
$K_w$	bulk modulus of water (0 for drained material)
$\gamma_w$	unit weight of water
$\gamma_{bulk}$	bulk unit weight of soil
$k_x$	permeability in $x$ direction
$k_y$	permeability in $y$ direction
$C$	shear variation constant
$m$	over-consolidation ratio ( $OCR$ ) exponent
$n$	mean effective stress ( $p'$ ) exponent
$OCR_{ref}$	one-dimensional over-consolidation ratio
$m_{OCR}$	increment rate of $OCR$ with depth
$K_0$	lateral earth pressure coefficient

The critical state void ratio ( $e_{cs}$ ) can be derived from the following relationship:

$$e_{cs} = e_0 + (\lambda - \kappa) \ln\left(\frac{p' \cdot OCR}{2}\right) + \kappa \ln(p') \quad (108)$$

The  $OCR$  in relation to the  $OCR_{oedo}$  is given by:

$$OCR = \frac{OCR_{oedo}(1 + 2K_{0,NC})}{1 + 2K_0} \left[ 1 + \frac{9(1 - K_{0,NC})^2}{M^2(1 + 2K_{0,NC})^2} \right] \quad (109)$$

#### 6.11.4 Schofield

The model comprises of the original Cam clay yield criterion with a limiting stress Hvorslev surface and a “no tension” surface.

The material parameters required are:

Parameter	Definition
$y_{ref}$	reference elevation
$c_s$	slope of swelling line
$\kappa$	$R \cdot c_s / \ln 10$
$c_c$	slope of normal compression line
$\lambda$	$c_c / \ln 10$
$p'$	mean effective stress
$e_0$	initial void ratio
$e_{cs}$	critical state void ratio
$\phi_{cs}$	critical state friction angle
$M$	critical state frictional constant
$\nu$	Poisson's ratio
$K_w$	bulk modulus of water (0 for drained material)
$\gamma_w$	unit weight of water
$\gamma_{bulk}$	bulk unit weight of soil
$k_x$	permeability in $x$ direction
$k_y$	permeability in $y$ direction
$H$	slope of Hvorslev's surface along constant volume section in $q - p'$ space
$S$	slope of tensile crack region in $q - p'$ space
$k_{xt}$	permeability $x$ in tensile crack
$k_{yt}$	permeability $y$ in tensile crack
$OCR_{ref}$	one-dimensional over-consolidation ratio
$m_{OCR}$	increment rate of $OCR$ with depth
$K_0$	lateral earth pressure coefficient

The critical state void ratio ( $e_{cs}$ ) can be derived from the following relationship:

$$e_{cs} = e_0 + (\lambda - \kappa) \ln\left(\frac{p' \cdot OCR}{2.718}\right) + \kappa \ln(p') \quad (110)$$

The  $OCR$  in relation to the  $OCR_{oedo}$  is given by:

$$OCR = \frac{OCR_{oedo}(1 + 2K_{0,NC})}{1 + 2K_0} \exp\left[\frac{3}{M} \cdot \frac{1 - K_{0,NC}}{1 + 2K_{0,NC}}\right] \quad (111)$$

## 6.12 User definable

The user will need to have the knowledge of Fortran programming language and is able to compile the source code into a binary dynamic link library file (.dll).

User model interface **UMOD.F90** should contain at least one subroutine, **UDMAT**. Subroutine **UDMAT** is used to calculate the stress-strain matrix. There are two optional subroutines, one is **UPSTSPAR** and the other one is **UINIVAR**.

**UPSTSPAR** is used to update the stress variable or some parameters. This subroutine may not be required for elastic soil model.

**UINIVAR** is used to initialize the stress variable and some parameters at the in-situ stage for critical state user soil models.

User model (  ) can define up to 12 material parameters, P1-P6 and P11-P16. Material parameters P7-P10 is predefined as bulk modulus of water ( $K_w$ ), bulk unit weight of soil ( $\gamma_{bulk}$ ), permeability in the  $x$ -direction ( $k_x$ ) and permeability in the  $y$ -direction ( $k_y$ ) respectively.

A detailed instruction for implementation of user model will be given upon request.

## 6.13 Structure interaction

All structural elements are weightless. If the self-weight of the structure needs to be considered, elements with drained soil material properties may be used. Bending moments cannot be derived directly from these drained elements.

Placing the same structural element in soil or rock will affect its characteristics behaviour. Bending stiffness in a beam will take away some tensile forces. Typically, beams are used to model soil-nails. Geo-fabric doesn't have significant bending stiffness so it may not be appropriate to use the beam element. Where compressional stress or strain is observed in a geo-fabric model, avoid modeling it with bar or beam as these elements do not have compression cut-off mechanism.

**Warning:** Do not use bars or beams as non-vertical structural members in an axisymmetric model!

**Tips:** Structural elements cannot be used as non-vertical elements in axisymmetric models. A special class of axisymmetric shell element must be used. However, a very low stiffness structural beam can be embedded in an axisymmetric solid mesh to derive bending moments by scaling it up to the stiffness of the structural solid at the appropriate sections.

For reasonable representation of axial tensile force, ensure that the soil element mesh is sufficiently fine to generate effective coupling of soil nodes to the structural elements. This will prevent spurious tensile forces from arising.

The rotation matrix used for the transformation is referred to as  $y$ - $z$ - $x$  transformation. The angle of rotation are denoted as  $\beta$ ,  $\gamma$  and  $\alpha$  respectively. These series of rotations,  $[T']$ , about the  $y$ -,  $z$ - and  $x$ -axes, can be resolved into their respective vector components through the following transformations:

$$[T'] = [T_\alpha][T_\gamma][T_\beta] \quad (112)$$

where

$$[T_\alpha] = \begin{bmatrix} 1 & 0 & 0 \\ 0 & \cos\alpha & \sin\alpha \\ 0 & -\sin\alpha & \cos\alpha \end{bmatrix} \quad (113)$$

$$[T_\gamma] = \begin{bmatrix} \cos\gamma & \sin\gamma & 0 \\ -\sin\gamma & \cos\gamma & 0 \\ 0 & 0 & 1 \end{bmatrix} \quad (114)$$

$$[T_\beta] = \begin{bmatrix} \cos\beta & 0 & \sin\beta \\ 0 & 1 & 0 \\ -\sin\beta & 0 & \cos\beta \end{bmatrix} \quad (115)$$

$\beta$  is the rotation of global  $y$ -axis,  $\gamma$  is the rotation of global  $z$ -axis and  $\alpha$  is the rotation of global  $x$ -axis (angle of tilt).

Thus, expressed in terms of the direction cosines of the element:

$$[T'] = \begin{bmatrix} \frac{C_x}{\sqrt{C_x^2 + C_z^2}} & \frac{C_y}{\sqrt{C_x^2 + C_z^2} \cos \alpha} & \frac{C_z}{\sqrt{C_x^2 + C_z^2}} \\ \frac{-C_x C_y \cos \alpha - C_z \sin \alpha}{\sqrt{C_x^2 + C_z^2}} & & \frac{-C_y C_z \cos \alpha + C_x \sin \alpha}{\sqrt{C_x^2 + C_z^2}} \\ \frac{C_x C_y \sin \alpha - C_z \cos \alpha}{\sqrt{C_x^2 + C_z^2}} & -\sqrt{C_x^2 + C_z^2} \sin \alpha & \frac{C_x C_y \sin \alpha + C_z \cos \alpha}{\sqrt{C_x^2 + C_z^2}} \end{bmatrix} \quad (116)$$

where

$$C_x = \frac{x_j - x_i}{L}, C_y = \frac{y_j - y_i}{L}, C_z = \frac{z_j - z_i}{L}$$

and

$$L = \sqrt{(x_j - x_i)^2 + (y_j - y_i)^2 + (z_j - z_i)^2}$$

### 6.13.1 Bar elements

The material properties required for a bar element are:

- Young's modulus
- Poisson's ratio
- Cross sectional area of bar

Parameter	Definition
<b>Spacing</b>	distance between the centers of adjacent structures
<b><math>E_{actual}</math></b>	Young's modulus
<b><math>E_{smeared}</math></b>	Young's modulus divided by spacing
<b><math>\nu</math></b>	Poisson's ratio
<b><math>A</math></b>	cross sectional area

In 2 dimensions, a smeared value of Young's modulus is required by the input of bar spacing.

### 6.13.2 Beam elements

The material properties required for a bar element are:

- Young's modulus

- Poisson's ratio
- Cross sectional area
- Second moment of area of cross section

For a beam in 2-dimensions:

Parameter	Definition
<b><i>Spacing</i></b>	distance between the centers of adjacent structures
<b><i>E<sub>actual</sub></i></b>	Young's modulus
<b><i>E<sub>smeared</sub></i></b>	Young's modulus divided by spacing
<b><i>ν</i></b>	Poisson's ratio
<b><i>A</i></b>	cross sectional area
<b><i>I</i></b>	second moment of area of cross section
<b><i>f<sub>y</sub></i></b>	yield stress
<b><i>W<sub>el,xx</sub></i></b>	elastic modulus of cross section in <i>x-x</i> axis

In 2 dimensions, a smeared value of Young's modulus is required by the input of beam spacing.

For a beam in 3-dimensions:

Parameter	Definition
<b><i>E</i></b>	Young's modulus
<b><i>ν</i></b>	Poisson's ratio
<b><i>A</i></b>	cross sectional area
<b><i>I<sub>xx</sub></i></b>	second moment of area of cross section in <i>x-x</i> axis
<b><i>I<sub>yy</sub></i></b>	second moment of area of cross section in <i>y-y</i> axis
<b><i>α</i></b>	angle rotated about the beam axis
<b><i>J</i></b>	torsional constant of cross section
<b><i>f<sub>y</sub></i></b>	yield stress
<b><i>W<sub>el,xx</sub></i></b>	elastic modulus of cross section in <i>x-x</i> axis
<b><i>W<sub>el,yy</sub></i></b>	elastic modulus of cross section in <i>y-y</i> axis

**Good practice:** For modeling tapered beams or curved beams, the user needs to approximate such members into several elements. For the tapered beams the user needs to

*divide the beam into several elements and use an appropriate constant cross-section area and second moment of areas for each of these elements.*

This page is intentionally left blank.

## Chapter 7 In-Situ panel

Selecting **In-Situ** on the Workflow panel reveals a set of tools on the In-Situ panel.

The geometrical model should not contain overlapping elements during the in-situ stage. All elements required in the analysis shall be created in the in-situ stage and removed from the current mesh for subsequent addition in other stages. The removed element entities will be placed in an alternate mesh view and remain inactive until they are included in the current mesh. The alternate mesh view can be inspected by selecting the “exclude mesh” option.

The model should be adequately restrained. No incremental fixities shall be applied at this stage.

The elevation of groundwater table and the unit weight of water shall be specified in the in-situ stage.

**Tips:** *These initial conditions must be established correctly so that the analysis begins from an equilibrium state.*

### 7.1 In-situ stress workgroup

It is crucial that the internal stresses and external loads of the elements forming the current mesh are at equilibrium with each other. The program provides an easy way to do that by allowing the user to select an auto equilibration option for problems where the stresses vary in the horizontal direction. Three settings are provided to specify in-situ stress: ignore, auto and manual.



Figure 58: In-situ stress settings

**Bad practice:** Avoid wish-in-place new structures when doing auto equilibration.

### 7.1.1 Ignore

When in-situ stresses are ignored, no boundary fixities or loads can be applied to the mesh in this stage. The boundary fixities, pore-pressures and loads icons are all inactive. All in-situ stresses are assumed to be zero. Critical state models should not be used as they require to establish the size of their yield loci based on the in-situ stress levels.

### 7.1.2 Auto

The automatic computation of in-situ stress is based on gravity loading in two stages.

In the first stage, calculate the displacement from gravity loading. All the elements in this stage are converted to drained type because only the total stress is required in the computation of  $\sigma_y = \gamma h$ . All the materials are assumed to be linear elastic with a constant stiffness as no initial yielding is allowed. Newton Raphson's (NR) method is applied to redistribute any out-of-balance loads arising from any non-linearity in the computation. For NR method, we used slightly less stringent criteria for the convergence. The maximum iteration count is set to 5 and the tolerance is set to 0.001 (i.e. 0.1%). These values are 10 times larger than the values used for the NR method for loading steps.

In the second stage, based on the ground water table, the effective vertical stress  $\sigma'_y = \sigma_y - \gamma_w h_w$  is derived. The effective horizontal stresses  $\sigma'_x$  and  $\sigma'_z$  is computed based on  $\sigma'_y$  and  $K_0$ . If the  $K_0$  is not specified in the material database, the program will compute

its value by using linear elastic relationship for linear elastic materials or by using Jaky (1944) empirical relationship. The materials are replaced with the actual soil properties defined by the user. The stresses for the yielding condition will be checked in this stage and if the re-computed out-of-balance load is large, NR method is applied to redistribute the out-of-balance loads. For this, maximum iteration is set to 30 and the tolerance is set to 0.0005 (i.e. 0.05%).

**Tips:** *Newton Raphson's method redistributes out-of-balance loads arising from any non-linearity in the computation to maintain equilibrium at the start of the analysis.*

### 7.1.3 Manual

For the manual specification of in-situ stress, the mesh should be divided into a number of horizontal layers. If there are  $N$  in-situ reference points then there are  $N-1$  in-situ layers. When setting the in-situ stress from reference elevation, 2 sets of in-situ stress data can be specified for a single elevation. The user can create a linear variation of stresses by specifying values for the top and bottom of the mesh.

These points are in fact reference levels. Therefore the user specifies a set of reference points along a vertical section and the stresses at these points. The in-situ stresses at the integration points are interpolated from the stresses specified at these points. Either  $\sigma'_x$  and  $\sigma'_z$  or  $K_0$  is required to compute in-situ stresses. Also, either  $p'_c$  or  $OCR$  is required to define the yield surface of the critical state models. If both competing values are entered in either set, the former values will govern the analysis.

The in-situ reference points should cover the whole of the mesh. No part of the mesh which requires any in-situ stresses assigned to it should lie outside the range of the  $y$ -coordinates specified by the points 1- $N$ .

For most problem, the in-situ stresses do not vary in the horizontal direction and it is assumed that the stresses vary only with depth. This method of setting is not suitable for an undulating ground profile. In the problem where the stresses do vary in the horizontal direction, automatic computation of in-situ stresses should be used.

**Good practice:** *At the in-situ stage, equilibrium errors should be very close to zero, typically less than 0.1% for manual specification of in-situ stress.*

## 7.2 Translation (in-situ) workgroup

Boundaries can only be smooth if they are aligned with vertical or horizontal directions where the translational degree of freedoms can behave in an unrestrained manner. Rough boundaries can be created in any direction.

*Tips: Non-zero displacements cannot be specified in the in-situ stage.*

### 7.2.1 Node translational restraint

This fixity type is applicable to both 2-and 3-dimensional meshes. Only the vertex nodes can be fixed using this nodal type fixity as the control of nodes along element edges are not available to the users.

Icon	Description
	Fixes the translation in the $x$ -direction at a node in 2- or 3-dimension.
	Fixes the translation in the $y$ -direction at a node in 2- or 3-dimension.
	Fixes the translation in the $z$ -direction at a node in 3-dimension only.

### 7.2.2 Edge translational restraint

This fixity type is applicable to both 2-and 3-dimensional meshes.

Two different edges with the same length and in the same position (duplicates) will be fixed. So both edges are applied with the same fixity type and value. This will ensure that both the edges for initial and replacement elements are fixed.

Icon	Description
	Fixes the translation in the $x$ -direction along an edge of face in 2-dimension or edge of a solid in 3-dimension.
	Fixes the translation in the $y$ -direction along an edge of face in 2-dimension or edge of a solid in 3-dimension.
	Fixes the translation in the $z$ -direction along an edge of a solid in 3-dimension.

### 7.2.3 Face translational restraint

This fixity type is applicable to 3-dimensional meshes only.

Two different faces with same shape and in the same position (duplicates) will be fixed. So both faces are applied with the same fixity type and value. This will ensure that both the faces for initial and replacement elements are fixed.

Icon	Description
	Fixes the translation in the $x$ -direction on a face of a solid in 3-dimensional mesh only.
	Fixes the translation in the $y$ -direction on a face of a solid in 3-dimensional mesh only.
	Fixes the translation in the $z$ -direction on a face of a solid in 3-dimensional mesh only.

## 7.3 Rotation (in-situ) workgroup

The elements must contain rotational degrees of freedom for the fixity to take effect. Currently, the only element type available is beam.

### 7.3.1 Node rotational restraint

This fixity type is applicable to both 2- and 3-dimensional meshes. Only the vertex nodes can be fixed using this nodal type fixity as the control of nodes along element edges are not available to the users.

Icon	Description
	Fixes the rotation about the $x$ -direction at a node in 3-dimension only.
	Fixes the rotation about the $y$ -direction at a node in 3-dimension only.
	Fixes the rotation about the $z$ -direction at a node in 2- or 3-dimension.

## 7.4 Pore pressure (in-situ) workgroup

Pore pressure is not specified in a drained or an undrained analysis, only in a consolidation analysis. The user does not need to specify any pore pressure conditions for an impermeable boundary. All boundaries are automatically assumed to be impermeable.

There are two types of pore pressure fixity conditions at the in-situ stage. First, incremental excess pore pressure when the changes in excess pore pressure are known over the stages of application e.g. recharging boundary where the groundwater table is maintained and the hydraulic pressure head is unchanged with depth. Second, total head is specified when the hydraulic pressure head is known e.g. exposure of ground soil face to atmospheric pressure under loading condition.

Icon	Description
	Incremental excess pore pressure selector.
	Sets uniform incremental excess pore pressure to an edge in 2-dimensional or a face in 3-dimension.
	Sets linearly varying incremental excess pore pressure to an edge in 2-dimensional or a face in 3-dimension.
	Total hydraulic pressure head selector. Atmospheric pressure head is assumed to be zero.
	Sets uniform total hydraulic pressure head to an edge in 2-dimensional or a face in 3-dimension.
	Sets linearly varying total hydraulic pressure head to an edge in 2-dimensional or a face in 3-dimension.

#### 7.4.1 Node assignment

This fixity type is applicable to both 2-and 3-dimensional meshes. The nodal assignment is useful as a point source or sink for groundwater flow. This type of assignment is not available in the current version.

#### 7.4.2 Edge assignment

This fixity type is applicable to 2-dimensional meshes only. This type of assignment in 3-dimensional space is not available in the current version.

Two different edges with the same length and in the same position (duplicates) will be fixed. So both edges are applied with the same fixity type and value. This will ensure that both the edges for initial and replacement elements are fixed.

#### 7.4.3 Face assignment

This fixity type is applicable to 3-dimensional meshes only.

Two different faces with the same shape and in the same position (duplicates) will be fixed. So both faces are applied with the same fixity type and value. This will ensure that both the faces for initial and replacement elements are fixed.

#### 7.4.4 Constraints removal

Removing of constraint will eliminate it from all stages. There are two ways of removing constraints from the tree view. Each constraint assignment is grouped at entity level. To remove the constraint as an assignment group, expand the constraint type to reveal the assignment group, right-click on the group and select "Delete". To remove the assignment at entity level, expand the assignment group to show individual entities,

right-click on the entity with the undesired assignment and select "Remove". Make sure that the selection is correct by ensuring the desired constraint is highlighted in the model.

### 7.4.5 Constraints release

A constraint is considered released when it does not take part further in the analysis stages. To release the constraint, expand the constraint type to reveal the assignment group, right-click on the group and select "Release Fixity".

## 7.5 Load (in-situ) workgroup

The conventions that are adhered to in the input and output data files are:

- Positive normal loads are compressive
- Negative normal loads are tensile
- Positive shear acts on element edges in an anti-clockwise direction about the element centre.

Three types of static loading are available. They are:

- nodal load,
- edge load and
- face load.

The edge and face loads are applied directly to the edges and faces of elements. The solver converts that element loading to an equivalent nodal loads behind the scenes during solution.

Icon	Description
	Nodal load is available in 2- and 3-dimensional analyses. The load can be applied to vertex nodes only.
	Edge load selector.
	Sets uniformly distributed load to an edge in 2- or 3-dimension. The load can be applied to straight or curved edges.
	Sets linearly varying distributed load to an edge in 2- or 3-dimension. The load can be applied to straight or curved edges.
	Sets parabolically distributed load to an edge in 2- or 3-dimension. The load can be applied to straight or curved edges.
	Face load selector for 3-dimension only.

Icon	Description
	Sets uniformly distributed load to a face in 3-dimension. The load can be applied to flat or curved faces.
	Sets distributed load that varies linearly along the $x$ -direction to a face in 3-dimension. The linear load variation is interpolated between two user specified load values and $x$ -ordinates. The load can be applied to flat or curved faces.
	Sets distributed load that varies linearly along the $y$ -direction to a face in 3-dimension. The linear load variation is interpolated between two user specified load values and $y$ -ordinates. The load can be applied to flat or curved faces.
	Sets distributed load that varies linearly along the $z$ -direction to a face in 3-dimension. The linear load variation is interpolated between two user specified load values and $z$ -ordinates. The load can be applied to flat or curved faces.
	Sets distributed load that is interpolated from 3 or 4 user specified corner values on a face in 3-dimension. Specifying 3 corner values give a coplanar variation of the load while 4 corner values give a bilinearly interpolated load distribution over the face. The load can be applied to face with 3 or 4 edges only.

### 7.5.1 Loads removal

Removing of load will eliminate it from all stages. There are two ways of removing loads from the tree view. Each load assignment is grouped at entity level. To remove the load as an assignment group, expand the constraint type to reveal the assignment group, right-click on the group and select "Delete". To remove the load at entity level, expand the assignment group to show load entities, right-click on the entity with the undesired load and select "Remove". Make sure that the selection is correct by ensuring the desired load is highlighted in the model.

### 7.5.2 Loads release

A load is considered released when it does not take part further in the analysis stages. To release the load, expand the load type to reveal the assignment group, right-click on the group and select "Release Load".

## 7.6 Common (in-situ) workgroup

This workgroup simplifies the application of some common boundary conditions by grouping different fixity conditions into one operation.

Icon	Description
	Fixes the translations for all distal boundaries parallel to the $x$ - $y$ and $y$ - $z$ planes in the out-of-plane directions and the bottom most horizontal boundary in all directions. This condition is applied to edges in 2-dimension or faces in 3-dimension. Oblique planes will not be fixed.
	Maintains the pore pressure head at the selected face. This is commonly used to set the far-field groundwater recharging condition at the mesh boundaries. This condition is applied to edges in 2-dimension or faces in 3-dimension.
	Fixes the translations and rotations at one end of a beam element. This simulates the fixed end of a beam. This condition is applied to nodes only.
	Fixes the translations but not the rotations at one end of a beam element. This simulates the pinned end of a beam. This condition is applied to nodes only.
	Fixes the rotation but not the translations at one end of a beam element to model a zero slope condition. This simulates the mid-span condition for an uniform beam with symmetrical loading. This condition is applied to nodes only.

## 7.7 State (in-situ) workgroup

Icon	Description
	Views the objects that are currently active in the finite element mesh. While the view is active, selecting objects and press "ENTER" will exclude the selections from the current mesh.
	Views the objects that are inactive in the finite element mesh. While the view is active, selecting objects and press "ENTER" will include the selections into the current mesh.

This page is intentionally left blank.

# Chapter 8 Stages panel

Selecting **Stages** on the Workflow panel reveals a set of tools on the Stages panel. Soil constructions or excavation can be modelled in an analysis via the addition or removal of elements as the analysis progresses.

## 8.1 Staged construction

One important concept of an add and remove operation is the immediate contribution of stiffness to the mesh while the effect of the body forces will be distributed over the number of increments within the stage.

The individual elements are generally grouped as mesh entities for user's convenience during pre-processing stage. How the elements are grouped will be at their user's discretion.

Realistic loading can be simulated by applying loads, fixities, boundary conditions and construction sequences to the finite element mesh. These are modelled as discrete stages in an incremental formulation.

Each stage consists of user defined number of increments as the unit of analysis as the solution progresses. Any displacement or stress change will be applied equally over the number of increments in the stage.

The smallest unit of increments is one. Owing to the non-linear nature of real-world problems, several increments should be specified over which the conditions are gradually applied. Alteration of loads and boundary conditions is not allowed within a stage.

By splitting an analysis into a number of stages, load and boundary conditions can be altered so that each stage is used to model a different process or event.

In a consolidation analysis, a time duration shall be specified and that duration is divided equally over the increments.

Each stage will comprise of gravity increment, load and fixities with inclusion and exclusion data organized into a single data block. As the finite element formulation is incremental, the gravity value is also incremental. Therefore, the gravity increment input field needs to be populated only once where needed. The user might need to populate this field more than once for centrifugal setups. The data block description can be modified to give each block a meaningful and unique name.

All elements required in the analysis shall be created in the in-situ stage and removed from the current mesh for subsequent addition in other stages. The removed element entities will be placed in an alternate mesh view and remain inactive until they are included in the current mesh. The alternate mesh view can be inspected by selecting the “Exclude mesh” option. The user can only select entities that are visible in the Workspace. The “Include mesh” and “Exclude mesh” options are catered for building up construction sequences by adding or removing elements from the mesh.

With the above function and a fair bit of imagination, swapping of soil elements with concrete elements to model replacement is achievable. For the building of embankments, the embankment elements may start off removed and be constructed later. However, it shall be noted that the added elements will have a zero stress state and will not be in equilibrium with the surrounding elements. As such, equilibrium errors will be reflected as out-of-balance loads in the analysis. This out-of-balance loads can be redistributed using Newton-Raphson’s scheme selectable at the start of the analysis.

The user cannot add any element which has a stress history, hence elements which are added to represent a construction event cannot have critical state material types associated with them. Such elements will have to be modelled as an elastic or elastic perfectly plastic material. A small value should be provided for cohesion if Mohr Coulomb or Drucker Prager yield criteria are used to prevent the initial zero stress state being on the yield surface.

## 8.2 Translation (stage) workgroup

Boundaries can only be smooth if they are aligned with vertical or horizontal directions where the translational degree of freedoms can behave in an unrestrained manner. Rough boundaries can be created in any direction.

There are two important concepts to note when applying displacement to the mesh. The first is inheritance characteristic and the second is the incremental nature of the solution method.

All displacement fixities can be released so that the nodes are completely unrestrained. The computation proceeds with the prevailing value of displacement.

Boundaries can only be smooth if they are aligned with vertical or horizontal directions where the translational degree of freedoms can behave in an unrestrained manner. Rough boundaries can be created in any direction.

### 8.2.1 Node translational restraint

This fixity type is applicable to both 2- and 3-dimensional meshes. Only the vertex nodes can be fixed using this nodal type fixity as the control of nodes along element edges are not available to the users.

Icon	Description
	Fixes the translation in the $x$ -direction at a node in 2- or 3-dimension.
	Fixes the translation in the $y$ -direction at a node in 2- or 3-dimension.
	Fixes the translation in the $z$ -direction at a node in 3-dimension only.

For zero value (fully-fixed), there is no need to set thus not possible to set this fixity type at the same node until after it is released at the subsequent stage because of the inheritance characteristic of this type of fixity.

Icon	Description
	Sets the translation in the $x$ -direction to a certain value at a node in 2- or 3-dimension.
	Sets the translation in the $y$ -direction to a certain value at a node in 2- or 3-dimension.
	Sets the translation in the $z$ -direction to a certain value at a node in 3-dimension only.

A fixed value translation can be applied to the same node over different stages. Due to the inheritance characteristic, the successive applications of this fixity type are interpreted as incremental values.

### 8.2.2 Edge translational restraint

This fixity type is applicable to both 2- and 3-dimensional meshes.

Two different edges with the same length and in the same position (duplicates) will be fixed. So both edges are applied with the same fixity type and value. This will ensure that both the edges for initial and replacement elements are fixed.

Icon	Description
	Fixes the translation in the $x$ -direction along an edge of face in 2-dimension or edge of a solid in 3-dimension.

Icon	Description
	Fixes the translation in the $y$ -direction along an edge of face in 2-dimension or edge of a solid in 3-dimension.
	Fixes the translation in the $z$ -direction along an edge of a solid in 3-dimension.

For zero value (fully-fixed), there is no need to set thus not possible to set this fixity type at the same edge until after it is released at some stage because of the inheritance characteristic of this type of fixity.

Icon	Description
	Sets the translation in the $x$ -direction to a certain value along an edge of face in 2-dimension or edge of a solid in 3-dimension.
	Sets the translation in the $y$ -direction to a certain value along an edge of face in 2-dimension or edge of a solid in 3-dimension.
	Sets the translation in the $z$ -direction to a certain value along an edge of a solid in 3-dimension.

A fixed value translation can be applied to the same edge over different stages. Due to the inheritance characteristic, the successive applications of this fixity type are interpreted as incremental values.

### 8.2.3 Face translational restraint

This fixity type is applicable to 3-dimensional meshes only.

Icon	Description
	Fixes the translation in the $x$ -direction on a face of a solid in 3-dimensional mesh only.
	Fixes the translation in the $y$ -direction on a face of a solid in 3-dimensional mesh only.
	Fixes the translation in the $z$ -direction on a face of a solid in 3-dimensional mesh only.

Strictly no faces should be fixed with zero displacement twice. Thus, it is not possible to set this fixity type at the same face until after it is released at some stage because of the inheritance characteristic of this type of fixity.

Icon	Description
	Sets the translation in the $x$ -direction to a certain value on a face of a solid in 3-dimensional mesh only.
	Sets the translation in the $y$ -direction to a certain value on a face of a solid in 3-dimensional mesh only.
	Sets the translation in the $z$ -direction to a certain value on a face of a solid in 3-dimensional mesh only.

A fixed value translation can be applied to the same face over different stages. Due to the inheritance characteristic, the successive applications of this fixity type are interpreted as incremental values.

Two different faces with same shape and in the same position (duplicates) will be fixed. So both faces are applied with the same fixity type and value. This will ensure that both the faces for initial and replacement elements are fixed.

The combination of nodal, edge and face prescribed translations can be applied on the same edge or face of an element. However, user has to note that when such combination is applied, the translational value of node will take precedence over that of the edge and the face and translational value of edge will take precedence over that of the face.

### 8.3 Rotation (stage) workgroup

The elements must contain rotational degrees of freedom for the fixity to take effect. Currently, the only element type available is beam.

#### 8.3.1 Node rotational restraint

This fixity type is applicable to both 2- and 3-dimensional meshes. Only the vertex nodes can be fixed using this nodal type fixity as the control of nodes along element edges are not available to the users.

Icon	Description
	Fixes the rotation about the $x$ -direction at a node in 3-dimension only.
	Fixes the rotation about the $y$ -direction at a node in 3-dimension only.
	Fixes the rotation about the $z$ -direction at a node in 2- or 3-dimension.

For zero value (fully-fixed), there is no need to set thus not possible to set this fixity type at the same node until after it is released in the subsequent stage because of the inheritance characteristic of this type of fixity.

Icon	Description
	Sets the rotation about the $x$ -direction to a certain value at a node in 3-dimension only. The unit is in radians.
	Sets the rotation about the $y$ -direction to a certain value at a node in 3-dimension only. The unit is in radians.
	Sets the rotation about the $z$ -direction to a certain value at a node in 2- or 3-dimension. The unit is in radians.

A fixed value rotation can be applied to the same node over different stages. Due to the inheritance characteristic, the successive applications of this fixity type are interpreted as incremental values.

## 8.4 Pore pressure (stage) workgroup

Pore pressure is not specified in a drained or an undrained analysis, only in a consolidation analysis. The user does not need to specify any pore pressure conditions for an impermeable boundary. All boundaries are automatically assumed to be impermeable.

There are three types of pore pressure fixity conditions. First, absolute excess pore pressure can be applied when the magnitude of the pore pressure in excess of the hydrostatic pore pressure is known. Second, incremental excess pore pressure when the changes in excess pore pressure are known over the stages of application e.g. introduction of a recharging boundary where the hydraulic pressure head is maintained. Third, total head is specified when the hydraulic pressure head is known e.g. exposure of vertical soil face to atmospheric pressure in an excavation.

All pore pressure fixities can be released and the computation proceeds with the prevailing pore pressure. After the release, the boundary becomes impermeable.

Icon	Description
	Incremental excess pore pressure selector.
	Sets uniform incremental excess pore pressure to an edge in 2-dimensional or a face in 3-dimension.
	Sets linearly varying incremental excess pore pressure to an edge in 2-dimensional or a face in 3-dimension.
	Absolute excess pore pressure selector.
	Sets uniform excess pore pressure to an edge in 2-dimensional or a face in 3-dimension.
	Sets linearly varying excess pore pressure to an edge in 2-dimensional or a face in 3-dimension.

Icon	Description
	Total hydraulic pressure head selector. Atmospheric pressure head is assumed to be zero.
	Sets uniform total hydraulic pressure head to an edge in 2-dimensional or a face in 3-dimension.
	Sets linearly varying total hydraulic pressure head to an edge in 2-dimensional or a face in 3-dimension.

### 8.4.1 Node assignment

This fixity type is applicable to both 2-and 3-dimensional meshes. The nodal assignment is useful as a point source or sink for groundwater flow. This type of assignment is not available in the current version.

### 8.4.2 Edge assignment

This fixity type is applicable to 2-dimensional meshes only. This type of assignment in 3-dimensional space is not available in the current version.

Two different edges with the same length and in the same position (duplicates) will be fixed. So both edges are applied with the same fixity type and value. This will ensure that both the edges for initial and replacement elements are fixed.

For zero value, there is no need to set thus not possible to set this fixity type at the same edge until after it is released at some stage because of the inheritance characteristic of this type of fixity.

A fixed value can be applied to the same edge over different stages. Due to the inheritance characteristic, the successive applications of this fixity type are interpreted as incremental values.

### 8.4.3 Face assignment

This fixity type is applicable to 3-dimensional meshes only.

Two different faces with the same shape and in the same position (duplicates) will be fixed. So both faces are applied with the same fixity type and value. This will ensure that both the faces for initial and replacement elements are fixed.

Strictly no faces should be fixed with zero pressure twice. Thus, it is not possible to set this fixity type at the same face until after it is released at some stage because of the inheritance characteristic of this type of fixity.

A fixed pressure can be applied to the same face over different stages. Due to the inheritance characteristic, the successive applications of this fixity type are interpreted as incremental values.

## 8.5 Load (stage) workgroup

There are two important concepts to note when applying loads to the mesh. The first is inheritance characteristic and the second is the incremental nature of the solution method.

The conventions that are adhered to in the input and output data files are:

- Positive normal loads are compressive
- Negative normal loads are tensile
- Positive shear acts on element edges in an anti-clockwise direction about the element centre.

Three types of static loading are available. They are:

- nodal load,
- edge load and
- face load.

Icon	Description
	Nodal load is available in 2- and 3-dimensional analyses. The load can be applied to vertex nodes only.
	Edge load selector.
	Sets uniformly distributed load to an edge in 2- or 3-dimension. The load can be applied to straight or curved edges.
	Sets linearly varying distributed load to an edge in 2- or 3-dimension. The load can be applied to straight or curved edges.
	Sets parabolically distributed load to an edge in 2- or 3-dimension. The load can be applied to straight or curved edges.
	Face load selector for 3-dimension only.
	Sets uniformly distributed load to a face in 3-dimension. The load can be applied to flat or curved faces.
	Sets distributed load that varies linearly along the $x$ -direction to a face in 3-dimension. The linear load variation is interpolated between two user specified load values and $x$ -ordinates. The load can be applied to flat or curved faces.
	Sets distributed load that varies linearly along the $y$ -direction to a face in 3-dimension. The linear load variation is interpolated between two user specified load values and $y$ -ordinates. The load can be applied to flat or curved faces.

Icon	Description
	Sets distributed load that varies linearly along the z-direction to a face in 3-dimension. The linear load variation is interpolated between two user specified load values and z-ordinates. The load can be applied to flat or curved faces.
	Sets distributed load that is interpolated from 3 or 4 user specified corner values on a face in 3-dimension. Specifying 3 corner values give a coplanar variation of the load while 4 corner values give a bilinearly interpolated load distribution over the face. The load can be applied to face with 3 or 4 edges only.

***Tips:** It is recommended to avoid applying external loads and pore pressure boundary conditions in the same increment. This is because the pore pressure at a given node is changed by two different sources.*

The desired distributed tractions on portions of the mesh are defined by interpolation patches.

The load applied in a stage will be equally divided across the number of increments in the stage.

All loads can be released and the program takes care of that load application by applying the same magnitude of the load in the opposite direction.

### 8.5.1 Node assignment

This fixity type is applicable to both 2-and 3-dimensional meshes.

A nodal load can be applied to the same node over different stages. Due to the inheritance characteristic, the successive applications of this fixity type are interpreted as incremental values.

Although the equation solver in the finite element program deals with nodal loads, the user is advised against converting distributed loads manually unless the user has in-depth knowledge of the theory of consistent nodal loads in finite element method.

### 8.5.2 Edge assignment

This fixity type is applicable to both 2-and 3-dimensional meshes.

The load distribution can be applied to the same edge over different stages. Due to the inheritance characteristic, the successive applications of this fixity type are interpreted as incremental values.

### 8.5.3 Face assignment

This fixity type is applicable to 3-dimensional meshes only.

A face pressure load can be applied to the same face over different stages. Due to the inheritance characteristic, the successive applications of this fixity type are interpreted as incremental values.

## 8.6 Common (stage) workgroup

This workgroup simplifies the application of some common boundary conditions by grouping different fixity conditions into one operation.

Icon	Description
	Fixes the translations for all distal boundaries parallel to the $x$ - $y$ and $y$ - $z$ planes in the out-of-plane directions and the bottom most horizontal boundary in all directions. This condition is applied to edges in 2-dimension or faces in 3-dimension. Oblique planes will not be fixed.
	Maintains the pore pressure head at the selected face. This is commonly used to set the far-field groundwater recharging condition at the mesh boundaries. This condition is applied to edges in 2-dimension or faces in 3-dimension.
	Fixes the translations and rotations at one end of a beam element. This simulates the fixed end of a beam. This condition is applied to nodes only.
	Fixes the translations but not the rotations at one end of a beam element. This simulates the pinned end of a beam. This condition is applied to nodes only.
	Fixes the rotation but not the translations at one end of a beam element to model a zero slope condition. This simulates the mid-span condition for an uniform beam with symmetrical loading. This condition is applied to nodes only.

## 8.7 State (stage) workgroup

Icon	Description
	Views the objects that are currently active in the finite element mesh. While the view is active, selecting objects and press "ENTER" will exclude the selections from the current mesh.
	Views the objects that are inactive in the finite element mesh. While the view is active, selecting objects and press "ENTER" will include the selections into the current mesh.

# Chapter 9 Solution panel

Selecting **Solution** on the Workflow panel reveals a set of tools on the Solution panel.

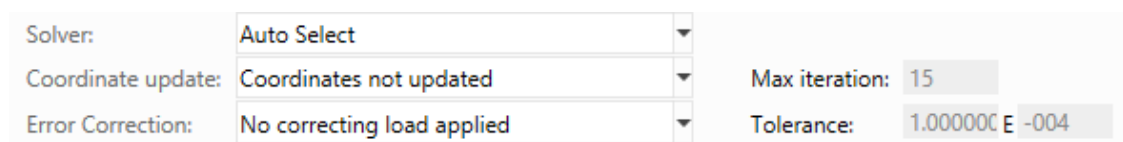


Figure 59: Solution settings

## 9.1 Solver

A number of iterative solvers are provided for the solution of different types of problems. Not all solvers are created equal. Depending on the problem type, user has to select the appropriate solver. However, a novice user who has little or no prior knowledge of iterative solvers and their characteristics may find it difficult to select an appropriate solver for the problem. Auto-select solver is designed to select the solver using a predefined set of rules.

## 9.2 Coordinates update

### 9.2.1 Coordinates not updated

This corresponds to the normal assumption that is made in linear elastic finite element formulation. External loads and internal stresses are assumed to be in equilibrium in relation to the undeformed geometry of the finite element mesh. This is known as the small displacement assumption.

### 9.2.2 Coordinates updated

This option updates the nodal coordinates after each increment of the analysis by adding the displacement undergone by the nodes during the increment to the coordinates. The stiffness matrix of the continuum is then calculated with respect to these new coordinates during the next analysis increment. The intention of this process is that at the end of the analysis, equilibrium will be satisfied in the deformed configuration.

Although this approach would seem to be intuitively more appropriate when there are significant deformations, it should be noted that it does not constitute a rigorous treatment of the large strain behaviour for a new definition of stresses and strains are required. In most situations, the inclusion of large strain effects leads to a stiffer load-deformation response near failure or some enhancement of the load carrying capacity. This response cannot be simulated in the coordinates update option.

### 9.2.3 Updated Lagrangian scheme

The updated Lagrangian scheme is the general continuum mechanics formulations for geometric nonlinear problems resulting from large displacement. It linearizes the equation of the principle of virtual displacements. This formulation refers to all the static and kinematic variables corresponding to the last calculated configuration.

During the linearization process, the nonlinear strain terms are ignored resulting in out-of-balance load. In order to reduce the “out-of-balance” virtual work form, we need to perform iteration in the above process until the difference between the internal and the external virtual work is negligible within a certain convergence measure. Thus, Newton Raphson’s scheme should be used.

## 9.3 Error correction

It is necessary to specify external loading that is in equilibrium with the in-situ stresses at the start of the analysis. Equilibrium checks are carried out in the in-situ stage and at the end of each increment.

The out-of-balance load will be generated when the total load from the self-weight and external pressure does not add up to the nodal loads equivalent to the element stresses.

During in-situ equilibrium check, this happens when:

- The specified external loads were not accounted in the in-situ reference stress.
- There are two sets of elements occupying the same space.
- Boundaries are inappropriately restrained.
- There are gaps in the mesh.

During stage increments, errors arise because:

- Too little increments are used for the stage.
- Stress points turn plastic.
- Boundaries are inappropriately restrained.
- Highly nonlinear characteristic is encountered; geometric and material nonlinearities.
- Stress redistribution by the correction scheme is ineffective.

For analyses using any elastic perfectly plastic constitutive model without Newton Raphson's scheme, equilibrium errors up to 20% are acceptable. While elastic or critical state constitutive models are used, equilibrium errors should not exceed 5%. These errors arise from the estimation of nonlinear behaviour in the soil (material nonlinearity) by a system of linear equations.

The appropriate stress correction scheme should be Newton Raphson's scheme. This scheme corrects the equilibrium errors within each increment. Only the out-of-balance loads are checked based on input tolerance value and maximum Newton-Raphson's iteration allowed by the user. The Newton-Raphson's tolerance criterion will adjust dynamically if the system diverges or remains stagnant. The Newton Raphson's scheme ensures that the equilibrium errors will be sufficiently small before proceeding to the next increment.

Applying the correction load in the next increment is not exactly appropriate and the last increment will have its out-of-balance loads discarded. It will lead to erroneous results if the discarded loads are large.

Other options of not applying correction should only be used for elastic material where the stress-strain relationship is linear or for test-runs.

## 9.4 Running the analysis

Option is provided to store results for all increments in the analysis or only at the end of each block to conserve hard disk space utilisation. Begin the analysis by clicking on the green arrow button. The green arrow icon will be changed into a red square icon indicating that the analysis is in progress.

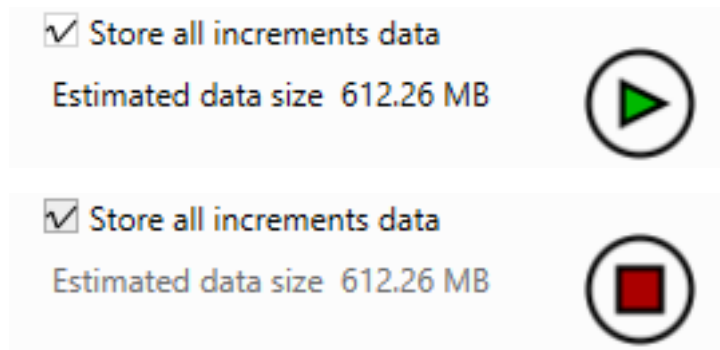


Figure 60: Starting and stopping the analysis

A solution status window will appear during the solution process presenting the analysis progress and the convergence of the iterative methods in use. When the analysis is completed, "Status: Completed" will be displayed. Proceed to click the "OK" button to view results.

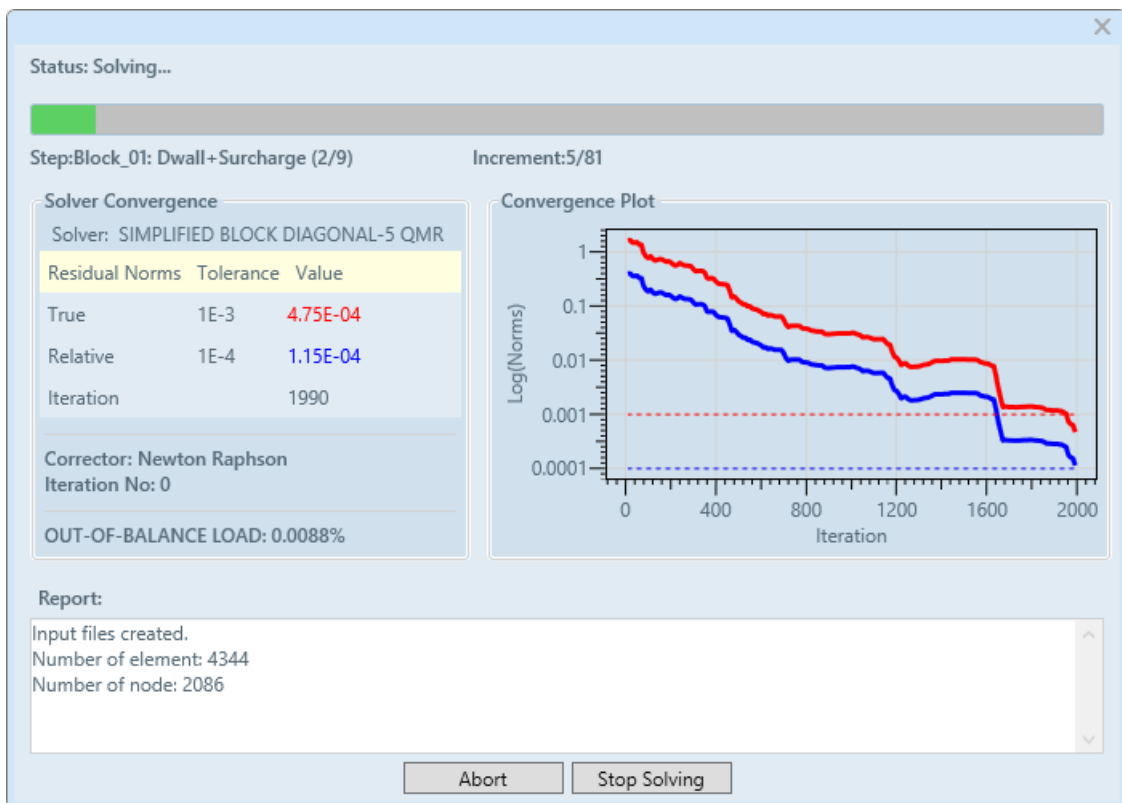


Figure 61: Solution in progress

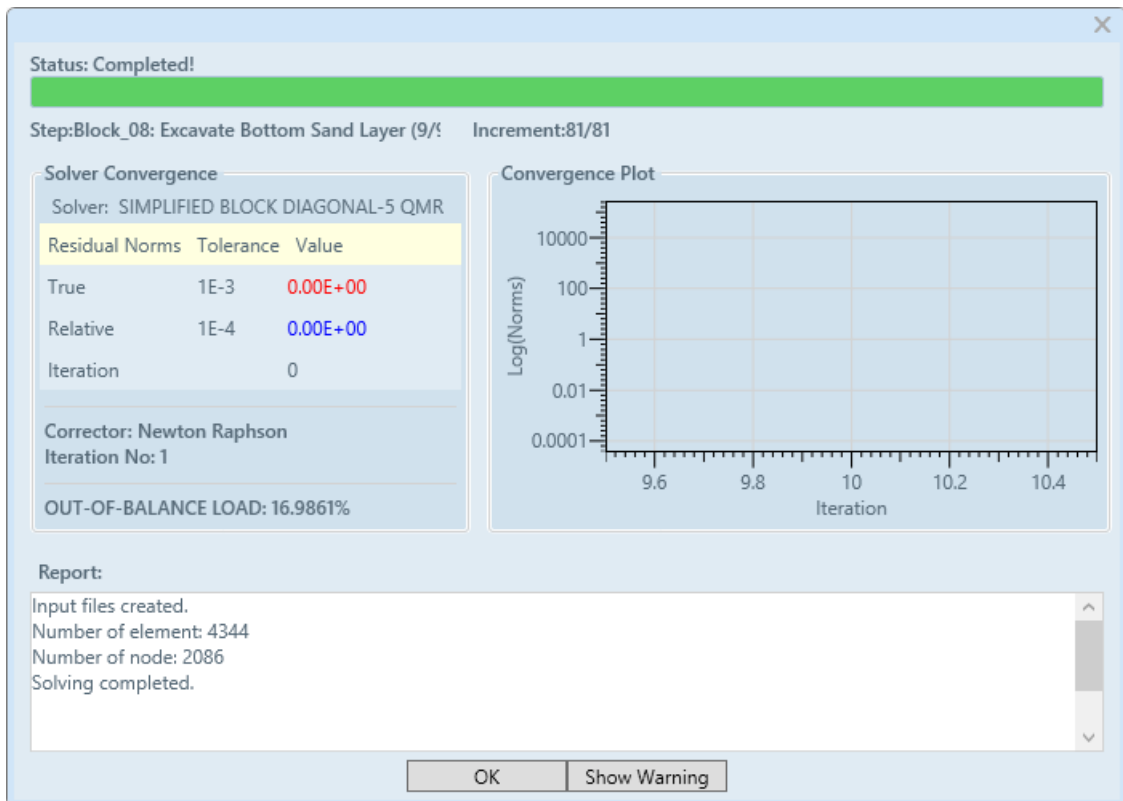


Figure 62: Solution completed

**Tips:** Frontal solution is not an iterative method.  
 Convergence plot will not appear when Frontal solver is used.

This page is intentionally left blank.

# Chapter 10 Result panel

Selecting **Result** on the Workflow panel reveals a set of tools on the Result panel.

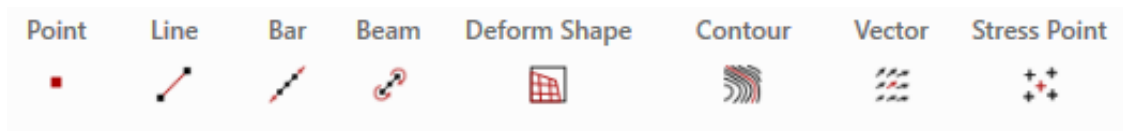


*Figure 63: Result panel*

## 10.1 Point

Point plot identifies results at the desired locations and generates a 2D graph of the selected variable versus solution steps, time or another variable. Values from all increments will be plotted.

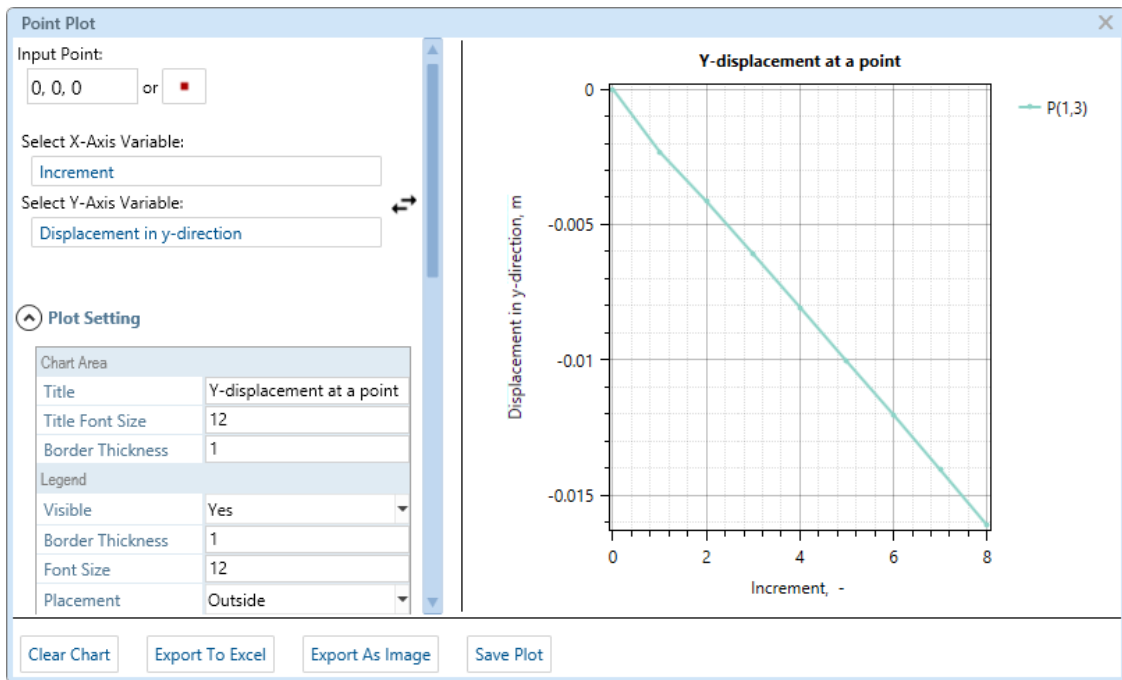


Figure 64: Point plot window

"Input Point" allows selection through coordinate input or simply clicking on the desired location on the mesh. The "Show Grid" option in the Common Work Panel must be enabled for click selection.

The variables on the  $x$ -axis and the  $y$ -axis can be interchanged by clicking on the switch button to the side of the variables selection.

The plot is customisable for the options provided in the "Plot Setting". A few noteworthy settings are:

- Chart and axes titles can be renamed.
- Marker shape can be changed.
- Legends can be repositioned.
- Order of values can be ascending or descending.

Plot Setting

Chart Area	
Title	Chart Title
Title Font Size	12
Border Thickness	1
Legend	
Visible	Yes
Border Thickness	1
Font Size	12
Placement	Outside
Position	RightTop
Line	
Style	Solid
Marker	
Size	2
Type	Circle
X Axis	
Font Size	12
Line Thickness	1
Major Grid Thickness	1
Minor Grid Thickness	1
Sequence	Ascending
Visible	Yes
X Axis Title	
Name	X Axis Title
Position	10
Font Size	12
Y Axis	
Font Size	12
Line Thickness	1
Major Grid Thickness	1
Minor Grid Thickness	1
Sequence	Ascending
Visible	Yes
Y Axis Title	
Name	Y Axis Title
Position	20
Font Size	12

Figure 65: Plot setting

## 10.2 Line

Line plot generates a 2-D graph of the desired result on a selected edge of the model. The graph displays the result versus actual model distance along the selected edge. This option is available when you select only one edge.

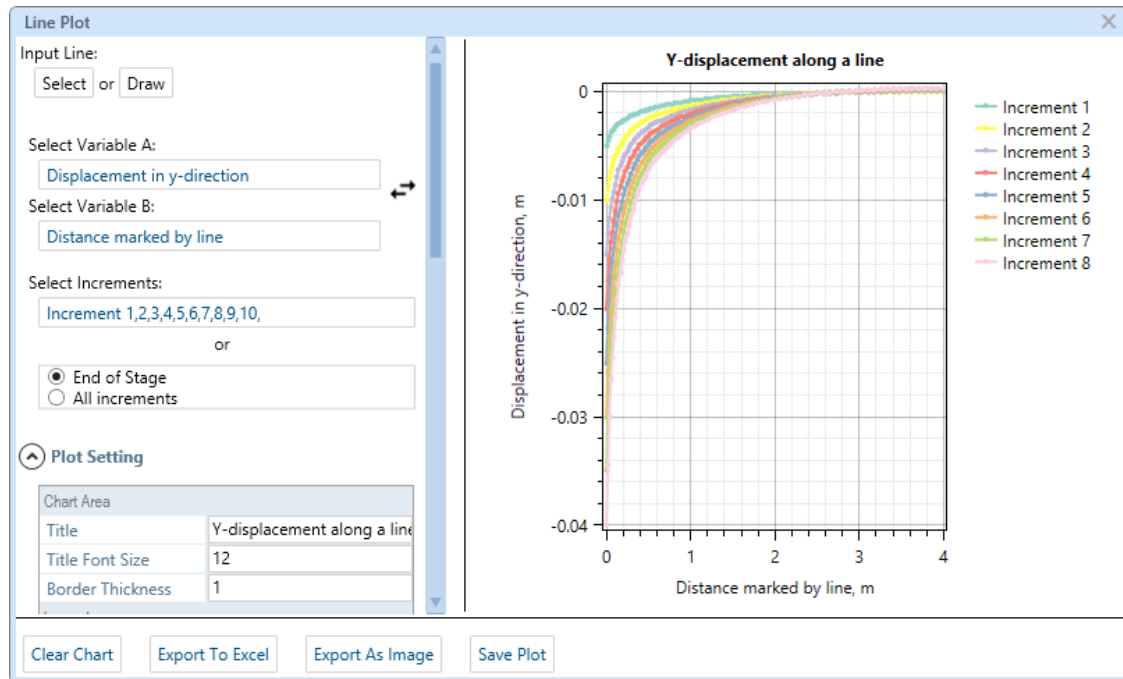


Figure 66: Line plot window

"Input Line" allows selection through clicking on the desired line on the mesh or draw a user defined line for processing.

The variables on the  $x$ -axis and the  $y$ -axis can be interchanged by clicking on the switch button to the side of the variables selection.

"Select Increment" allows the number of increments to be selected as desired.

The plot is customisable for the options provided in the "Plot Setting".

The graph data can be exported as Microsoft Excel or image (PNG/JPEG) format.

## 10.3 Bar

The bar plot opens the viewing result environment for bar element only.

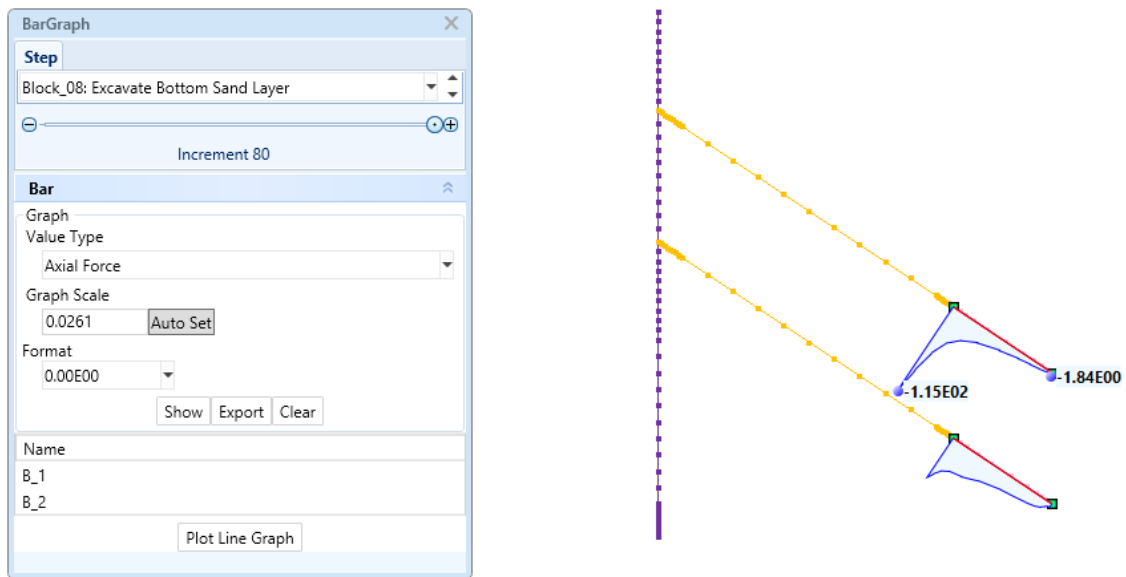


Figure 67: Bar result window

The "Value Types" of result for bar consist:

- Axial force
- $x$ -displacement
- $y$ -displacement
- $z$ -displacement (3-dimension analysis only)
- displacement normal

The data profile for the selected variable in the current stage will be plotted along the bar element upon clicking "Show". Multiple bar entities can be selected if desired. The graph can be exported to Microsoft Excel by clicking on "Export".

**Good practice:** Use a single continuous line to represent the bar entity when creating geometry as much as possible. This make selection of the entity easy during the post-processing operation.

"Graph Scale" will scale the graph plotted on the bar according to the factor. An auto scaling feature is available for user where the scale factor is not crucial to the presentation.

"Format" option allows formatting of the values shown on the display.

A multi-stage line graph can be plotted for the selected bar elements. The bar entities that are available for selection are named in increasing numerical order. Select the desired entity and the corresponding on-screen plot will be highlighted.

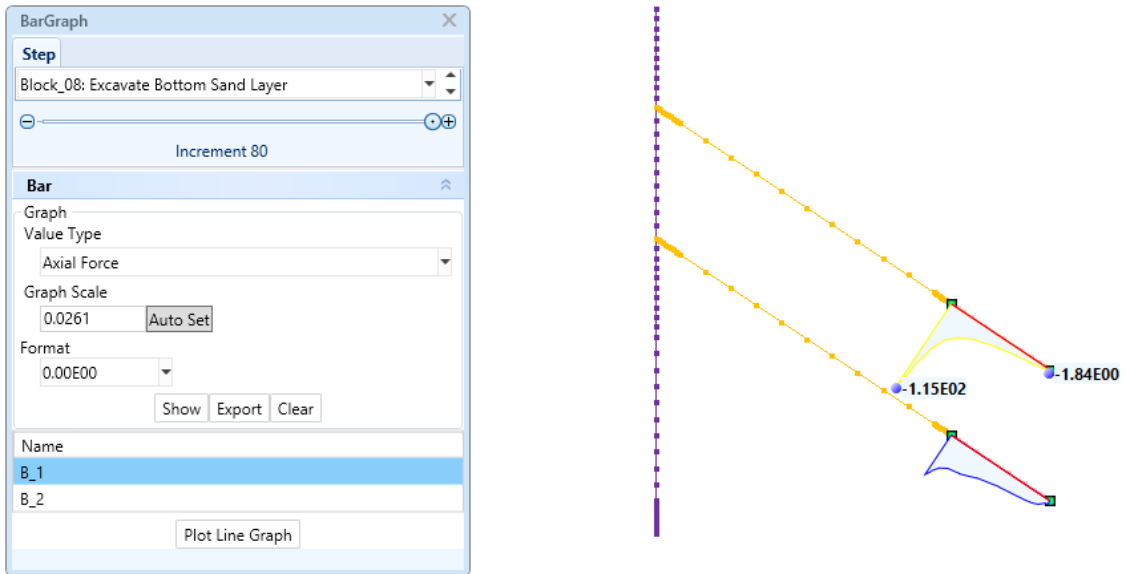


Figure 68: Selection of bar entity for line graph in result window

Click "Plot Line Graph" to generate the multi-stage line graph for the selected entity.

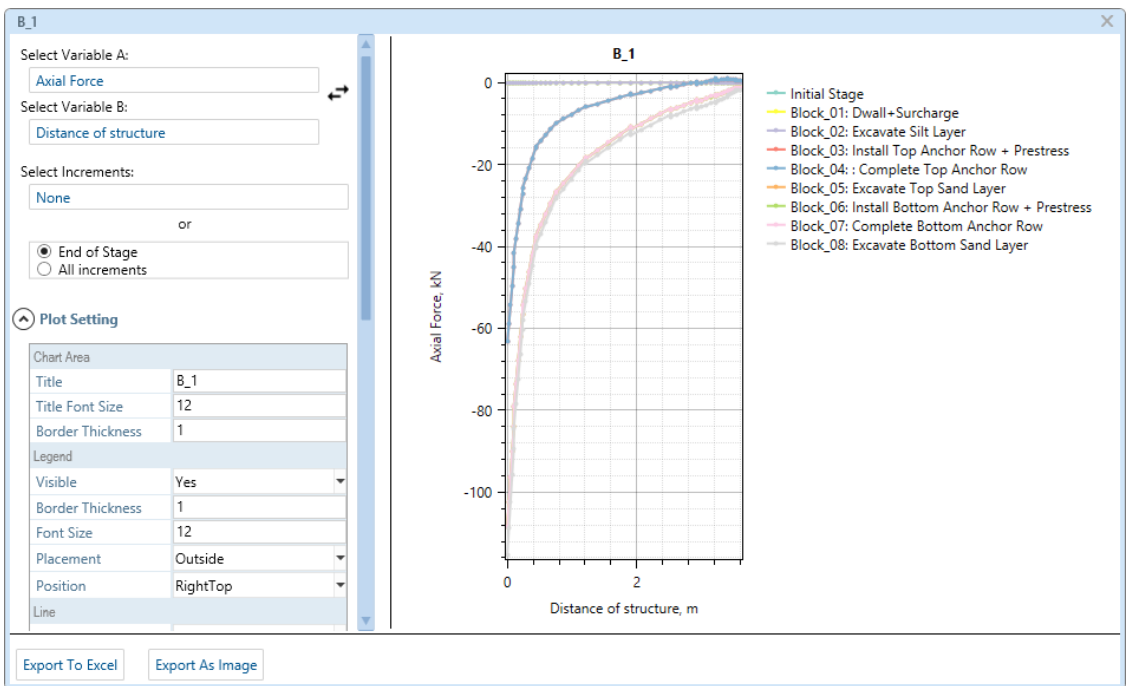


Figure 69: Line graph for selected of bar entity

The plot can be similarly customized or exported as described in the line plot.

Click "Clear" to remove the plot along the bar and the line graph.

## 10.4 Beam

The beam plot opens the viewing result environment for beam element only.

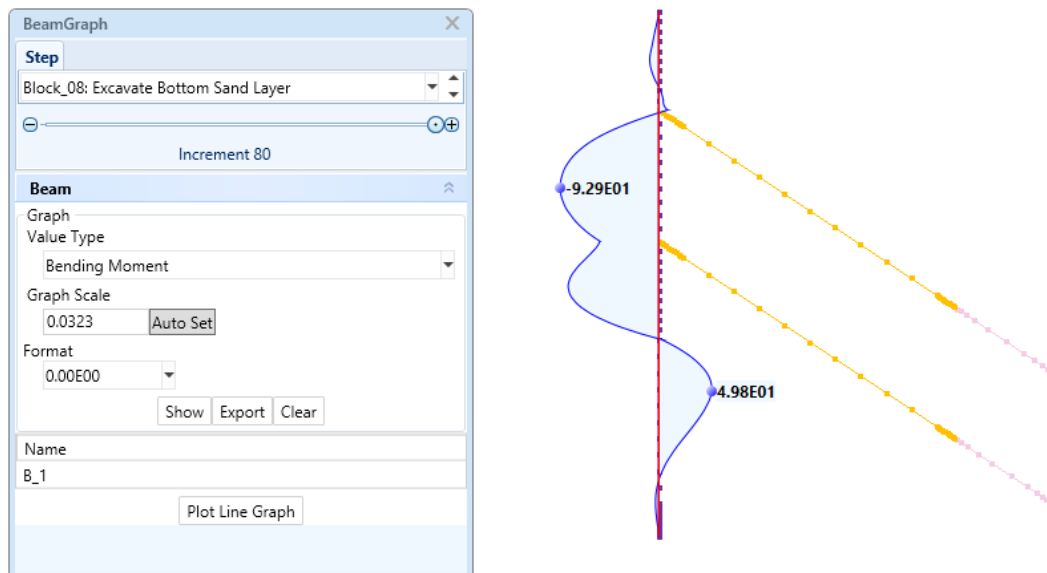


Figure 70: Beam result window

The "Value Types" of result for beam consist:

- Axial force
- Shear force
- Bending moment about  $x$ -axis (3-dimension analysis only)
- Bending moment about  $y$ -axis (3-dimension analysis only)
- Bending moment about  $z$ -axis
- $x$ -displacement
- $y$ -displacement
- $z$ -displacement (3-dimension analysis only)
- displacement normal

The graph for the selected variable will be plotted along the beam element. The plot can be similarly customized or exported as described in the bar plot. The bending moment envelope throughout the construction stages can be derived from the multi-stage line graph option.

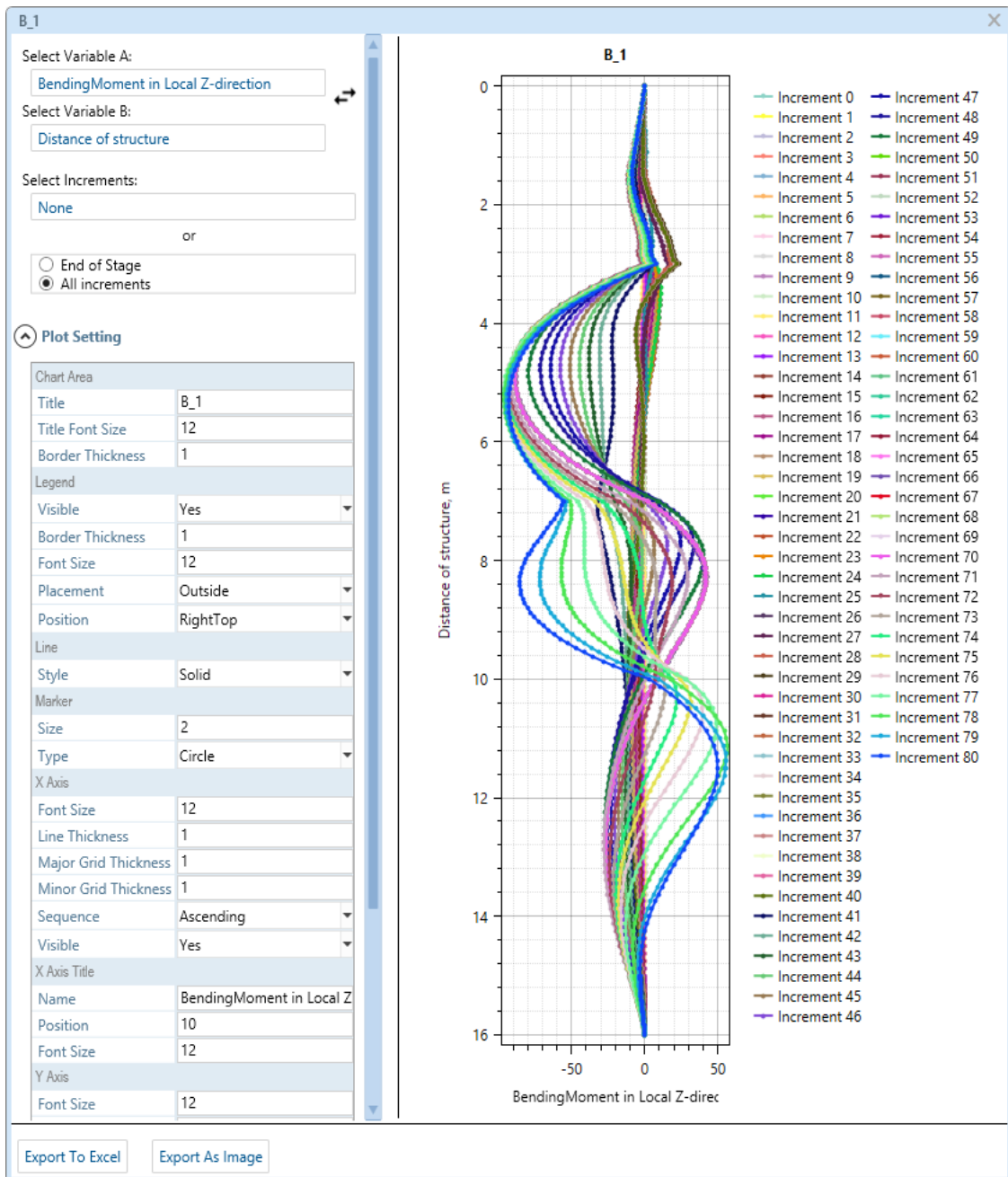


Figure 71: Line graph for selected of beam entity

"Graph Scale" will scale the graph plotted on the beam according to the factor. An auto scaling feature is available for user where the scale factor is not crucial to the presentation.

"Format" option allows formatting of the values shown on the display.

## 10.5 Deform shape

A deformed plot shows the shape of your model according to the values of a nodal displacement.

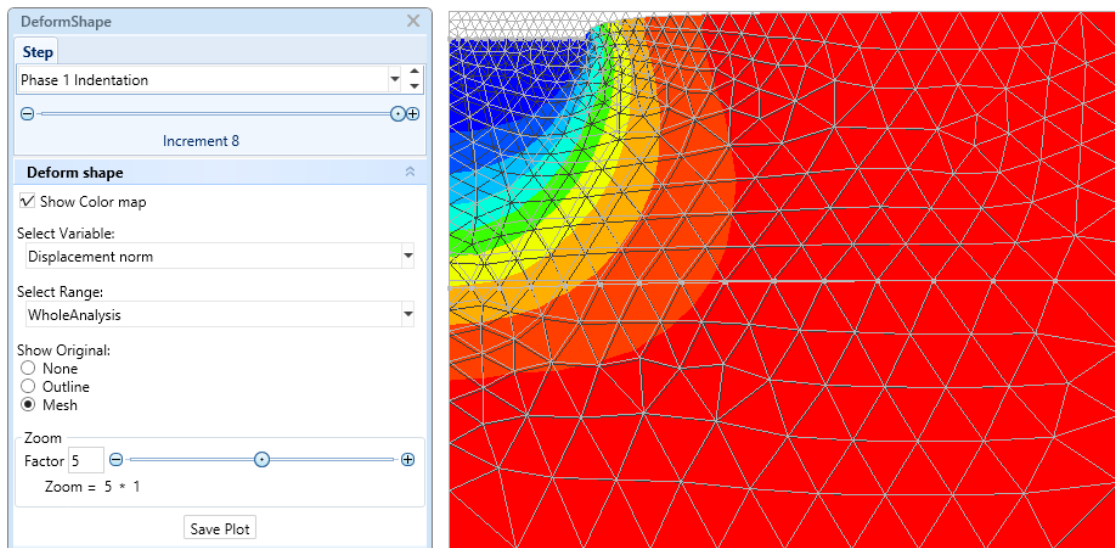


Figure 72: Deform mesh plot

"Show Color Map" checkbox allows the mesh to be contoured and coloured according to nodal displacement values when checked.

"Select Variables" only have one variable, displacement norm, currently.

"Select Range" defines the maximum and minimum displacement of the contour values. The options are: "WholeAnalysis", "CurrentStep", "SurfaceValue" and "IncrementalChange". "WholeAnalysis" contours the current view against the extreme displacement values found in the whole analysis. "CurrentStep" contours the current view against the extreme values found within the stage in view. "SurfaceValue" contours the current view against the extreme values found on the surface of the current mesh view. "IncrementalChange" computes the difference in nodal displacement between the current and previous stages. The contours reflects the incremental displacement from the previous stage.

"Show Original" option superimposes the undeformed geometry of the mesh according to the selected radio button.

"Zoom" sets the displaced node position according to zoom factor applied to the actual displacement value.

## 10.6 Contour

During result extraction on a plane, coordinates labelled “U” and “V” are used. These are simply different letters chosen to avoid confusion over “X”, “Y” and “Z”. The processed image like contour plot is normally laid out on a flat, two-dimensional plane. Each point on the image can be identified by X and Y coordinates. Points on/in the object have X, Y and Z coordinates. So to avoid confusion, the points on the image are identified using U and V to label their coordinates instead of X and Y. We then refer to “UV mapping” as the process of determining where each (U, V) image point ends up on the (X, Y, Z) object. This “UV mapping” allows the contour values any points to be extracted where necessary.

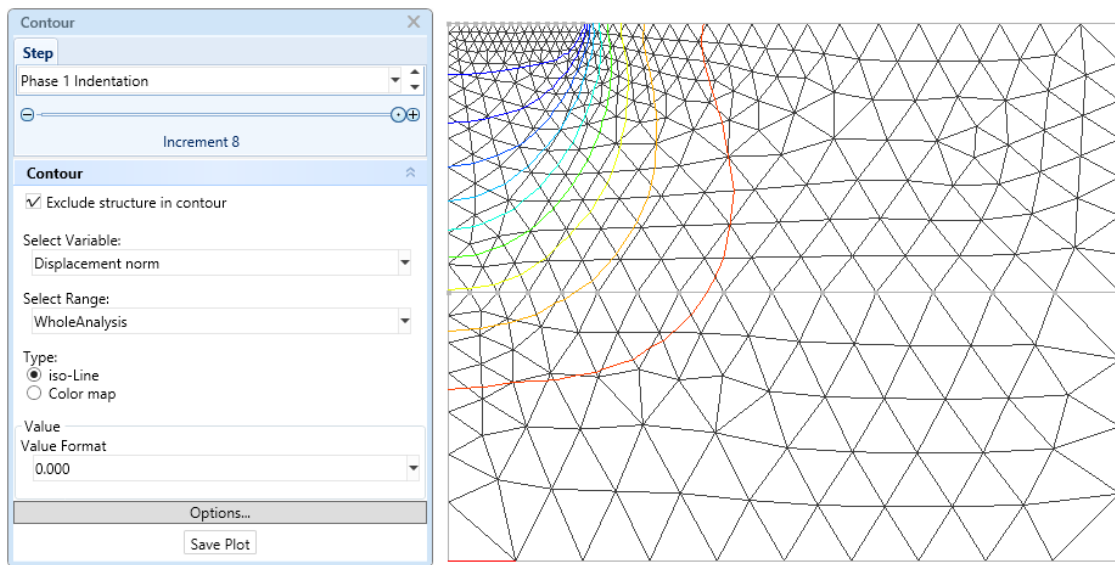


Figure 73: Contour plot using iso-lines option

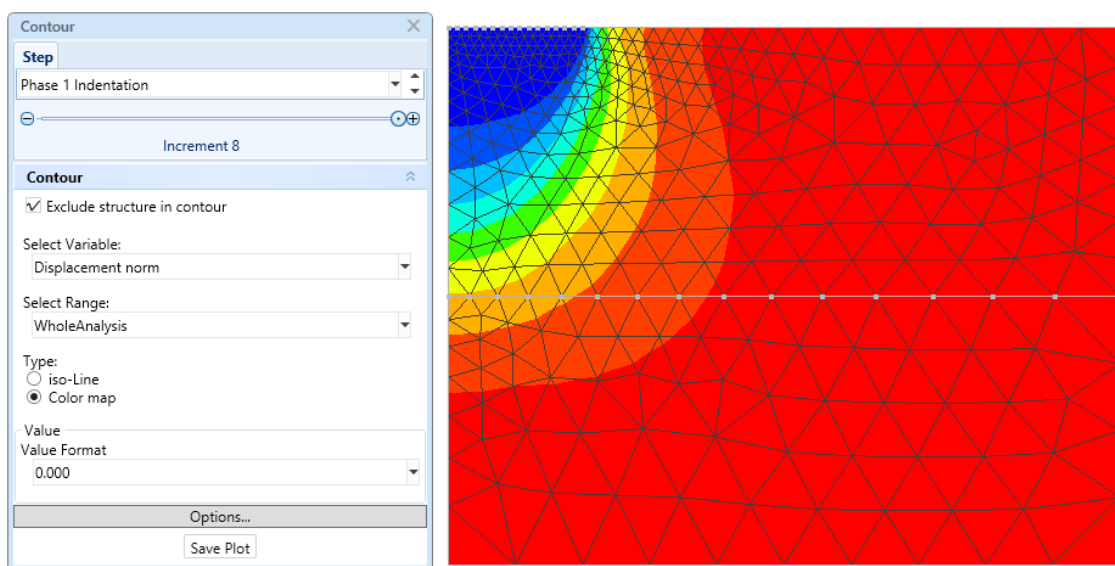


Figure 74: Contour plot using colour map option

"Exclude structure in contour" checkbox, when checked, omits the stresses within the structure from the contours computation.

"Select Variables" determined which variables will be plotted. Displacement vectors will show arrow head on each shaft of the direction vector to indicate the direction of movement. Stress vectors will not have arrow heads but shafts to indicate the stress orientation.

"Select Range" defines the extreme values of the results. The options are: "WholeAnalysis", "CurrentStep", "SurfaceValue" and "IncrementalChange". "WholeAnalysis" contours the current view against the extreme values found in the whole analysis. "CurrentStep" contours the current view against the extreme values found within the stage in view. "SurfaceValue" contours the current view against the extreme values found on the surface of the current mesh view. "IncrementalChange" computes the difference in values of the selected variable between the current and previous stages. The contours reflects the incremental change from the previous stage.

"Type" option allows the contours to be shown as either iso-lines or color map.

"Value" option allows formatting of the values shown on the display.

## 10.7 Vector

A vector plot is a type of cartesian chart where each point has an  $x$ ,  $y$  and  $z$  position, a length, and a direction. Vectors are drawn as arrows.

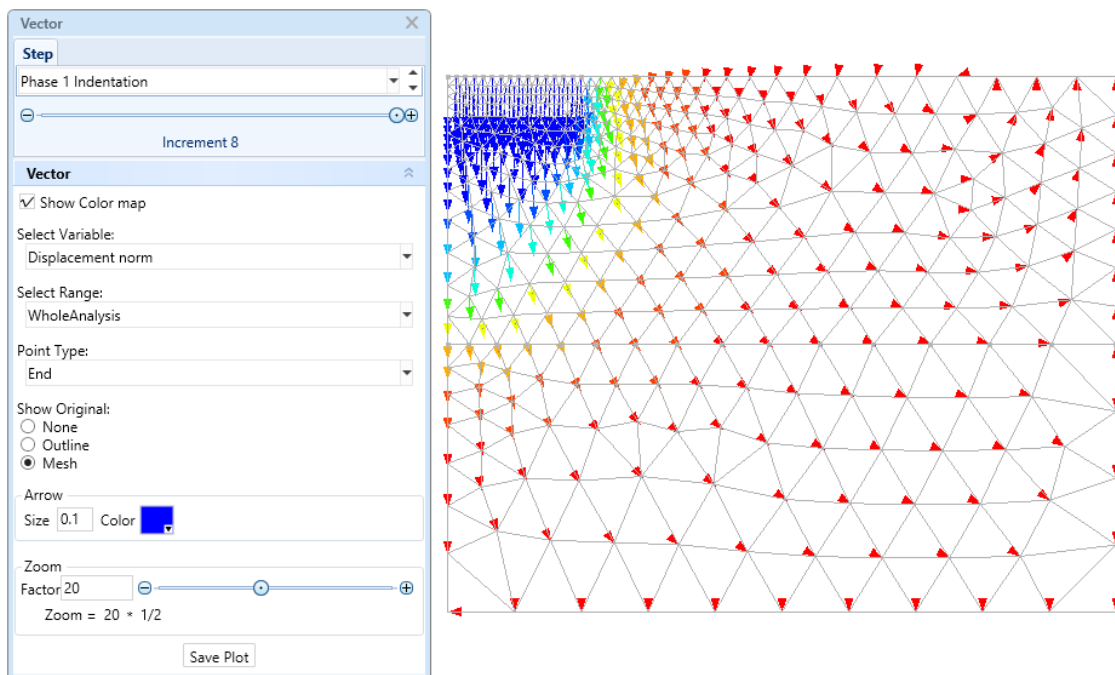


Figure 75: Vector plot

"Show Color Map" checkbox allows the vectors to be coloured according to their magnitude when checked.

"Select Variables" determined which variables will be plotted. Displacement vectors will show arrow head on each shaft of the direction vector to indicate the direction of movement. Stress vectors will not have arrow heads but shafts to indicate the stress orientation.

"Select Range" defines the extreme values of the results. The options are:

"WholeAnalysis", "CurrentStep", "SurfaceValue" and "IncrementalChange".

"WholeAnalysis" contours the current view against the extreme values found in the whole analysis. "CurrentStep" contours the current view against the extreme values found within the stage in view. "SurfaceValue" contours the current view against the extreme values found on the surface of the current mesh view. "IncrementalChange" computes the difference in values of the selected variable between the current and previous stages. The contours reflects the incremental change from the previous stage.

"Point Type" option sets the vector's point of rotation that could be the "Start", the "Center", or the "End". For displacement vectors, the default setting is "End" while for stress vectors is "Center".

"Show Original" option superimposes the undeformed geometry of the mesh according to the radio button selection.

"Arrow" sets the absolute size and the color (when the "Show Color Map" is unchecked) of the visual elements.

"Zoom" sets the relative size of each arrow according to zoom factor applied to the vector's magnitude.

## 10.8 Stress point

The stress point plots illustrate:

- "Yield Code" - the stress points that have turned plastic.
- "Local Factor of Safety" - the ratio of the current stress to the failure stress. In the elastic perfectly plastic models, the failure is defined by the yield envelope (the ratio of the shear strength versus its current mobilised strength). In the critical state models, the failure is considered at the critical state (the ratio of the current deviator stress,  $q$  versus  $q_{cs}$ ).

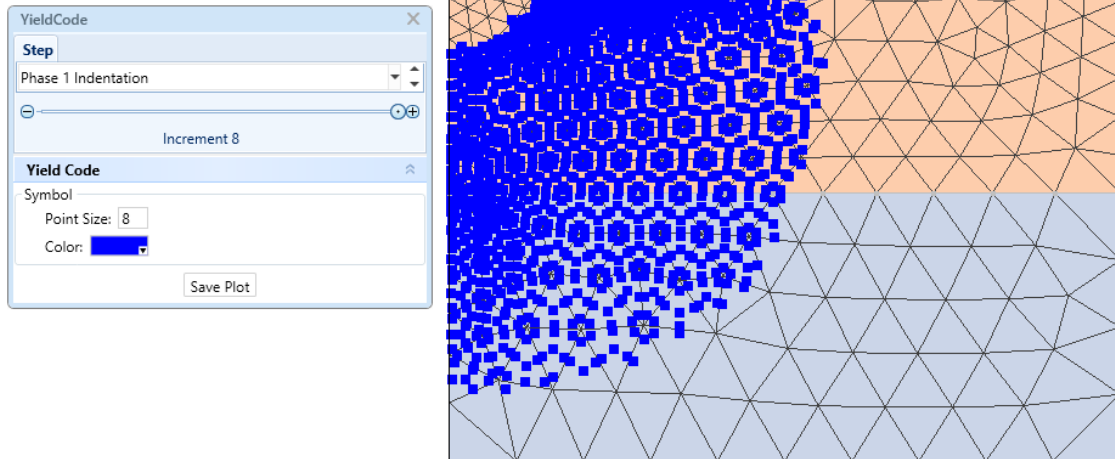


*Figure 76: Stress point plot*

"Symbol" sets the size and colour of the stress point markers.

This page is intentionally left blank.

# Chapter 11 Model explorer

The Model explorer located on the left side of the screen, below the Workflow explorer, allows the user to inspect the model entities. This is useful during setting up of construction stage. The various entities can be included in or excluded from the model by selecting from the entities listed.

The Model explorer consists of four tabbed panels: Model, Selection, Hidden and Layer.

The "Model" tab panel lists all the entities in the finite element model in a tree structure. "Model" tab panel exists in 2 modes: stage mode and result mode.

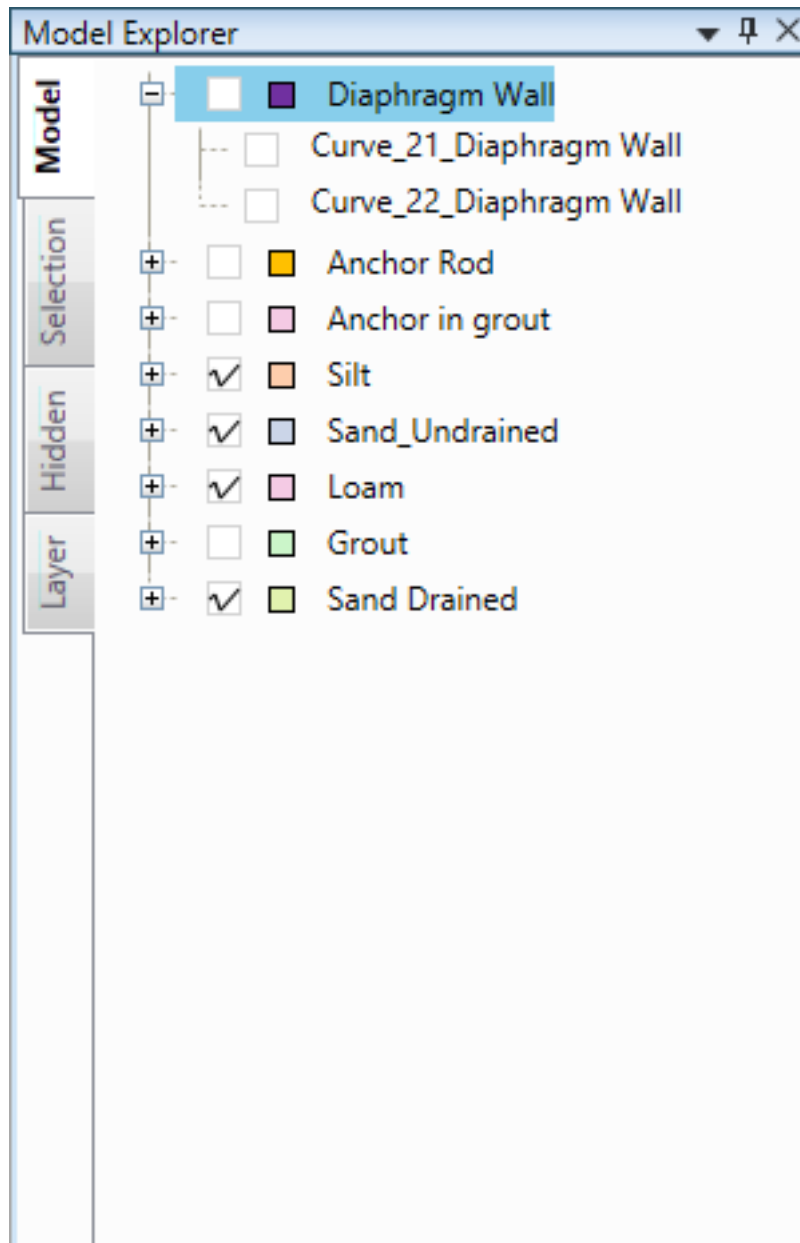


Figure 77: Model tab panel in model explorer (stage mode)

When the "Model" tab panel is in the stage mode, a series of check boxes appears at the front of each entity or each group of entities. The presence of a tick mark in the check box indicates that the corresponding entity is included in the mesh for the current stage as shown in the workspace. Unchecking the box will remove the entity from the mesh in the current stage. This function serves as an alternative way to include and exclude entities from the mesh at each stage.

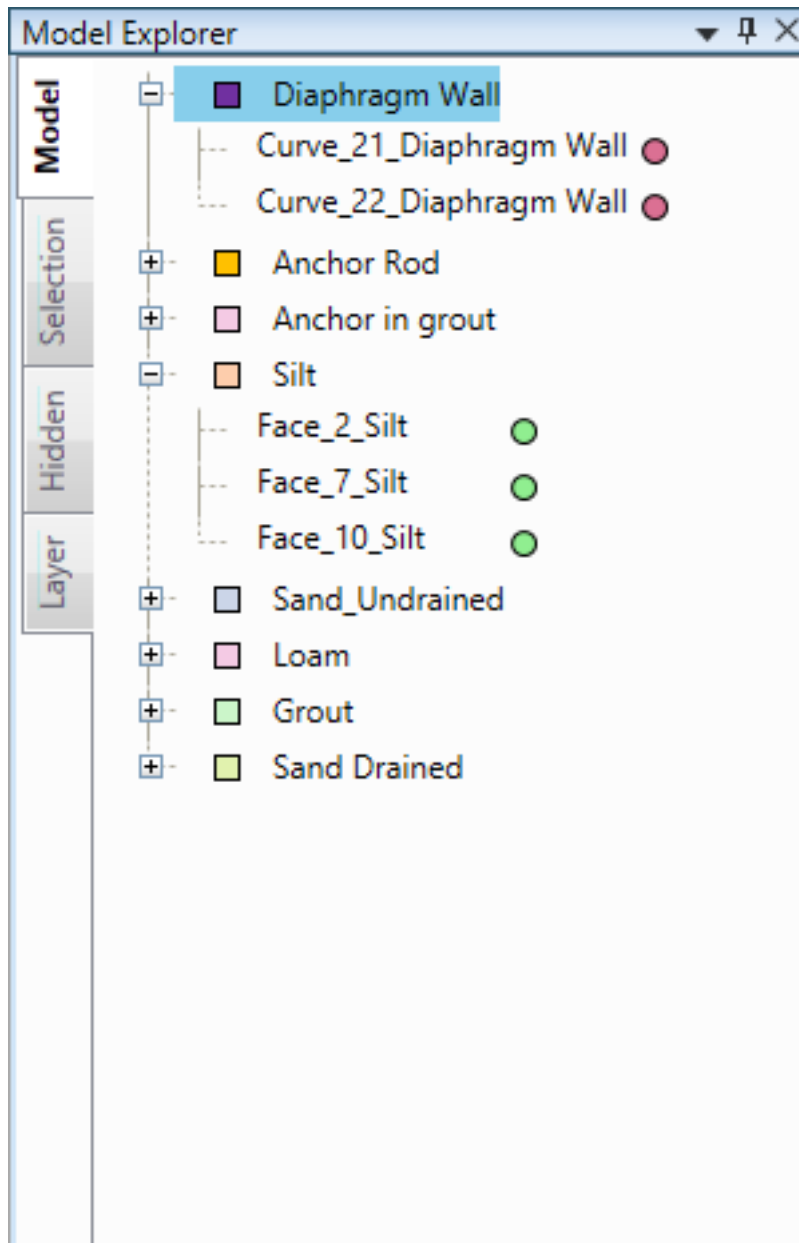
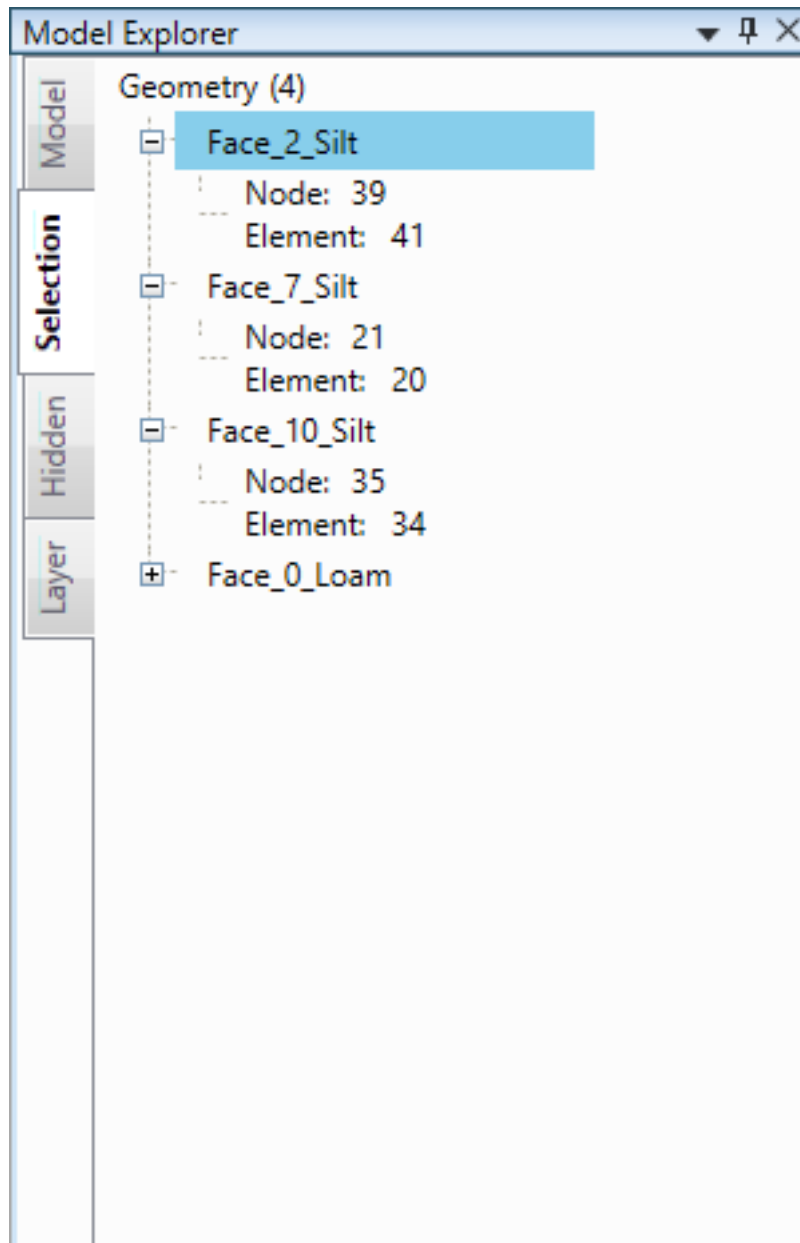


Figure 78: Model tab panel in model explorer (result mode)

When the "Model" tab panel is in the result mode, there is an indicator at the end of each entity name reflecting the presence of that entity in the current stage shown in the workspace. The indicator will only be shown after solution and the result folder is available. A green indicator indicates that the entity is currently included in the mesh and a red indicator indicates otherwise.



*Figure 79: Selection tab panel in model explorer*

The "Selection" tab panel lists the entities that are currently selected by the user. This is useful in locating and referencing the named entities. The number of nodes and elements contained in each entity can be shown by expanding the entity tree.

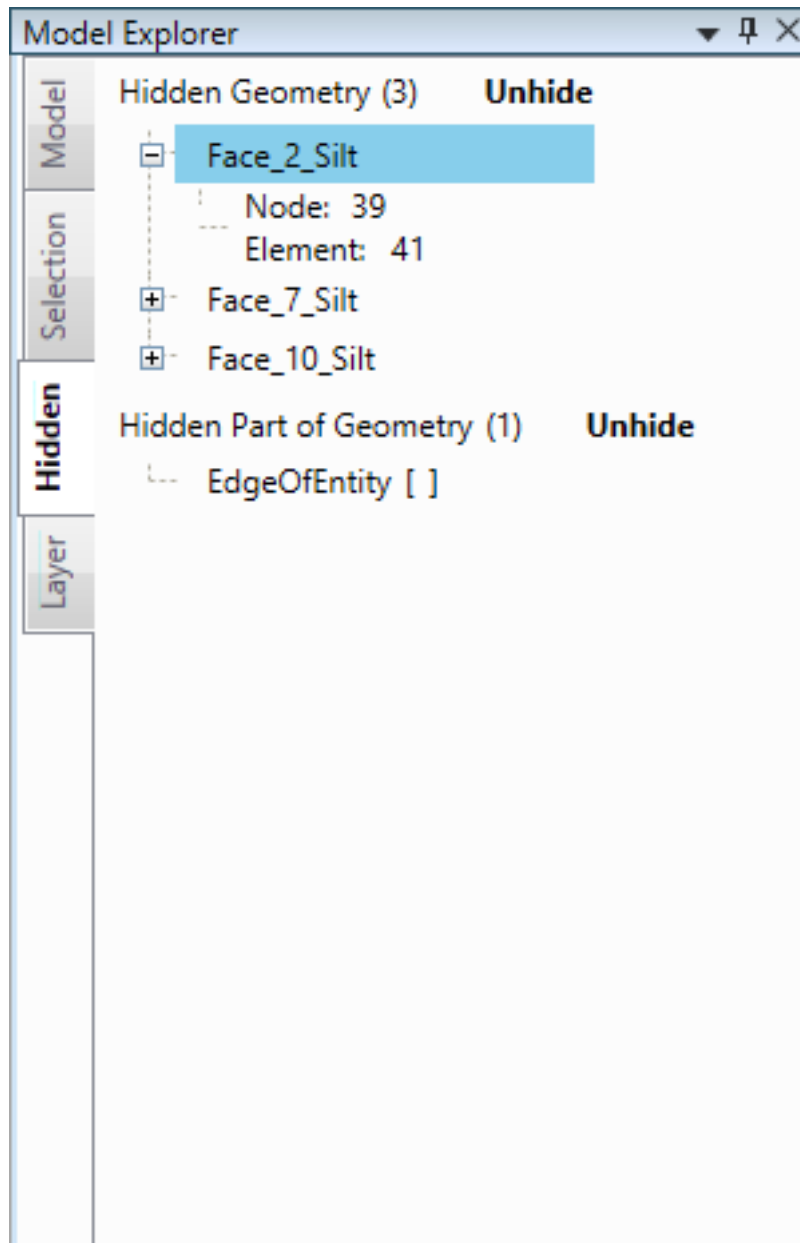


*Figure 80: Hidden tab panel in model explorer*

The "Hidden" tab panel lists the entities that are currently hidden by the user. This allows user to unhide the desired individual entities. Select the desired entity and click "Unhide". The name for part of geometry will be followed by a square bracket indication which entity the part belongs.

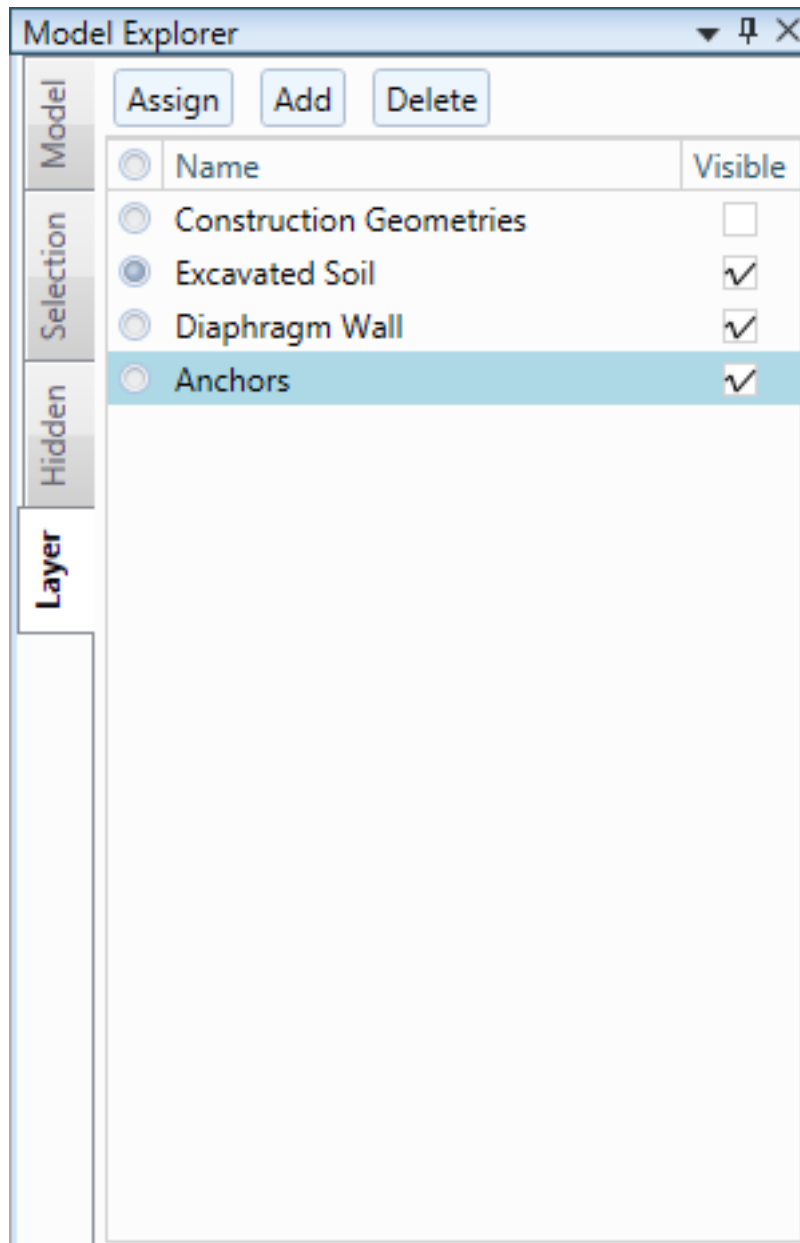


*Figure 81: Layer tab panel in model explorer*

The "Layer" tab panel segregate the objects into functional groups as desired by user. It allows grouping of entities with similar function rather than similar material type.

Add a named functional group within the panel. There are two methods to add entities to the functional group. First method is to identify the functional group by selecting the corresponding radio button. This results in all objects created thereafter to be assigned to that current functional group.

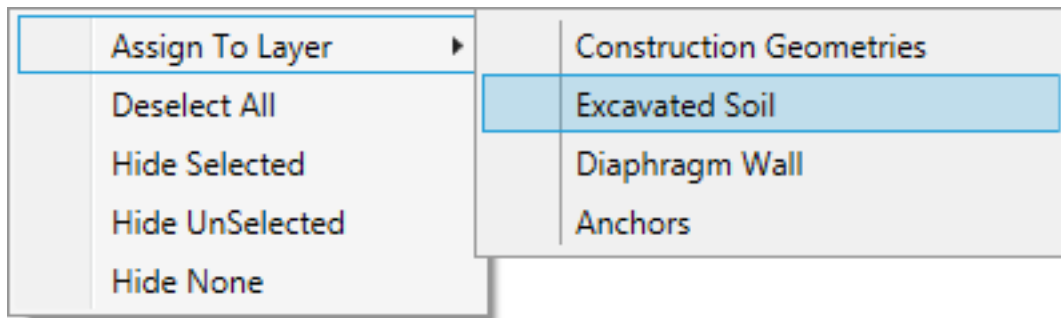


*Figure 82: Layer assignment to functional group*

Second method is to select the desired entity and right-click the entity to assign. Select "Assign to Layer" drops down a list of functional groups created. Select the desired functional group. The visibility of the entity in this functional group can be turned on or off by checking its "Visible" column.

This page is intentionally left blank.

# References

- Balasubramaniam, A.S., Phien-wej, N., Indraratna, B., and Bergado, D.T. (1989). Predicted Behaviour of a Test Embankment on a Malaysian Marine Clay. International Symposium on Trial Embankments on Malaysian Marine Clays, Kuala Lumpur, Malaysia, Vol. 2, pp. 1.1–1.18.
- Biot, M.A. (1941). General Theory of Three Dimensional Consolidation. *Journal of Applied Physics*, Vol. 12, pp. 155–164.
- Bolton, M. (1991). *A Guide to Soil Mechanics*. London: Macmillan Education Ltd.
- Bolton, M.D. (1986). The Strength and Dilatancy of Sands. *Geotechnique*, Vol. 36, No. 1, pp. 65-78.
- BSI (2015) BS 8002:2015: Code of practice for earth retaining structures. London: British Standards Institution.
- Carman, P.C. (1956). *Flow of Gases Through Porous Media*. New York: Academic Press Inc.
- Cryer, C.W. (1963). A Comparison of Three Dimensional Theories of Biot and Terzaghi. *Quarterly Journal of Mechanics and Applied Mathematics*, Vol. 16, No. 4, pp. 72–81.
- Dolinar, B., and Škrabl, S. (2013). Atterberg Limits in Relation to Other Properties of Fine-grained Soils. *Acta Geotechnica Slovenica*, Vol. 10, pp. 4–13.
- Drucker, D.C., and Prager, W. (1952). Soil Mechanics and Plastic Analysis on Limit Design. *Quarterly of Applied Mathematics*, Vol. 10, pp. 157–165.
- Duncan, J.M., and Buchignani, A.L. (1973). Failure of Underwater Slope in San Francisco Bay. *Proceedings of ASCE Journal of Soil Mechanics and Foundations Division*, Vol. 99, No. SM9, pp. 687–704.
- Hardin, B.O., and Black, W.L. (1969). Closure to vibration modulus of normally consolidated clays. *Proceedings of ASCE Journal of Soil Mechanics and Foundations Division*, Vol. 95, No. SM6, pp. 1531–1537.

- Hardin, B.O., and Drnevich, V.P. (1972) Shear modulus and damping in soils: Design equations and curves. Proceedings of ASCE Journal of Soil Mechanics and Foundations Division, Vol. 98, No. SM7, pp. 667–692.
- Hardin, B.O., and Richart, E.F.Jr. (1963). Elastic Wave Velocities in Granular Soils. Proceedings of ASCE Journal of Soil Mechanics and Foundations Division, Vol. 89, No. SM1, pp. 33–65.
- Hashiguchi, K. (1993). Fundamental requirements and formulation of elastoplastic constitutive equations with tangential plasticity. International Journal of Plasticity, Vol. 9, No. 5, pp. 525–549.
- Hatanaka, M., and Uchida, A. (1996). Empirical Correlation between Penetration Resistance and Effective Friction Angle of Sandy Soil. Soils & Foundations, Vol. 36, No. 4, pp. 1–9.
- Holtz, R.D., and Kovacs, W.D. (1981). An Introduction to Geotechnical Engineering. Englewood Cliffs, New Jersey: Prentice-Hall.
- Hough, B.K. (1957). Basic Soils Engineering. 1st Edition. New York: The Ronald Press Company.
- Jaky, J. (1944). The Coefficient of Earth Pressure at Rest. J. Soc. Hungarian Arch. Engrs., Vol. 78, No. 22, pp. 355–358 (in Hungarian). Cited from Hanna, A. and Ghaly, A. (1992). Effect of  $K_0$  and Overconsolidation on Uplift Capacity. Journal of Geotechnical Engineering ASCE, Vol. 118, No. 9.
- Kulhawy, F.H., and Mayne, P.H. (1990). Manual on Estimating Soil Properties for Foundation Design. Report EL-6800 Electric Power Research Institute, Palo Alto: Electric Power Research Institute.
- Ladd, C., Foot, R., Ishihara, K., Schlosser, F., and Poulos, H. (1977). Stress-deformation and Strength Characteristics. Proceedings of the 9th International Conference on Soil Mechanics and Foundation Engineering, Japanese Society of Soil Mechanics and Foundation Engineering, Tokyo, Japan. Vol. 2, pp. 421–494.
- Lee, J., Kim, G., Kim, I., Kim, D., and Byun, B. (2016) Effect of Inter-particle Strength on  $K_0$  Correlation for Granular Materials. Proceedings of the 5th International Conference on Geotechnical and Geophysical Site Characterisation, ISC 2016, (Sydney: Australian Geomechanics Society). Vol. 2, pp. 1003–1007.
- Liao, S.S., and Whitman, R.V. (1986). Overburden Correction Factors for SPT in Sand. Journal of Geotechnical Engineering, Vol. 112, No. 3, pp. 373–377.
- Masing, G. (1926). Eigenspannungen und Verfestigung beim Messing. Proceedings of 2nd International Congress of Applied Mechanics.
- Mayne, P.W., and Kulhawy, F.H. (1982).  $K_0$ -OCR Relationships in Soil. Journal of Geotechnical Engineering Division, ASCE, Vol. 108, No. GT6, pp. 851–872.
- Mayne, P.W. (1992). In-situ characterization of Piedmont residuum in eastern US. Proceedings of NSF US-Brazil Geo-Workshop: Application of Classical Soil Mechanics to Structured Soils, Belo Horizonte, pp. 89–93.

- Muir Wood, D. (1990). *Soil Behaviour and Critical State Soil Mechanics*. Cambridge: Cambridge University Press.
- NAVFAC (1986). *Foundations and Earth Structures, Design Manual NAVFAC DM-7.02*. Naval Facilities Engineering Command (NAVFAC), Washington, D.C.: U.S. Government Printing Office.
- Nasim, A.S.M. (1999). *Numerical Modelling of Soil Profile and Behaviour in Deep Excavation Analyses*. M. Eng. Thesis, National University of Singapore.
- Poulos, H.G., Lee, C.Y., and Small, J.C. (1989). Prediction of Embankment Performance on Malaysian Marine Clays. *International Symposium on Trial Embankments on Malaysian Marine Clays, Kuala Lumpur, Malaysia, Vol. 2*, pp. 1.22–1.31.
- Rendulic, L.(1936). Porenziffer und Porenwasserdruck in Tonen. *Der Bauingenieur*, Vol. 17, pp. 559–564.
- Roscoe, K.H., and Burland, J. B. (1968). On the Generalised Stress-strain Behaviour of 'Wet' Clay. in J. Heyman and F.A. Leckie (eds.), *Engineering Plasticity* pp. 535-609. Cambridge: Cambridge University Press.
- Roscoe, K.H., and Schofield, A.N. (1963). *Mechanical Behaviour of an Idealised 'Wet' Clay*. *Engineering Plasticity*. Cambridge: Cambridge University Press.
- Schanz, T., and Vermeer P.A. (1996). Angles of Friction and Dilatancy of Sand. *Geotechnique*, Vol. 46, No. 1, pp. 145-151.
- Schmidt, B. (1966). Discussion: Earth Pressures At Rest Related to Stress History. *Canadian Geotechnical Journal*, Vol. 3, No.4, pp. 239–242.
- Skempton, A.W. (1944). Notes on Compressibility of Clays. *Quarterly Journal of the Geological Society, London*, Vol. 100, No. 2 pp. 119–135.
- Skempton, A.W. (1954). Discussion: Sensitivity of Clays and the  $c/p$  Ratio in Normally Consolidated Clays. *Proceedings of the American Society of Civil Engineers, Separate Vol. 478*, pp. 19–22.
- Skempton, A.W. (1957). Discussion: Further Data on the  $c/p$  Ratio in Normally Consolidated Clays. *Proceedings of the Institution of Civil Engineers, Vol. 7*, pp. 305–307.
- Skempton, A.W. (1986). Standard Penetration Test Procedures and The Effects in Sands of Overburden Pressure, Relative Density, Particle Size, Ageing and Overconsolidation. *Geotechnique*, Vol. 36, No. 3, pp. 425–447.
- Sowers, G.B. (1970). *Introductory Soil Mechanics and Foundations*. 3rd Edition. MacMillan Company, London: Collier-MacMillan Limited.
- Stas, C. V., and Kulhawy, F. H. (1984). Critical evaluation of design methods for foundations under axial uplift and compression loading. Report EL-3771 Electric Power Research Institute, Palo Alto: Electric Power Research Institute.
- Stroud, M.A. (1974). The Standard Penetration Test in Sensitive Clays and Soft Rocks. *Proceedings of the European Seminar on Penetration Testing, Stockholm. Vol. 2, No. 2*, pp. 366–375.

Tavenas, F., Jean, P., LeBlond, P., and Leroueil, S. (1983). The Permeability of Natural Soft Clays. Part II, Permeability Characteristics. *Canadian Geotechnical Journal*, Vol. 20, No. 4, pp. 645-660.

Terzaghi, K. (1943). *Theoretic Soil Mechanics*. New York: John Wiley and Sons, Inc..

Terzaghi, K., and Peck, R.B. (1967). *Soil Mechanics in Engineering Practice*. New York: John Wiley & Sons, Inc..

Vardanega, P.J., and Bolton, M.D. (2011). Strength Mobilization in Clays and Silts. *Canadian Geotechnical Journal*, Ottawa: NRC Research Press, Vol. 48, No. 10, pp. 1485–1503.

Viggiani, G., and Atkinson, J.H. (1995). Stiffness of Fine-grained Soil at Very Small Strain. *Geotechnique*, Vol. 45, No. 2, pp. 249–265.

Wroth C.P. (1975). In-situ Measurement of Initial Stress and Deformation Characteristics. *Proceedings of the Specialty Conference on In-Situ Measurement of Soil Properties*, Raleigh, North Carolina (New York: ASCE), Vol. 2, pp. 181–230.

Wroth, C.P., and Wood, D.M. (1978). The Correlation of Index Properties with Some Basic Engineering Properties of Soils. *Canadian Geotechnical Journal*, Vol. 15, pp. 137–145.



